TECHNICAL NOTE

D- 236

PRESSURE DISTRIBUTIONS AND AERODYNAMIC CHARACTERISTICS OF SEVERAL SPOILER CONTROLS ON A 40° SWEPTBACK WING AT A MACH NUMBER OF 1.61

By Emma Jean Landrum and K. R. Czarnecki

Langley Research Center
Langley Field, Va.

NATIONAL AERONAUTICS AND SPACE ADMINISTRATION

WASHINGTON

April 1960

NATIONAL AERONAUTICS AND SPACE ADMINISTRATION

TECHNICAL NOTE D-236

PRESSURE DISTRIBUTIONS AND AERODYNAMIC CHARACTERISTICS OF SEVERAL SPOILER CONTROLS ON A 40° SWEPTBACK WING AT A MACH NUMBER OF 1.61

By Emma Jean Landrum and K. R. Czarnecki

SUMMARY

An investigation has been made at a Mach number of 1.61 to determine the pressure distributions and aerodynamic characteristics of a series of five spoiler controls on a 40° sweptback wing having an aspect ratio of 3.1 and a taper ratio of 0.4. Wing angle-of-attack range for these tests was -15° to 15°. The Reynolds number was 3.6×10^6 based on the mean aerodynamic chord of 11.72 inches.

Incremental pressure distributions due to the spoilers were in good agreement with previous flat-plate results and also with the results of tests of similar spoilers on a trapezoidal wing. The location of the spoiler apex determined the most forward influence of the spoilers on the pressures. The spanwise normal-force and pitching-moment loadings due to the spoilers were dependent on the relative location of the spoiler to the wing trailing edge, on spoiler sweep angle, on whether the spoiler was stepped, and on wing angle of attack. For all the spoiler configurations that were tested exclusive of the half-span trailing-edge spoiler there was decreased stability in the high negative angle-of-attack range. Spoiler effectiveness in reducing wing lift and bending-moment coefficients generally was greatest for the full-span swept spoiler and least for the half-span unswept spoiler. The spoilers generally had little effect on the wing pitching moment except at the largest negative angles of attack and except for the trailing-edge spoiler.

INTRODUCTION

As part of a general program of research on controls, an investigation has been made in the Langley 4- by 4-foot supersonic pressure tunnel to determine the important parameters in the design of controls for use on a 40° sweptback wing at supersonic speeds. The tabulated pressure data from the investigation are presented in reference 1. Several control configurations were investigated as follows: six flaps,

one horn balance, one tip control, one lower-surface spoiler, and five upper-surface spoilers. All controls were mounted on a wing having 40° sweepback of the quarter-chord line, an aspect ratio of 3.1, and a taper ratio of 0.4.

An analysis of the pressure distributions obtained on eight movable-control configurations has been presented in reference 2. The purpose of this report is to present an analysis of the pressure distributions and integrated coefficients obtained on the five upper-surface spoiler controls.

The wing angle-of-attack range for these tests was -15° to 15°. Reynolds number was 3.6×10^6 based on the mean aerodynamic chord of 11.72 inches for the test Mach number of 1.61.

SYMBOLS

C_L lift coefficient, $\frac{(\text{Normal force})(\cos \alpha)}{qS}$

C_b root bending-moment coefficient, $\frac{B}{2qSb}$

C_m pitching-moment coefficient, $\frac{M'}{qS(MAC)}$

c_m section pitching-moment coefficient (taken about quarter chord of mean aerodynamic chord)

c_n section normal-force coefficient

C_p pressure coefficient, $\frac{p_l - p}{q}$

B semispan wing-root bending moment

b/2 wing semispan

c wing chord

$\bar{c}$ wing average chord

L semispan-wing lift

M stream Mach number

M'	semispan-wing pitching moment about quarter chord of mean aerodynamic chord
p	stream static pressure
p_l	local surface pressure
q	stream dynamic pressure
R	Reynolds number based on mean aerodynamic chord
S	semispan-wing area
x	distance in chordwise direction from wing leading edge
y	distance in spanwise direction from wing-root chord
α	wing angle of attack, deg
Δ	prefix indicating increment due to spoiler

APPARATUS

Wind Tunnel

This investigation was conducted in the Langley 4- by 4-foot supersonic pressure tunnel at a Mach number of 1.61. During the tests the dewpoint was kept below -20° F so that the effects of water condensation in the supersonic nozzle were negligible.

Model and Model Mounting

The model used in this investigation consisted of a sweptback semispan wing with spoilers mounted at various locations on the upper surface of the wing as shown in figure 1. (The model numbers used in this paper correspond to those of ref. 1.) The spoilers had the same cross sections but different spans and sweep angles. Because a sufficient number of pressure tubes to instrument both surfaces of the model could not be brought through the torque tube, orifices were installed on only the upper surface. The chordwise and spanwise locations of the upper-surface pressure orifices are given in table 1.

The wing had 40° sweepback along the 25-percent-chord line, a root chord of 15.88 inches, a tip chord of 6.17 inches, a semispan of

17.02 inches, an aspect ratio of 3.1, and a taper ratio of 0.4. The wing section was 5 percent thick and was made up of a rounded NACA 65-series section extending from the leading edge to the 40-percent-chord line and a flat section, 0.79 inch thick at the root tapering to 0.31 inch thick at the tip, extending from the 40-percent-chord line to the trailing edge.

The wing was constructed of steel with the pressure tubes installed in grooves in the upper surface and faired over with plastic. The spoilers were constructed of 1/16-inch steel. The trailing edge of the wing was formed by maintaining the flap control at zero deflection.

The semispan wing was mounted horizontally in the tunnel from a turntable in a steel boundary-layer bypass plate which was located vertically in the test section about 10 inches from the tunnel wall.

TESTS AND TEST PROCEDURES

Angle of attack was changed by rotating the turntable on which the wing was mounted. Since the angular deflection of the wing under load was negligible, the angle of attack was measured by a vernier on the outside of the tunnel. The pressure distributions were determined from photographs of multitube manometer boards to which the leads from the model orifices were attached.

The angle-of-attack range for the tests was -15° to 15° at 3° increments. The tests were made at a tunnel stagnation pressure of 13 lb/sq in. abs at a Mach number of 1.61, corresponding to a Reynolds number of 3.6×10^6 based on the mean aerodynamic chord of 11.72 inches.

In order to insure a turbulent boundary layer over the model, 1/4-inch-wide strips of No. 60 carborundum grains were attached to both the upper and lower surfaces a short distance back from the leading edge. These strips completely spanned the model except within 1/4 inch of the orifice stations.

PRECISION OF DATA

The mean Mach number in the region occupied by the model is estimated from calibrations to be 1.61 with local variations of less than ± 0.02. Tunnel calibrations do not show evidence of any significant flow angularities. The estimated accuracy in setting wing angle of attack is $\pm 0.05^\circ$. The measured pressure coefficients are believed to be accurate within ± 0.01.

RESULTS AND DISCUSSION

Pressure Distributions

Basic distributions.- Upper-surface pressure distributions for each spoiler configuration at angles of attack of -12°, 0°, and 12° are presented in figures 2 to 6. In order that the changes due to the spoiler can be more readily seen, the corresponding pressure distributions for the no-spoiler condition are included in each figure.

For the wing without a spoiler, sharp pressure increases or decreases occur at the location of the leading edge of a full-span plain flap which forms the trailing edge of the wing. These discontinuities in pressure are most pronounced at angle of attack and result primarily from the bending deflection of the trailing-edge flap relative to the wing under load. The influence of these pressure discontinuities on the aerodynamic characteristics is negligible.

In general, the incremental pressure distributions due to the spoilers were in good agreement with previous flat-plate results (ref. 3), with the results of tests of similar spoilers on a trapezoidal wing (ref. 4), and with the data of reference 5. For all the configurations in the present investigation as in the previous investigation, flow separation, which occurs some distance ahead of the spoiler face, causes a rapid rise in pressure followed by a region of relatively constant pressure up to the spoiler face. At the spoiler, a rapid acceleration of the flow results in a negative-pressure peak which in turn is followed by a recompression of the flow in which the pressure approaches that for the spoiler-off configuration at some distance downstream. For the trailing-edge spoiler configuration (fig. 6), of course, the negative-pressure region and the recompression occur downstream of the wing.

As the wing angle of attack is increased and the local Mach number is increased, the separation point moves slightly rearward and the initial pressure rise decreases. (See figs. 2 to 6.) The rearward movement of the separation point with Mach number was shown in reference 3 and also occurred in tests of spoilers on a trapezoidal wing in reference 4. Because this rearward movement is slight the effect on the pressure rise is very small. There are two primary reasons for the decrease in pressure rise with increasing angle of attack. First, as the local Mach number is increased for a given separation angle, the pressure rise tends to decrease in terms of the local dynamic pressure. Secondly, as the local Mach number increases the local dynamic pressure decreases inasmuch as the stagnation conditions essentially remain the same.

Immediately downstream of the spoilers, there is only a slight increase in the negative pressures with increase in angle of attack. In most cases, the acceleration at the spoiler approaches the vacuum pressure (which is $C_p = -0.55$) at positive angles of attack. Further downstream, the recompression is much greater at the negative angles of attack as might be expected because of the higher pressure from which the initial disturbance started and to which the flow tends to return.

Configuration effects.- A comparison of figures 2 and 3 shows that reducing the spoiler span from 100 to 53 percent of the wing semispan has no effect on the pressures at orifice stations 1 to 3 and only a small effect on those at station 4, which for the half-span swept spoiler is close to the spoiler outboard edge and hence slightly influenced by end effects. Outboard of the half-span swept spoiler (stations 5 to 7) the influence of the spoiler on the local pressure diminishes with outward movement along the span as would be expected. There appears to be a merging of the influences of the positive-pressure increments ahead of the spoiler with those of the negative-pressure increments behind; this leads to a gradual weakening of the positive- and negative-pressure-increment regions rather than to the simple sweeping back of the unaltered pressure fields toward the wing trailing edge. As the angle of attack is increased the flow-acceleration effects of the half-span spoiler over the outboard portion of the wing tend to disappear and only the influence of the separation pressure (positive increments) can be seen. These trends result in a smaller decrease in spoiler effectiveness than might be anticipated from the magnitude of the reduction in spoiler span alone.

The effects of sweeping a half-span spoiler can be seen by comparing figures 3 and 4. In general (also shown in ref. 3) the effect of sweep is to broaden both the positive-pressure region ahead of and the negative-pressure region behind the spoiler and to decrease the magnitudes of the maximum positive or negative pressures with outboard movement along the span. Outboard of the spoilers was a tendency for the influence of the unswept spoiler to diminish more rapidly than that of the swept spoiler particularly at positive angles of attack. For the unswept spoiler the outboard movement along the span results in a large increase in the negative-pressure-increment region to the rear of the spoiler because of the sweepback of the wing trailing edge. Inasmuch as the recompression is generally not completed before the wing trailing edge is reached, there is a tendency for the negative-pressure regions behind the spoiler to cancel more of the negative lift ahead of the spoiler. This cancellation results in a decreasing effectiveness of the spoiler outboard along the spoiler span. This effect is not present for the swept spoiler investigated. Also, because the spoiler end effect appears to be stronger on the unswept spoiler and appears to accelerate the recompression to the rear of the spoiler, the loss in

relative effectiveness for the unswept spoiler at station 4 is less than the loss at station 3.

Changing the half-span swept spoiler configuration to a half-span step spoiler configuration, where the individual segments have no sweep but are swept relative to one another along the same sweep line as for the swept spoiler, generally decreased the size of the positive-pressure region ahead of the spoiler. (Compare figs. 3 and 5.) The change did, however, appear to reduce progressively the negative-pressure region behind the spoiler with inboard movement along the spoiler span. Outboard of the spoilers the effect of the step spoiler was generally smaller than that of the swept spoiler, particularly in the zero- and positive-angle-of-attack region.

The half-span trailing-edge spoiler (fig. 6) has a sweep angle between that of the half-span unswept spoiler (fig. 4) and that of the half-span swept spoiler (fig. 3). As expected, the characteristics of the pressures ahead of the trailing-edge spoiler lie between those of the half-span swept and half-span unswept spoilers. Of course, for the trailing-edge spoiler there is no detrimental effect of a negative-pressure region behind the spoiler as in the case of the other two spoilers.

Forward influence of spoilers.- Of interest in connection with the discussion of spoiler pressure fields is the effect of spoiler configuration on the most forward influence of the spoiler across the span. In order to illustrate this effect, the chordwise locations of the points where the pressure rise due to separation first appears at each spanwise station are plotted on the basic-wing plan form in figure 7 for the full-span and half-span swept spoilers (configurations 21 and 22, respectively) and for the half-span unswept spoiler (configuration 23).

The data indicate that for the unswept spoiler the variation across the spoiler span of this forward influence is somewhat less than that for the swept configurations. Outboard of the half-span spoilers there is little difference between any of the configurations. At $\alpha = -12^{\circ}$ the influence of all the spoilers reaches the wing leading edge at about half span. At $\alpha = 12^{\circ}$ the lack of points for the half-span configurations on the outboard half of the wing signifies the virtual disappearance of the disturbances rather than the pressure rise reaching the leading edge. (See figs. 3(c) and 4(c)). In general, it appears that the forward influence of a swept spoiler near the apex does not extend as far forward as the influence of the unswept spoiler. Farther out along the spoiler span the reverse is true. These results are in agreement with those presented in figure 5 of reference 3.

For the swept configurations there is little or no influence of spoiler span throughout the angle-of-attack range. This result suggests

that the forward influence of the spoiler across the wing span is determined by the location of the apex of the spoiler rather than by the individual spanwise sections for the spoiler sweep angles and Mach number under discussion.

The small effect of angle of attack on the forward influence of the full-span swept spoiler is shown in figure 8.

Spanwise Loadings

Basic loadings.- The spanwise normal-force and pitching-moment loadings for the various test configurations, determined by a step integration of the chordwise pressure distributions, are presented in figures 9 and 10, respectively. The contribution of the lower-surface pressures to these loadings was determined from the pressure distributions of the basic configuration without the spoilers. Examination of the results obtained on this configuration with the trailing-edge flap control deflected indicates that there is little, if any, effect of one surface of the wing on the other, even for the case where the shock from the apex of the control passes over the leading edge of the wing. In order to examine the loadings due to the spoilers in greater detail, the incremental spanwise normal-force and pitching-moment loadings are presented in figures 11 and 12, respectively.

In general, the spoilers tested decreased the normal-force loading over the span of the spoiler as was desired (fig. 11). The half-span unswept spoiler (fig. 11(c)), however, did exhibit a lack of effectiveness at station 3 $\left(\frac{y}{b/2} = 0.338\right)$ throughout the angle-of-attack range owing to the increasing distance from the spoiler to the wing trailing edge with outboard movement along the span. This region is influenced by the negative-pressure increments resulting from the incompleted recompression of the flow behind the spoiler as was described previously. At station 4 $\left(\frac{y}{b/2} = 0.506\right)$ the spoiler has recovered its effectiveness because of the influence of spoiler end effects. In the light of this reasoning the negative increment in lift measured at station 1 for the unswept spoiler appears too low. The explanation lies in the influence of the boundary layer of the wing mounting plate. A similar effect may be expected at a wing-fuselage juncture.

At very high negative angles of attack most of the configurations showed positive increments in normal force on the outboard wing stations (fig. 11), possibly because of some limitations imposed by the positive-pressure region reaching the wing leading edge. At high positive angles of attack the full- and half-span swept spoilers indicated an increased

negative lift effectiveness in the neighborhood of station 5 $\left(\frac{y}{b/2} = 0.670\right)$. This effect can be ascribed to the high negative pressures existing on the basic wing in this region which practically eliminates the appearance of the negative-pressure region behind the spoiler when the spoiler was installed.

The increment in pitching moment contributed by the spoilers when referred to the quarter-chord point of the mean aerodynamic chord was generally small for all the spoiler configurations with the exception of the trailing-edge spoiler at positive angles of attack and on the inboard half of the wing (fig. 12). On the outboard half of the wing the increments in spoiler pitching moments tended to be more positive in this α range, which indicated that the effective center of pressure of the increments in pressure due to the spoiler was to the rear of the moment center. As α was decreased the spoiler pitching-moment increments became negative across the complete wing span. Because of the more rearward location of the trailing-edge spoiler relative to the moment center (fig. 12(e)), the contribution of the spoiler to the pitching moment is always positive, but becomes smaller as α is increased.

Configuration effects.- A comparison of the spanwise normal-force coefficients for the full- and half-span swept spoilers (figs. 11(a) and 11(b), respectively) indicates identical characteristics over the inboard half of the wing and only a small decrease in normal-force increment due to the half-span spoiler over the outboard half. This trend results from the aforementioned more rapid disappearance of the negative-pressure increments relative to the positive-pressure influence. The same trend is reflected in the distributions of the spanwise pitching-moment increment (figs. 12(a) and 12(b)).

Sweeping the half-span spoiler increases its effectiveness in producing negative lifting increments across the span, generally, and eliminates the loss in effectiveness due to the increasing distance of the unswept spoiler relative to the wing trailing edge. (See figs. 11(b) and 11(c).) The effect of sweeping the half-span spoiler on the pitching-moment distribution was small except on the outboard half of the wing span.

In comparison with the swept and unswept half-span spoilers, the half-span trailing-edge spoiler, with a spoiler sweepback angle between that of the swept and unswept spoilers, produced the largest increments in negative lift over the spoiler span (compare figs. 11(b), 11(c), and 11(e)) because of the absence of negative pressures behind the spoiler. The trailing-edge spoiler generally also indicated the largest relative loss in effectiveness in lift carryover outboard of the spoiler control because of the short distance required to sweep the spoiler

effect off the wing. At negative angles of attack, nevertheless, the spoiler influence appears to extend close to the wing tip. This effect results from the lower Mach number on the upper surface of the wing in the negative angle-of-attack range. As has already been noted, the pitching-moment increments of the trailing-edge spoiler are considerably more positive than those of the swept and unswept half-span spoilers. (See figs. 12(b), 12(c), and 12(e).)

Angle-of-attack effects.- The effects of changes in angle of attack on the section normal-force and pitching-moment increments are presented in figure 13. Some of the effects have already been pointed out in the discussion of the span loadings and need not be covered in detail. Some of the trends, however, can be seen much more clearly in this form.

With the exception of the trailing-edge spoiler, all configurations tested tended to show an increase in the negative lift effectiveness as α was increased from the largest negative values toward zero. As α was increased still further in the positive angle-of-attack region, the section normal-force effectiveness remained constant for the full-span swept spoiler and over the inboard half of the wing for the half-span swept spoiler. For the half-span swept spoiler the effectiveness decreased with angle of attack near the wing tip. The half-span unswept spoiler had angle-of-attack trends similar to those for the half-span swept spoiler. The half-span stepped spoiler, on the other hand, showed a tendency for nearly all the stations to lose effectiveness with increasing values of α. In contrast with the other configurations, the trailing-edge spoiler generally lost effectiveness with increasing values of α in the negative angle-of-attack range and showed the largest losses in negative lift effectiveness over the spoiler span in the positive angle-of-attack range.

The increments in section pitching moment due to the spoilers show related trends. With the exception of the trailing-edge spoiler, all configurations show increasingly positive moment increments with increasing values of α in the negative angle-of-attack range. In the positive angle-of-attack range this increase in pitching moment continued at a very much reduced rate or disappeared. For the trailing-edge spoiler the results generally indicated a decreasing or more negative increment in section moment with increasing values of α through the entire angle-of-attack range.

Integrated Coefficients

Total coefficients.- The variations of lift, bending-moment, and pitching-moment coefficients with angle of attack are presented in figure 14 for the test configurations with and without the spoilers. These coefficients were obtained by integration of the spanwise-loading plots

shown in figures 9 and 10. The most noteworthy effect indicated in figure 14 is the decreased stability at the high negative angles of attack for all spoiler configurations except for the trailing-edge spoiler. For an airplane having a small margin of stability this could present a problem when the spoiler is extended.

Incremental coefficients.- The effect of configuration changes on spoiler effectiveness can be seen more readily in figures 15 to 18 which show the variations of incremental lift, bending-moment, and pitching-moment coefficients with angle of attack.

Spoiler effectiveness in reducing wing lift and bending moment generally was greatest for the full-span swept spoiler and least for the half-span unswept spoiler. Angle-of-attack effects on the spoiler effectiveness were variable. The incremental pitching moments due to the spoilers were small or negligible, with the exception of those of the trailing-edge configuration, over most of the angle-of-attack range; there was, however, a change to a more negative moment at the highest negative angles of attack.

In general, reducing spoiler span from 100 to 53 percent of the wing semispan had less effect on the incremental coefficients than might have been expected for the size of the reduction (fig. 15). In addition, the effect on C_m is much less than it is for the other coefficients except at the high positive angles of attack.

The effect of reducing spoiler sweep is shown in figure 16. The half-span swept spoiler shows more lift and bending-moment effectiveness than the half-span unswept spoiler. Incremental pitching-moment coefficient becomes more positive for the swept-spoiler configuration. The half-span step spoiler retains some of the lift and bending-moment effectiveness of the swept-spoiler configuration at the larger negative angles of attack but approaches the effectiveness of the unswept-spoiler configuration as α is increased. In the negative angle-of-attack range the incremental pitching-moment coefficient is more positive for the step spoiler than for the swept spoiler but is about the same as that for the unswept spoiler at the higher positive angles of attack.

The half-span trailing-edge spoiler is compared with the half-span swept spoiler in figure 17 and with the half-span unswept spoiler in figure 18. In each case, the trailing-edge spoiler produces more lifting effectiveness at the negative angles of attack. At positive angles of attack the lifting effectiveness for the trailing-edge spoiler is the same as that for the swept spoiler and better than that for the unswept spoiler. Bending-moment effectiveness for the trailing-edge spoiler is not as good as that for the swept spoiler at $\alpha > -4^\circ$, although at the more negative angles of attack the incremental bending-moment coefficient for the trailing-edge spoiler is more negative than that for the

swept spoiler. However, for the trailing-edge spoiler the incremental bending-moment coefficient is more negative throughout the α range than it is for the unswept spoiler. The large positive increments in pitching-moment coefficient for the trailing-edge spoiler are due to the location of the spoiler with respect to the center-of-gravity location which is the quarter chord of the mean aerodynamic chord.

CONCLUSIONS

An investigation has been made at a Mach number of 1.61 to examine the characteristics of several spoiler-type controls on a 40° sweptback wing. From an analysis of the chordwise pressure distributions, spanwise loadings, and integrated coefficients, the following conclusions may be made:

1. The incremental pressure distributions due to the spoilers were in good agreement with previous flat-plate results and with the results of tests of similar spoilers on a trapezoidal wing.

2. The effect of angle of attack on the pressures measured ahead of a spoiler was to decrease the magnitude of the incremental pressure rise due to the spoiler as the angle of attack was increased. Angle of attack had little effect on the negative pressures just behind a spoiler but did alter the relative magnitude of the recompression pressures further downstream.

3. Outboard of the half-span spoilers the influence of the negative-pressure region behind the spoiler appeared to deteriorate more rapidly than that of the positive pressure region ahead of the spoiler with outward movement along the span.

4. The most forward influence across the wing span of the more highly swept spoilers was determined by the location of the spoiler apex and was not affected by spoiler span.

5. In general, the spanwise normal-force loading due to the spoilers was dependent upon the relative location of the spoiler to the wing trailing edge, on spoiler sweep angle, on whether the spoiler was stepped, and on wing angle of attack. Outboard of the half-span spoilers there was a considerable carryover of normal force due to the spoilers.

6. The contribution of the spoilers to the wing pitching moments was dependent upon the same parameters. On the outboard half of the wing, beyond the half-span spoilers, the section pitching moments were strongly influenced by load carryover.

7. For all the spoiler configurations that were tested exclusive of the configuration with the half-span trailing-edge spoiler there was decreased stability in the high negative angle-of-attack range.

8. Spoiler effectiveness in reducing wing lift and bending moment generally was greatest for the full-span swept spoiler and least for the half-span unswept spoiler. Angle-of-attack effects on the spoiler effectiveness were variable.

9. The incremental pitching moments due to the spoilers were small or negligible, with the exception of those of the trailing-edge configuration, over most of the angle-of-attack range; there was, however, a change to a more negative moment at the highest negative angles of attack. The pitching-moment contribution of the trailing-edge spoiler was fairly large and positive throughout the angle-of-attack range.

Langley Research Center,
National Aeronautics and Space Administration,
Langley Field, Va., December 4, 1959.

REFERENCES

1. Lord, Douglas R.: Tabulated Pressure Data for a Series of Controls on a 40° Sweptback Wing at Mach Numbers of 1.61 and 2.01. NACA RM L57H30, 1957.

2. Lord, Douglas R.: Analysis of Pressure Distributions for a Series of Controls on a 40° Sweptback Wing at a Mach Number of 1.61. NASA TM X-139, 1959.

3. Lord, Douglas R., and Czarnecki, K. R.: Aerodynamic Loadings Associated With Swept and Unswept Spoilers on a Flat Plate at Mach Numbers of 1.61 and 2.01. NACA RM L55L12, 1956.

4. Lord, Douglas R., and Czarnecki, K. R.: Pressure Distributions and Aerodynamic Characteristics of Several Spoiler-Type Controls on a Trapezoidal Wing at Mach Numbers of 1.61 and 2.01. NACA RM L56E22, 1956.

5. Conner, D. William, and Mitchell, Meade H., Jr.: Effects of Spoiler on Airfoil Pressure Distribution and Effects of Size and Location of Spoilers on the Aerodynamic Characteristics of a Tapered Unswept Wing of Aspect Ratio 2.5 at a Mach Number of 1.90. NACA RM L50L20, 1951.

TABLE 1.- CHORDWISE AND SPANWISE LOCATION OF UPPER-SURFACE ORIFICE STATIONS

Orifice	Values of x/c at station -						
	1	2	3	4	5	6	7
	$\frac{y}{b/2} = 0.015$	$\frac{y}{b/2} = 0.168$	$\frac{y}{b/2} = 0.338$	$\frac{y}{b/2} = 0.506$	$\frac{y}{b/2} = 0.670$	$\frac{y}{b/2} = 0.834$	$\frac{y}{b/2} = 0.997$
1	0	0	0	0	0	0	0
2	.050	.050	.050	.050	.050	.050	.050
3	.100	.100	.100	.100	.100	.100	.100
4	.150	.150	.150	.150	.150	.150	.150
5	.200	.200	.200	.200	.200	.200	.200
6	.250	.250	.250	.250	.250	.250	.250
7	.300	.300	.300	.300	.300	.300	.300
8	.350	.350	.350	.350	.350	.350	.350
9	.400	.400	.400	.400	.400	.400	.400
10	.450	.450		.450	.450	.450	.450
11	.500	.500		.500	.500		
12	.550	.550		.550	.550	.550	.550
13	.600	.600	.600	.600	.600	.600	.600
14	.650	.650	.650	.650	.650	.650	.650
15	.700	.700	.700	.700	.700	.700	.700
16	.725	.725	.725	.725	.725	.725	.725
17		.725	.725	.725	.725	.725	.725
18		.750	.750	.750	.750	.750	.750
19	.800	.800	.800	.800	.800	.800	.800
20	.850	.850	.850	.850	.850	.850	.850
21	.900	.900	.900	.900	.900	.900	.900
22	.980	.980	.980	.980	.980	.980	.980

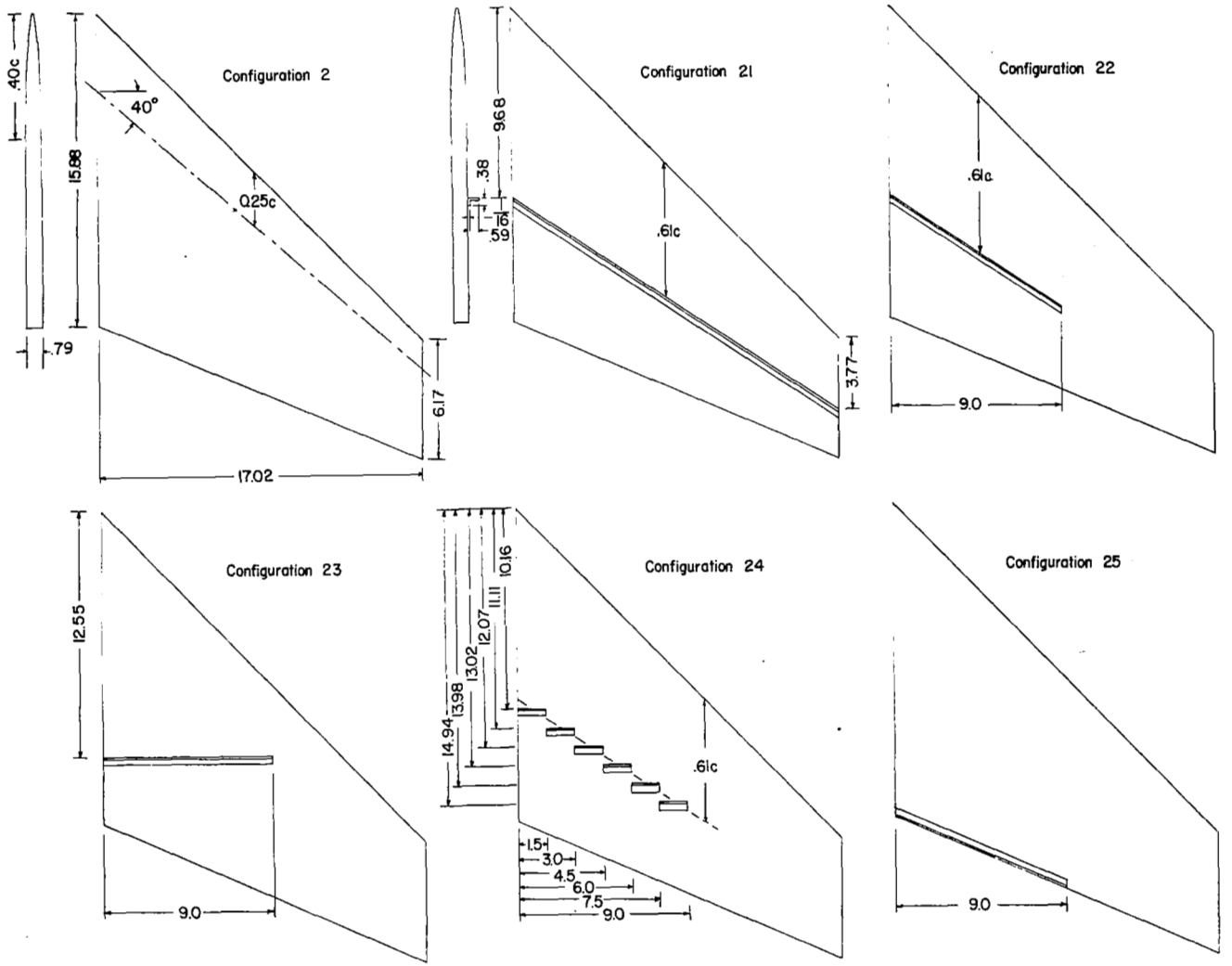

Figure 1.- Sketches of the configurations tested showing spoiler locations. All dimensions are in inches. Half-span spoilers are at 0.53b.

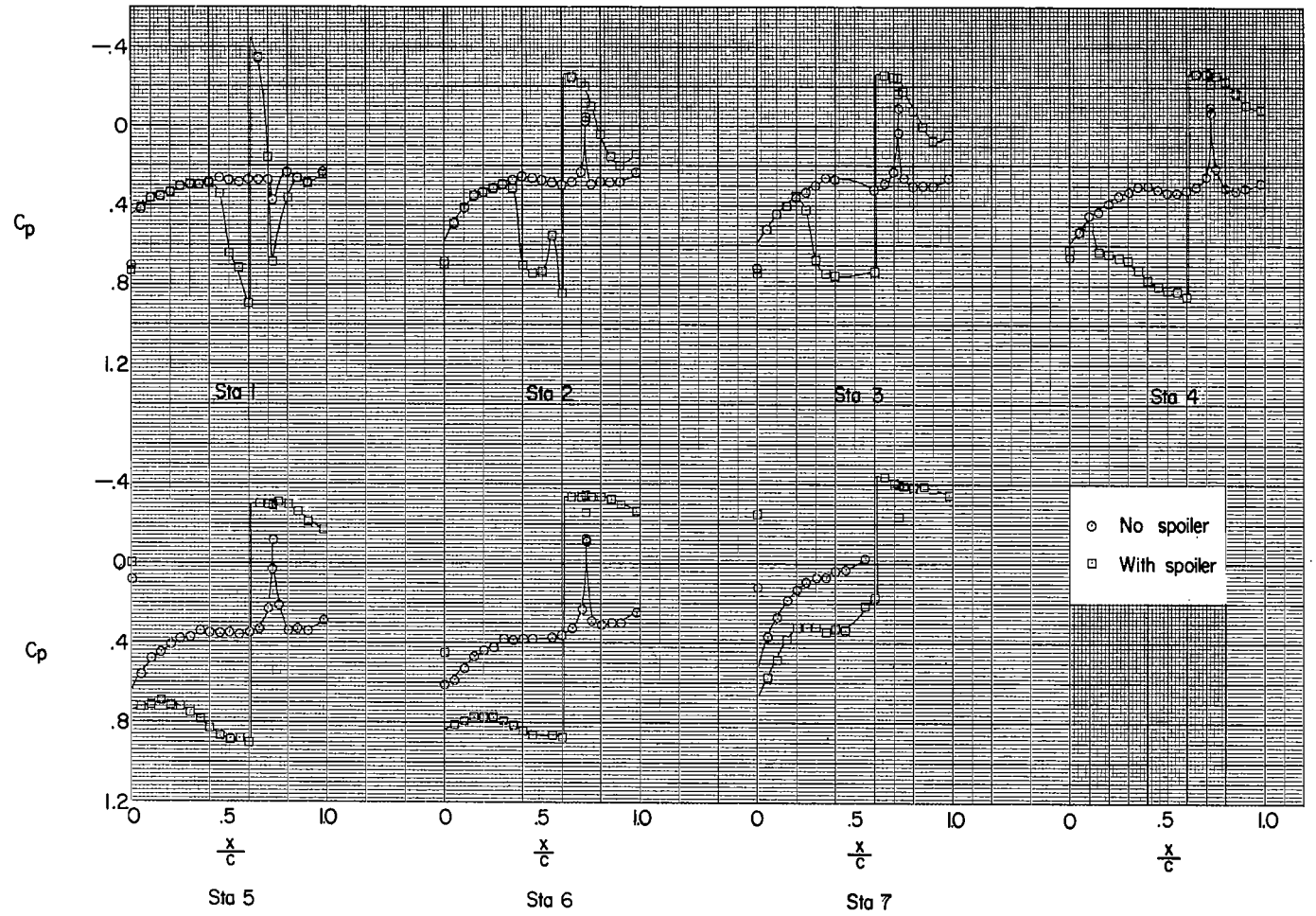

(a) $\alpha = -12^{\circ}$.

Figure 2.- Pressure distributions for full-span swept spoiler (configuration 21). M = 1.61; $R = 3.6 \times 10^{6}$.

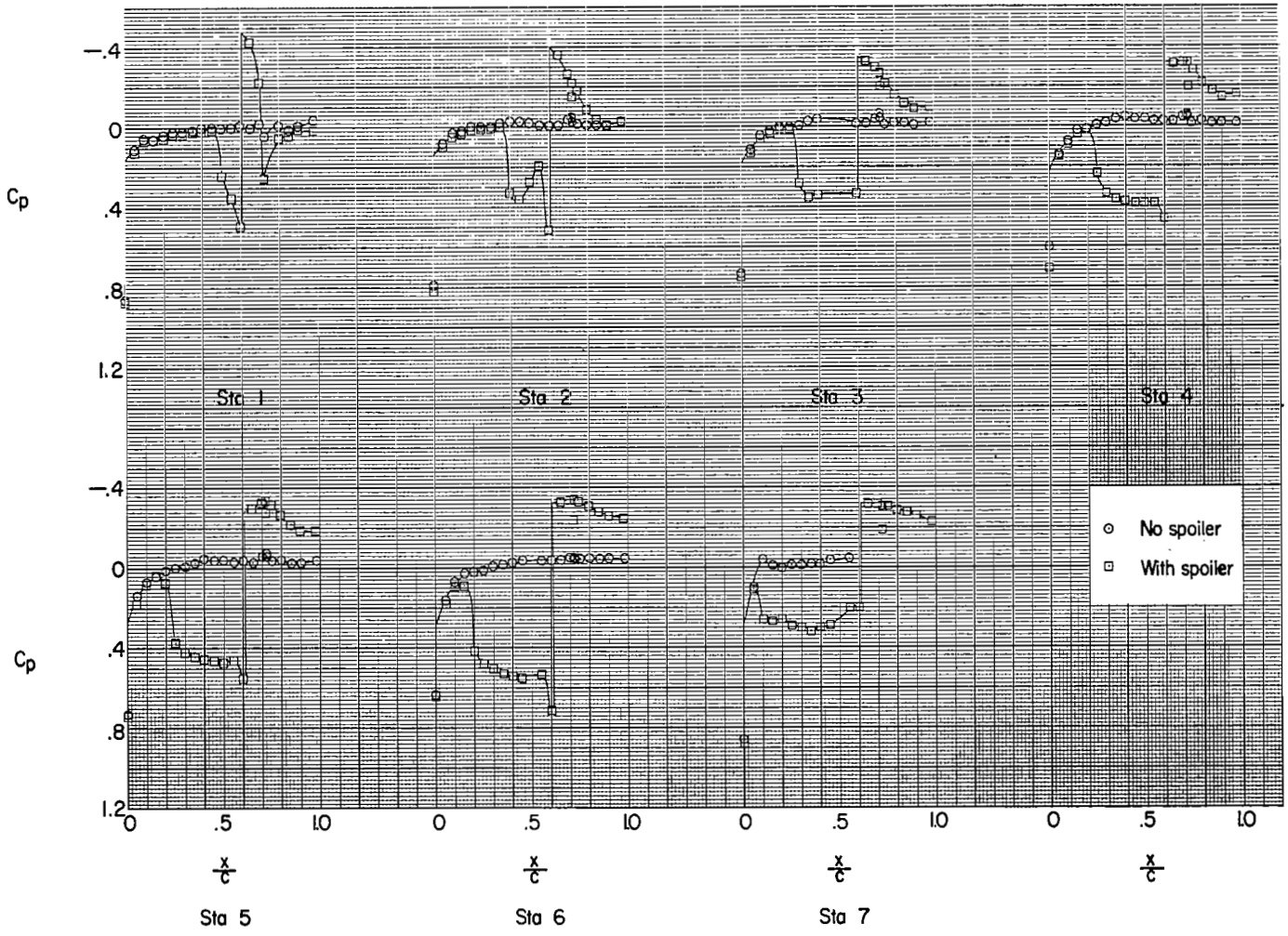

(b) $\alpha = 0^{\circ}$.

Figure 2.- Continued.

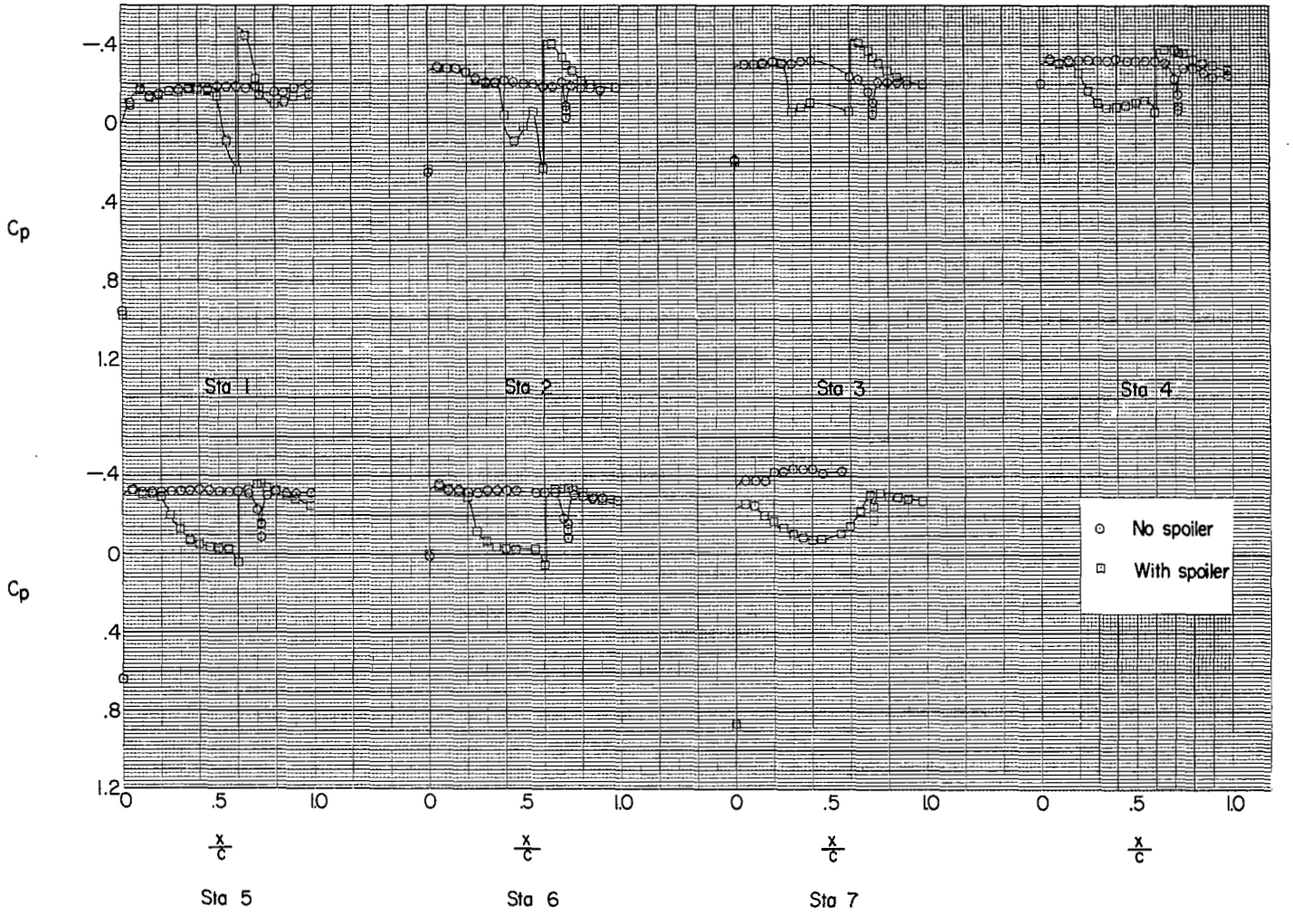

(c) $\alpha = 12^{\circ}$.

Figure 2.- Concluded.

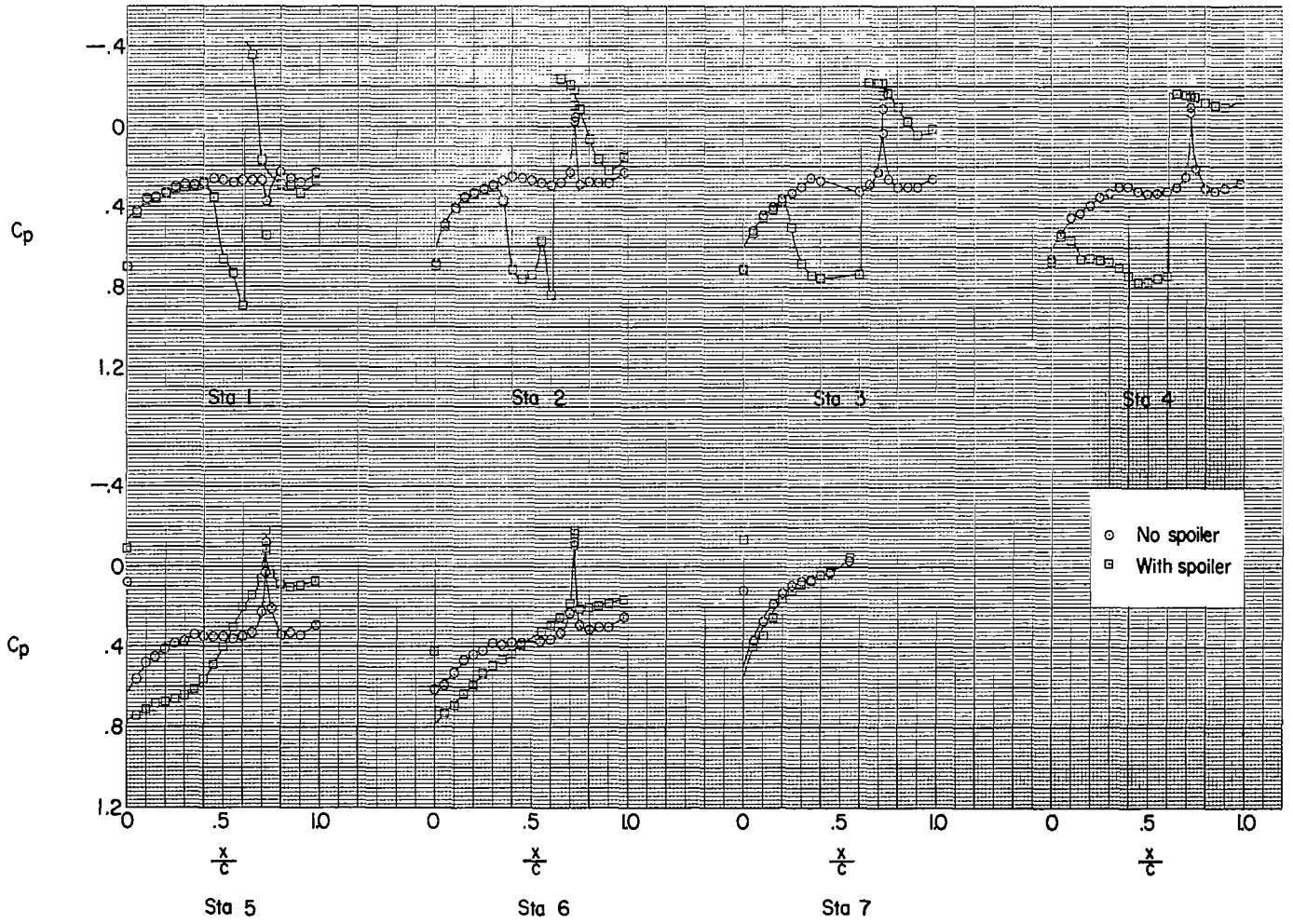

(a) $\alpha = -12^{\circ}$.

Figure 3.- Pressure distributions for half-span swept spoiler (configuration 22). M = 1.61; $R = 3.6 \times 10^6$.

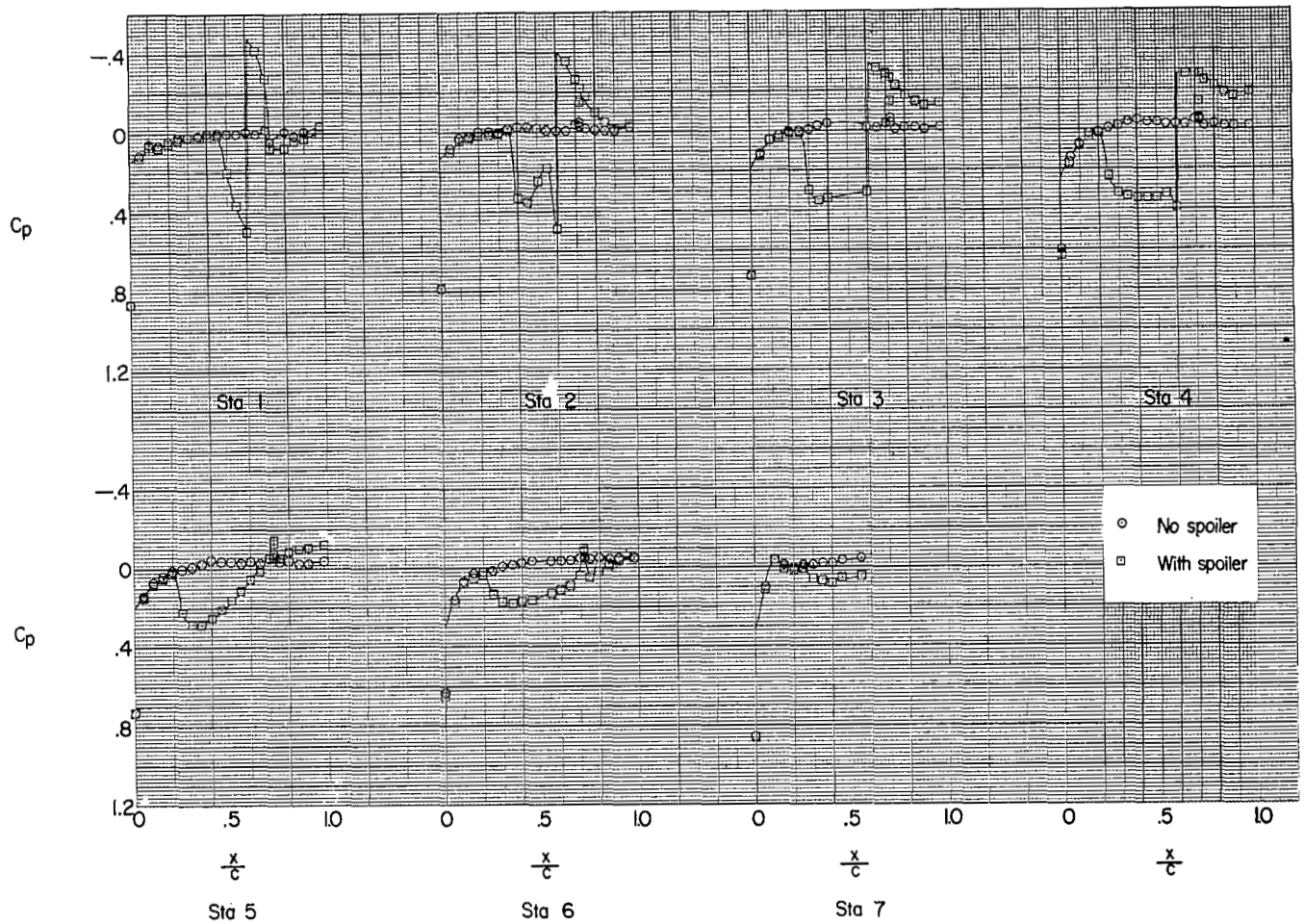

(b) $\alpha = 0^{\circ}$.

Figure 3.- Continued.

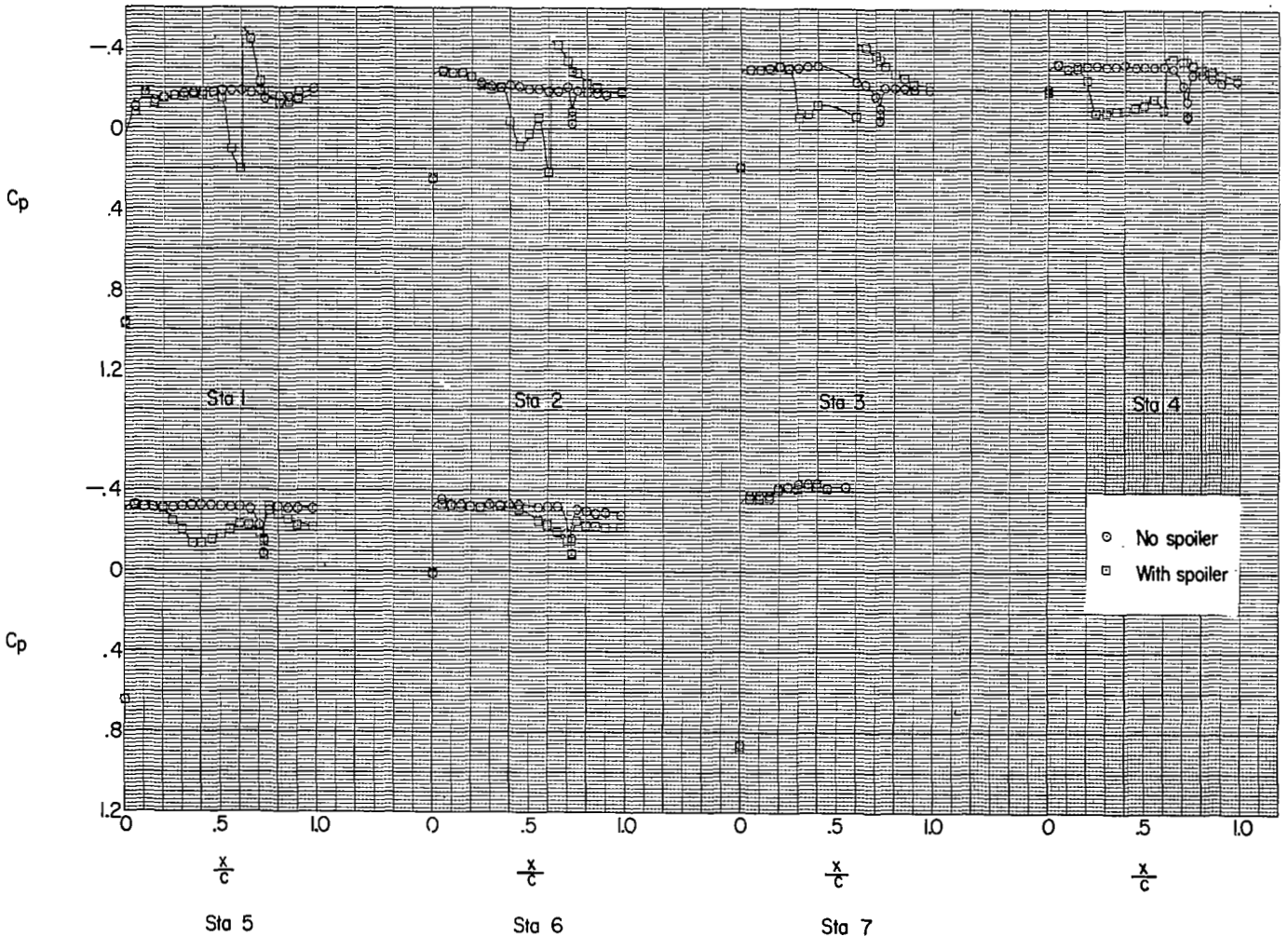

(c) $\alpha = 12^{\circ}$.

Figure 3.- Concluded.

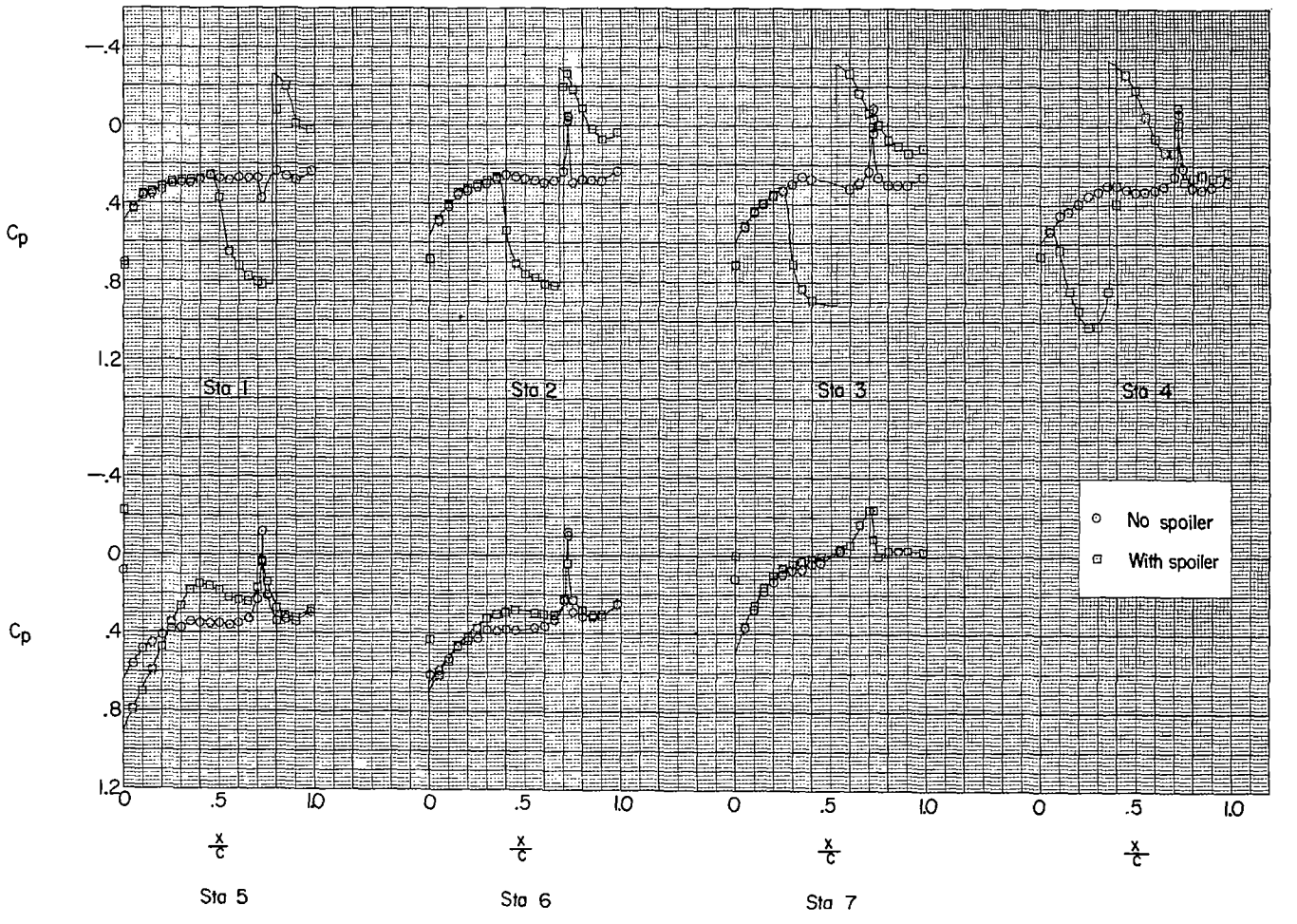

(a) $\alpha = -12^{\circ}$.

Figure 4.- Pressure distributions for half-span unswept spoiler (configuration 23). $M = 1.61$; $R = 3.6 \times 10^6$.

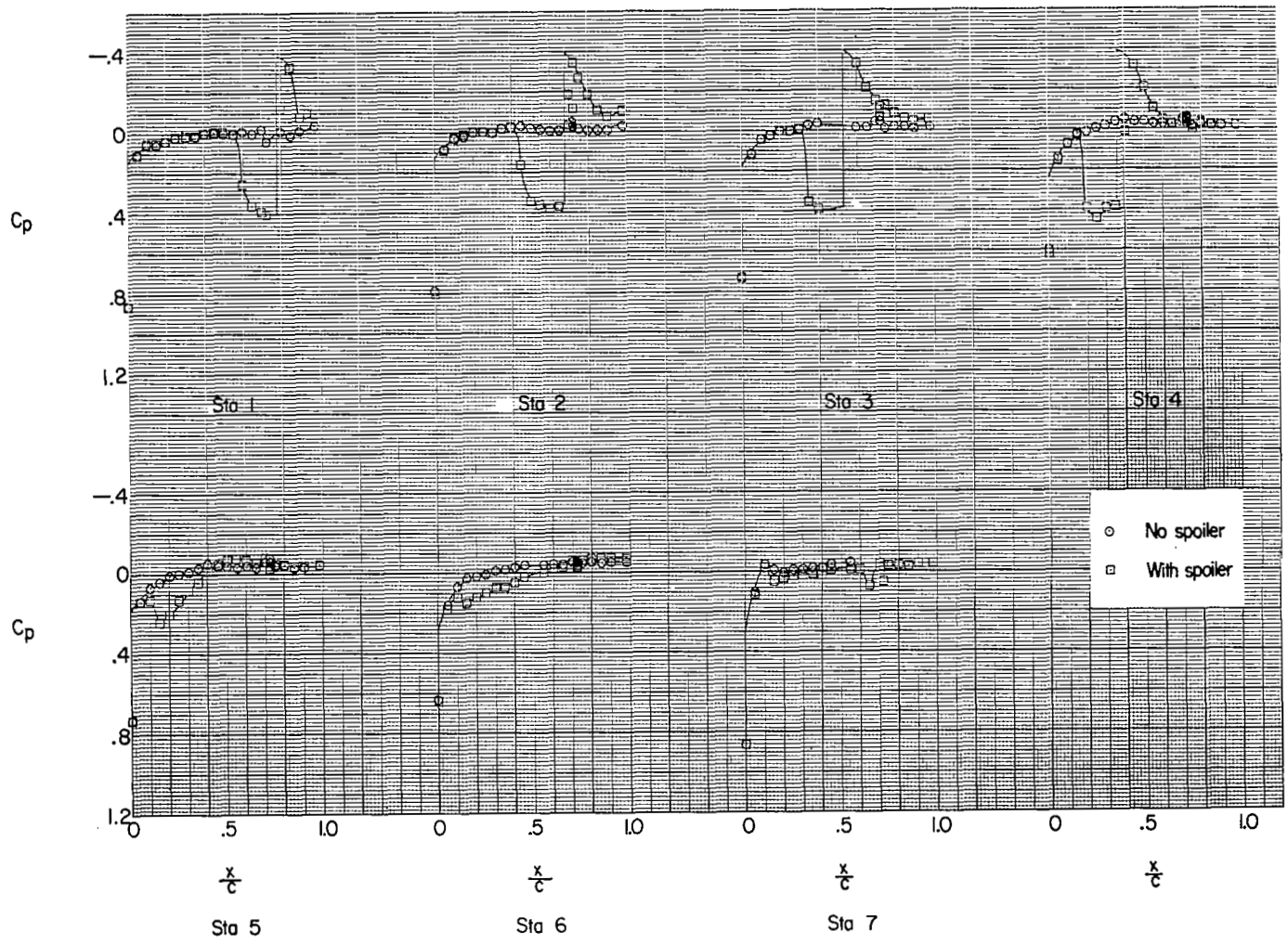

(b) $\alpha = 0^{\circ}$.

Figure 4.- Continued.

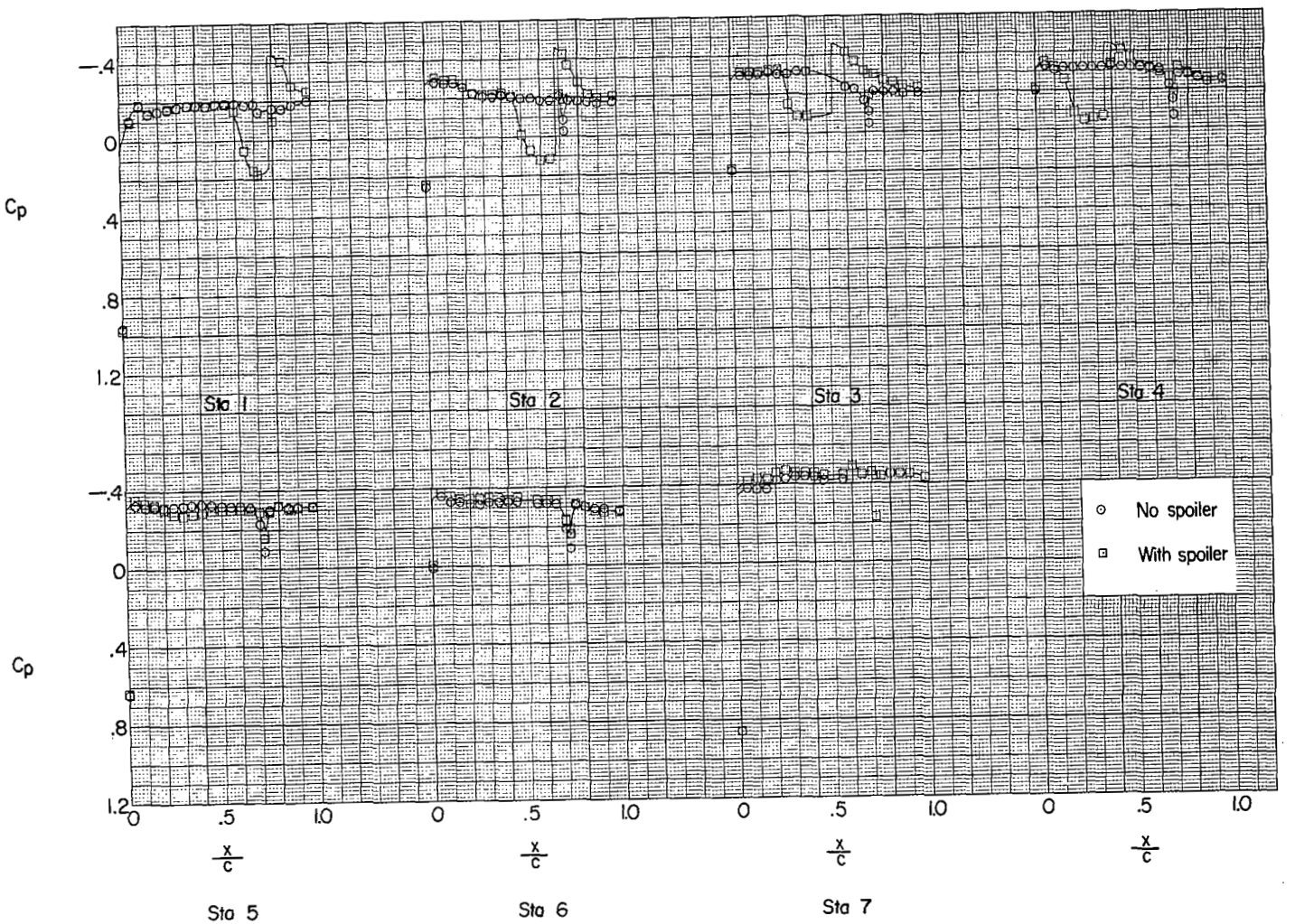

(c) $\alpha = 12^{\circ}$.

Figure 4.- Concluded.

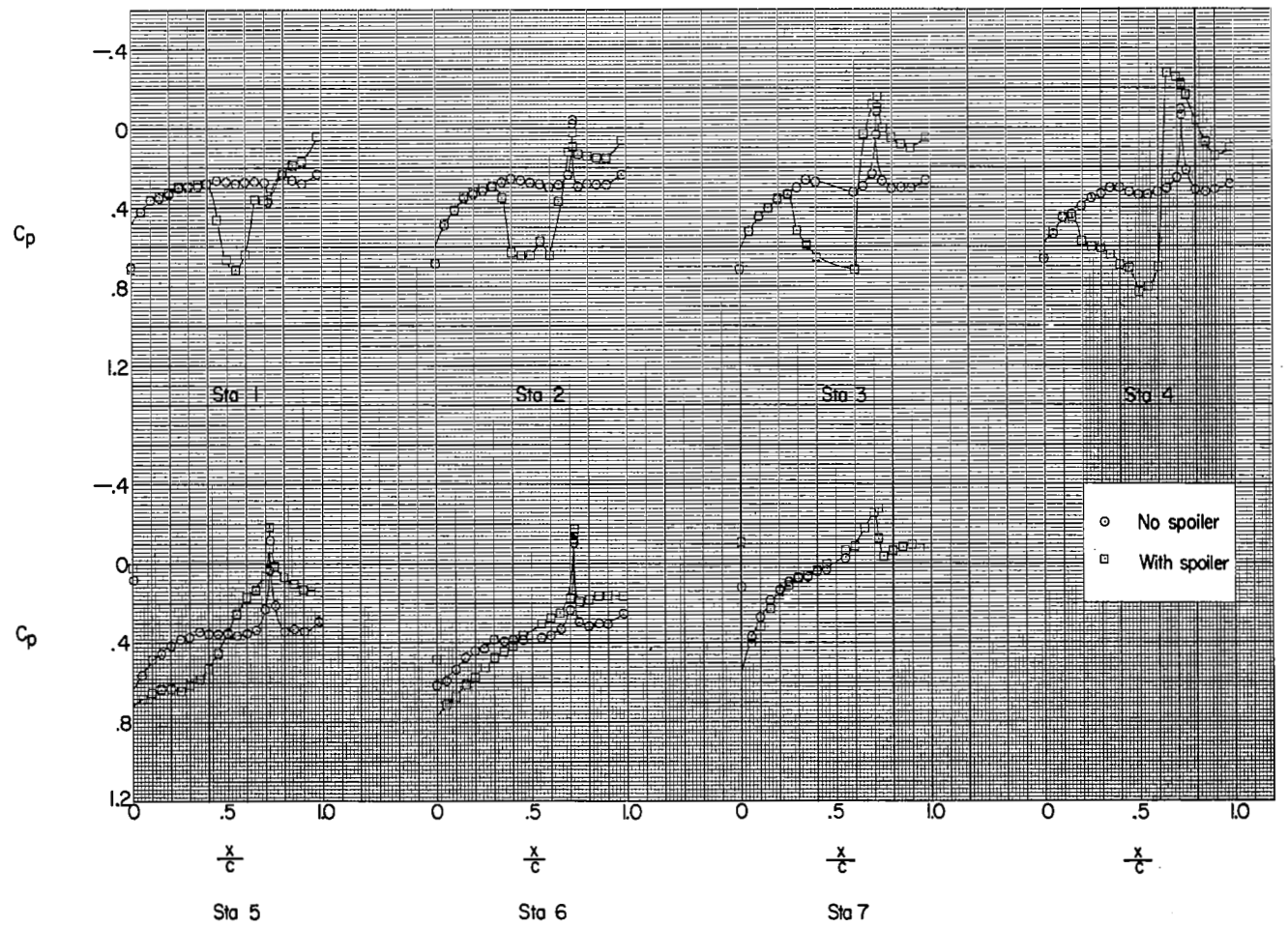

(a) $\alpha = -12^{o}$.

Figure 5.- Pressure distributions for half-span step spoiler (configuration 24). M = 1.61; $R = 3.6 \times 10^{6}$.

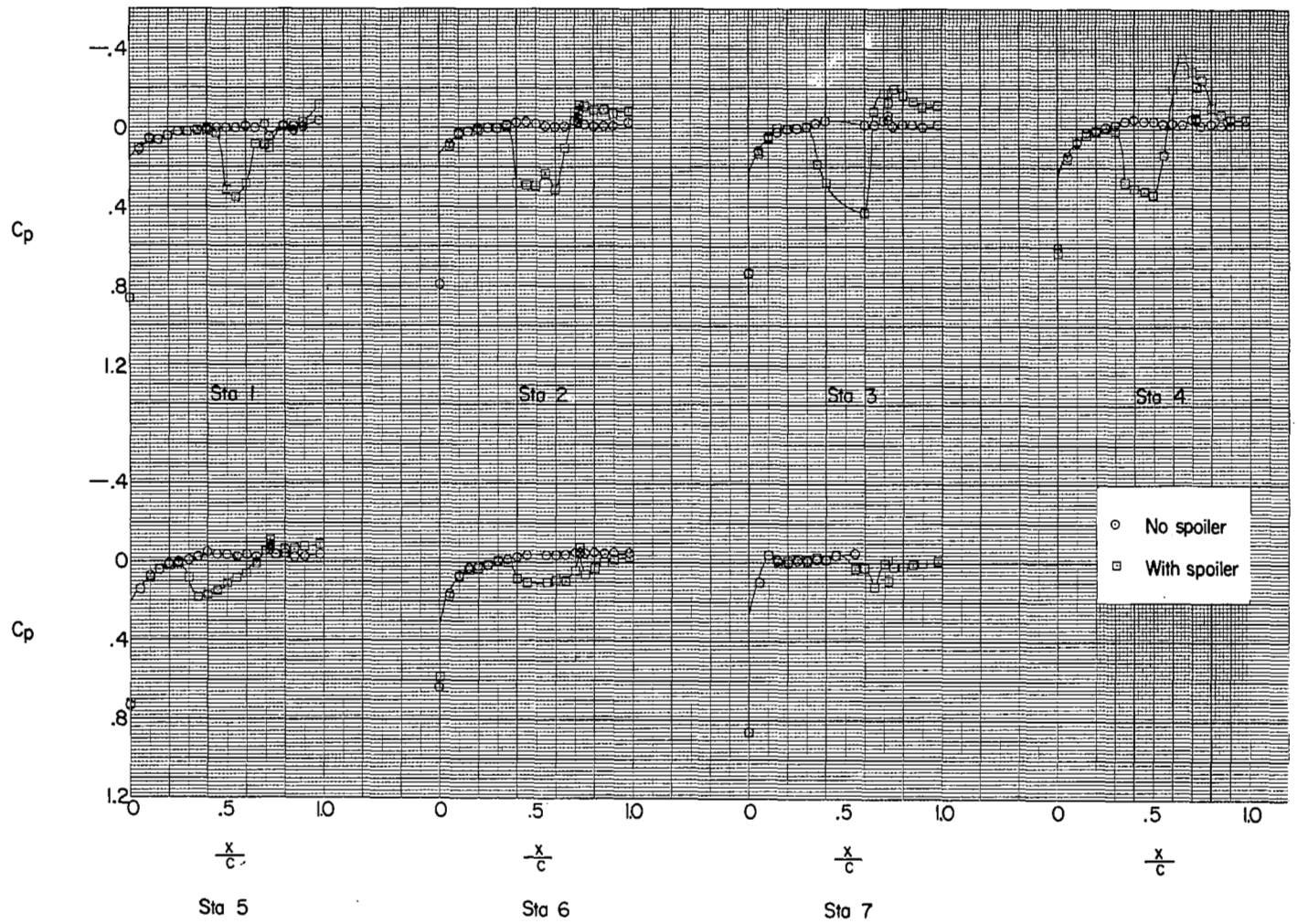

(b) $\alpha = 0^{\circ}$.

Figure 5.- Continued.

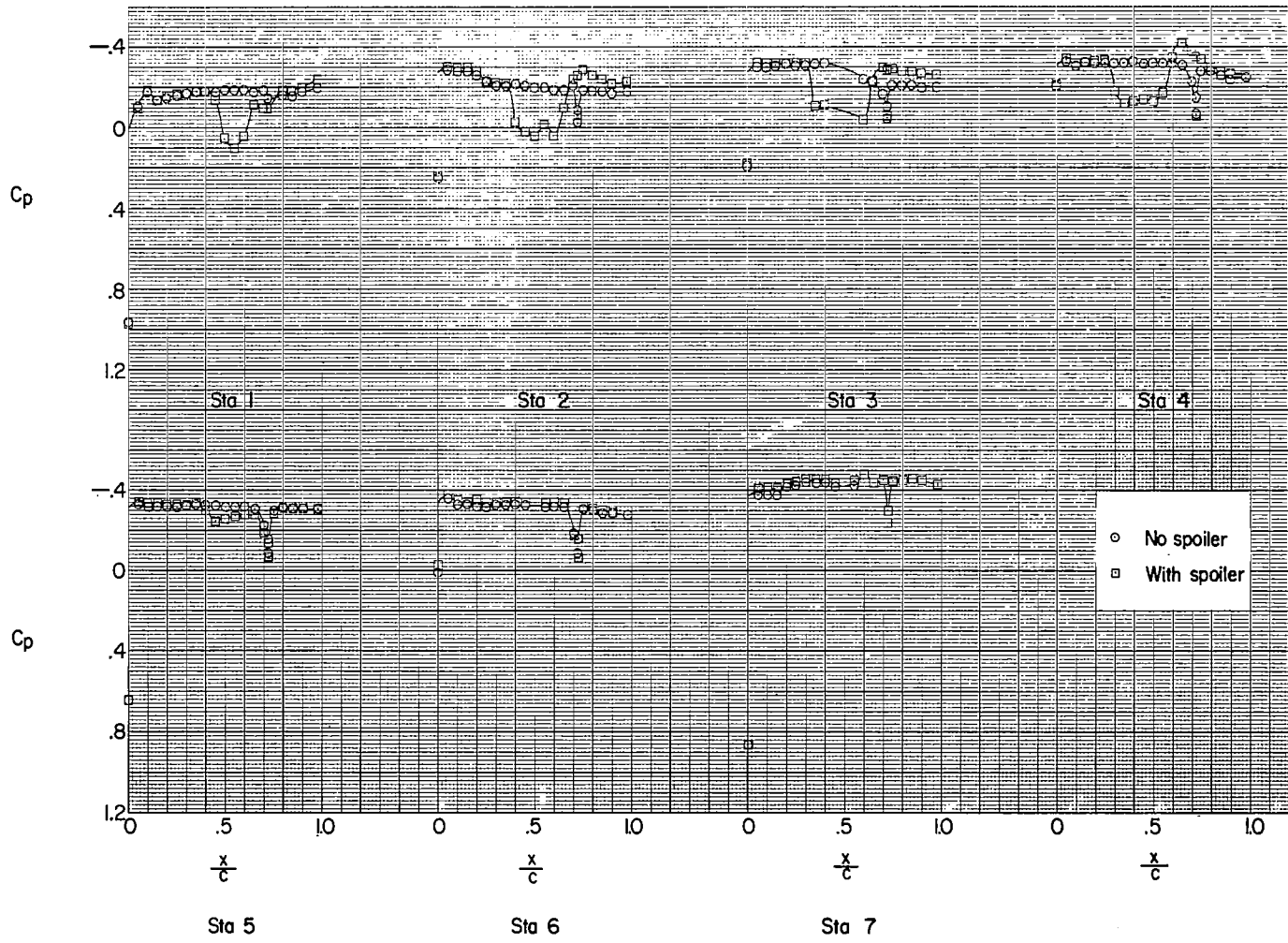

(c) $\alpha = 12^{\circ}$.

Figure 5.- Concluded.

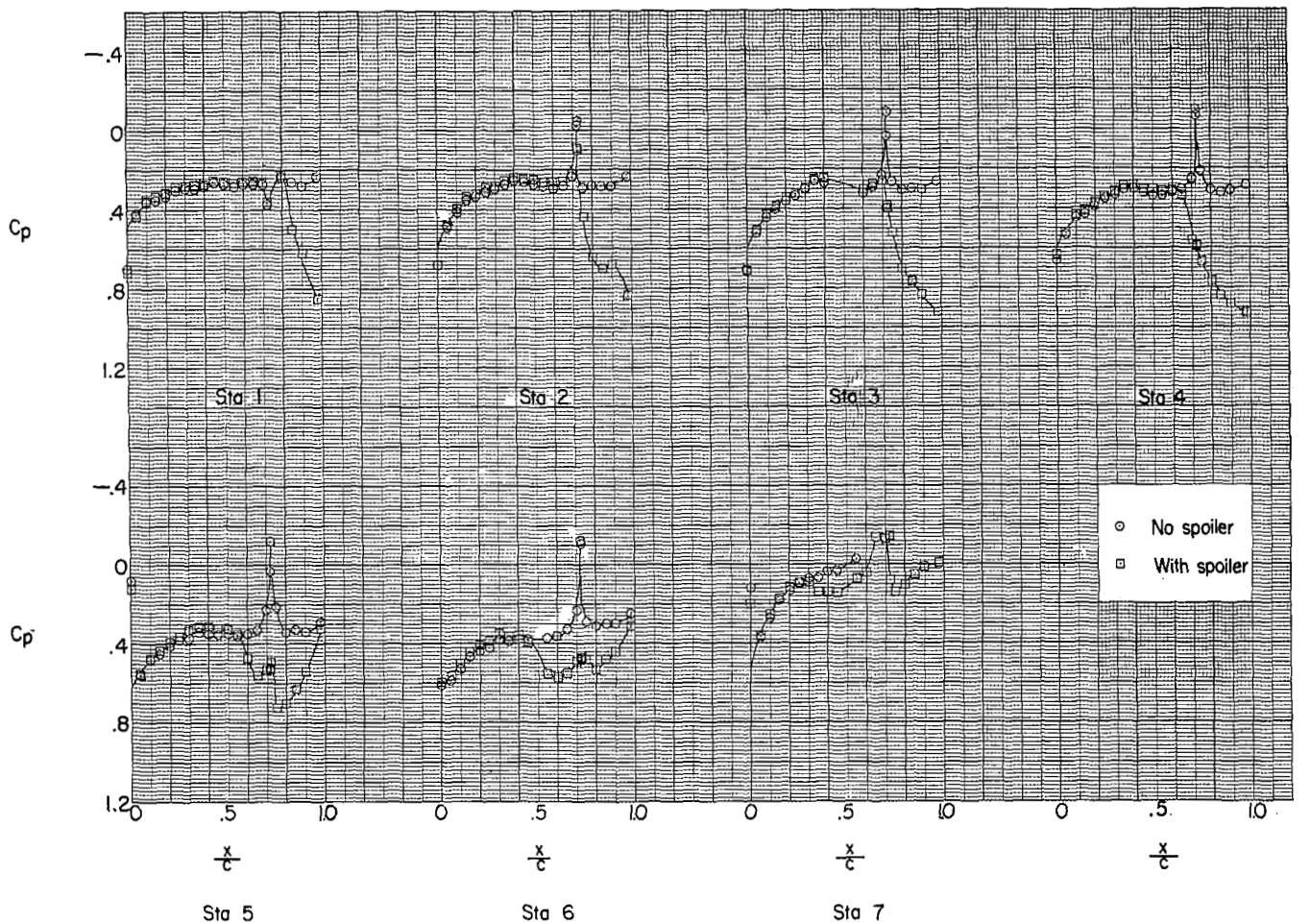

(a) $\alpha = -12^{\circ}$.

Figure 6.- Pressure distributions for half-span trailing-edge spoiler (configuration 25). $M = 1.61$; $R = 3.6 \times 10^6$.

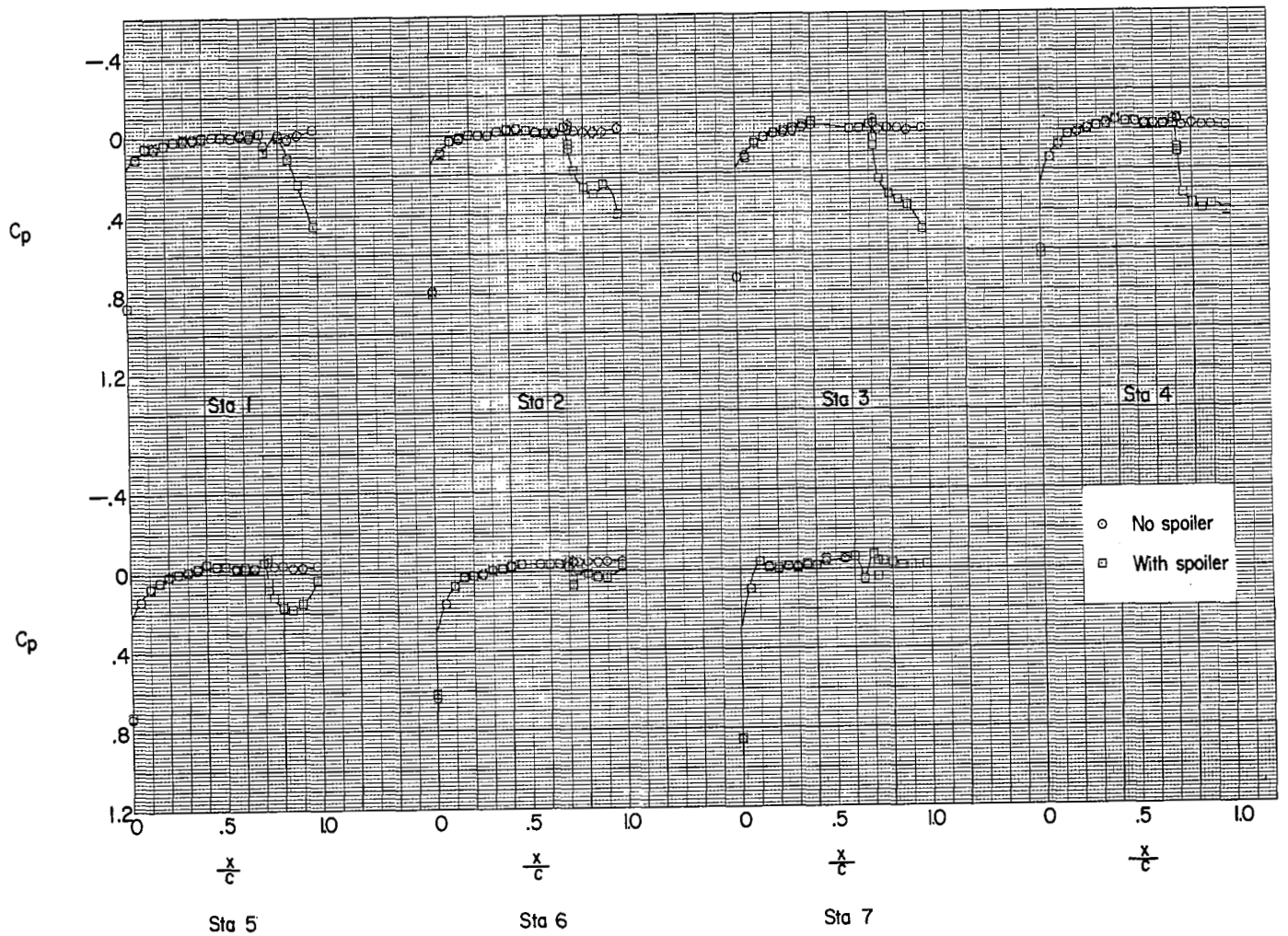

(b) $\alpha = 0^{\circ}$.

Figure 6.- Continued.

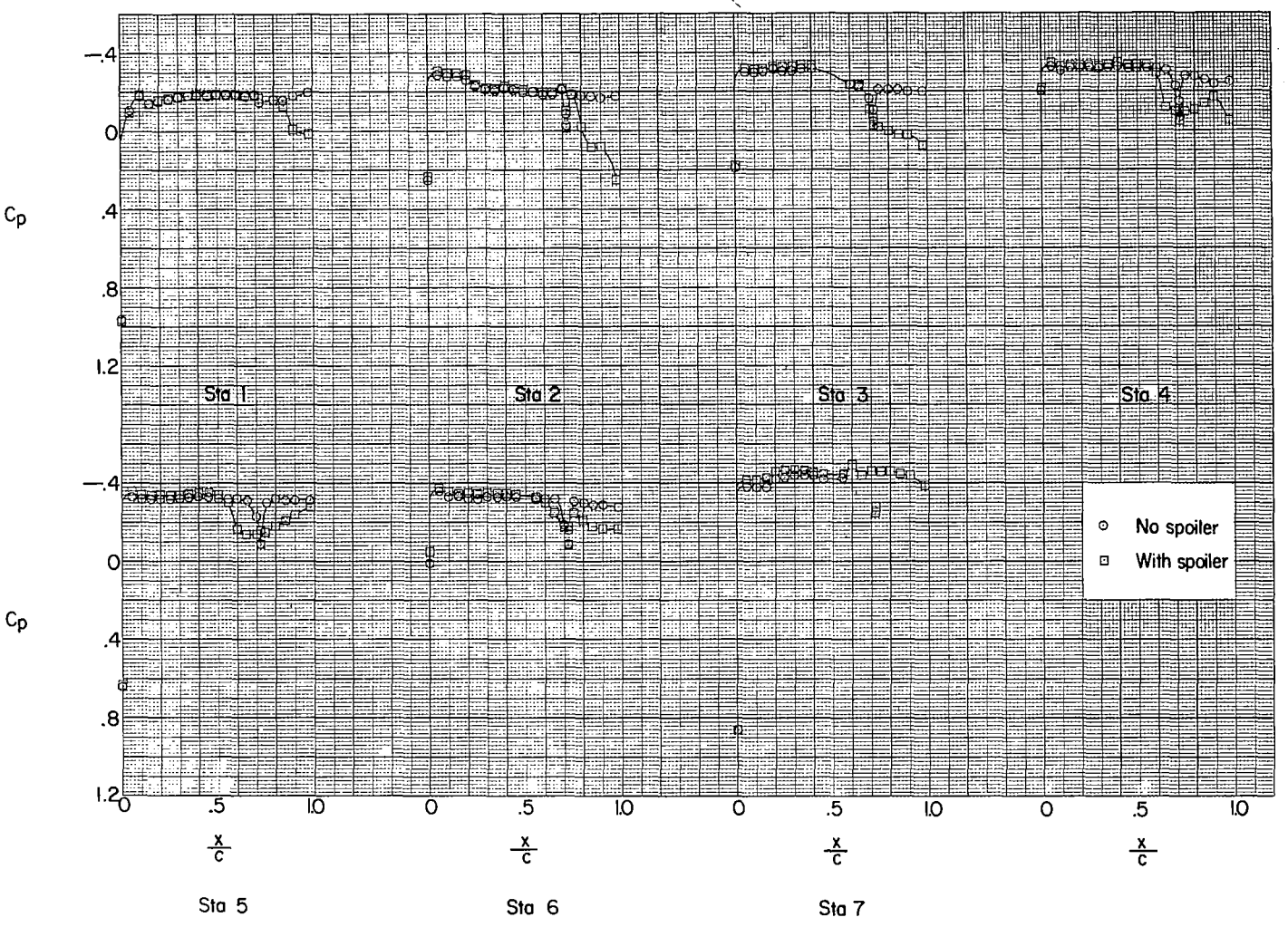

(c) $\alpha = 12^{o}$.

Figure 6.- Concluded.

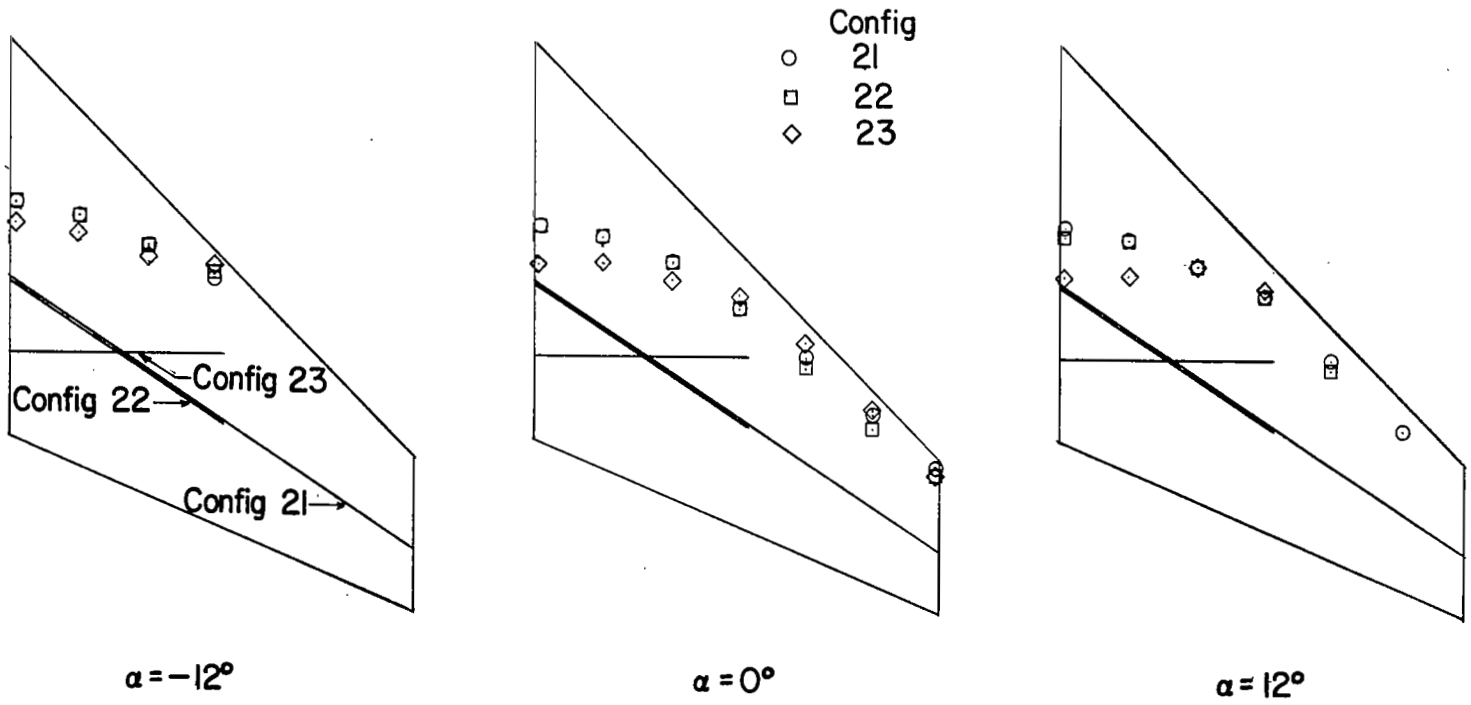

Figure 7.- Effect of spoiler span and spoiler sweep on flow-separation point.

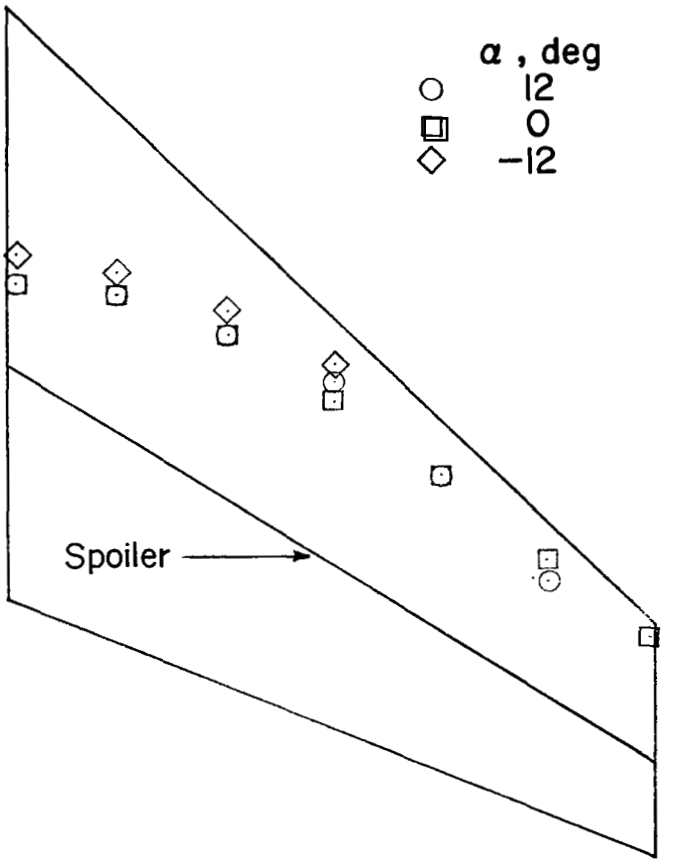

Figure 8.- Effect of angle of attack on flow-separation point for full-span swept spoiler (configuration 21).

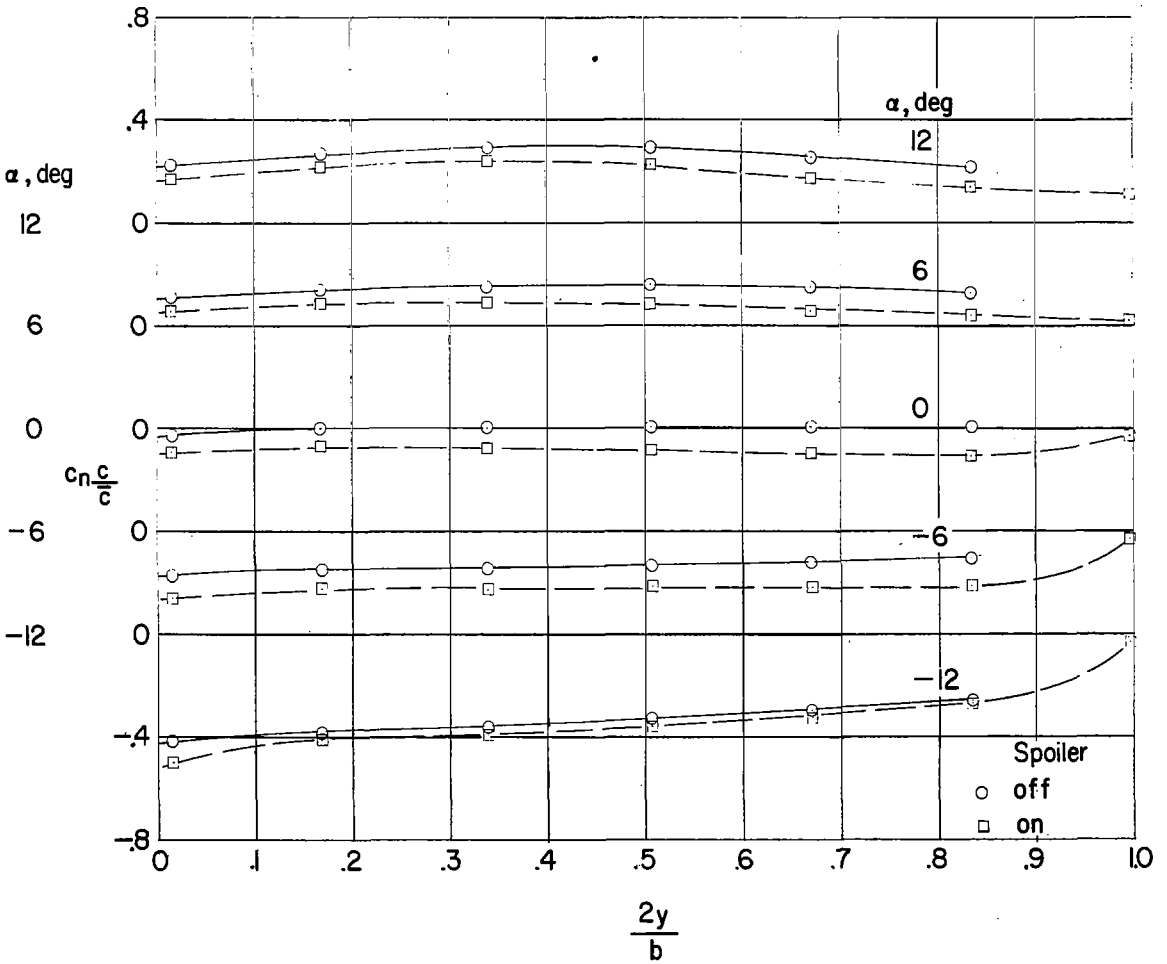

(a) Configuration 21, full-span swept spoiler.

Figure 9.- Spanwise variations of section normal-force coefficients for spoiler configurations tested.

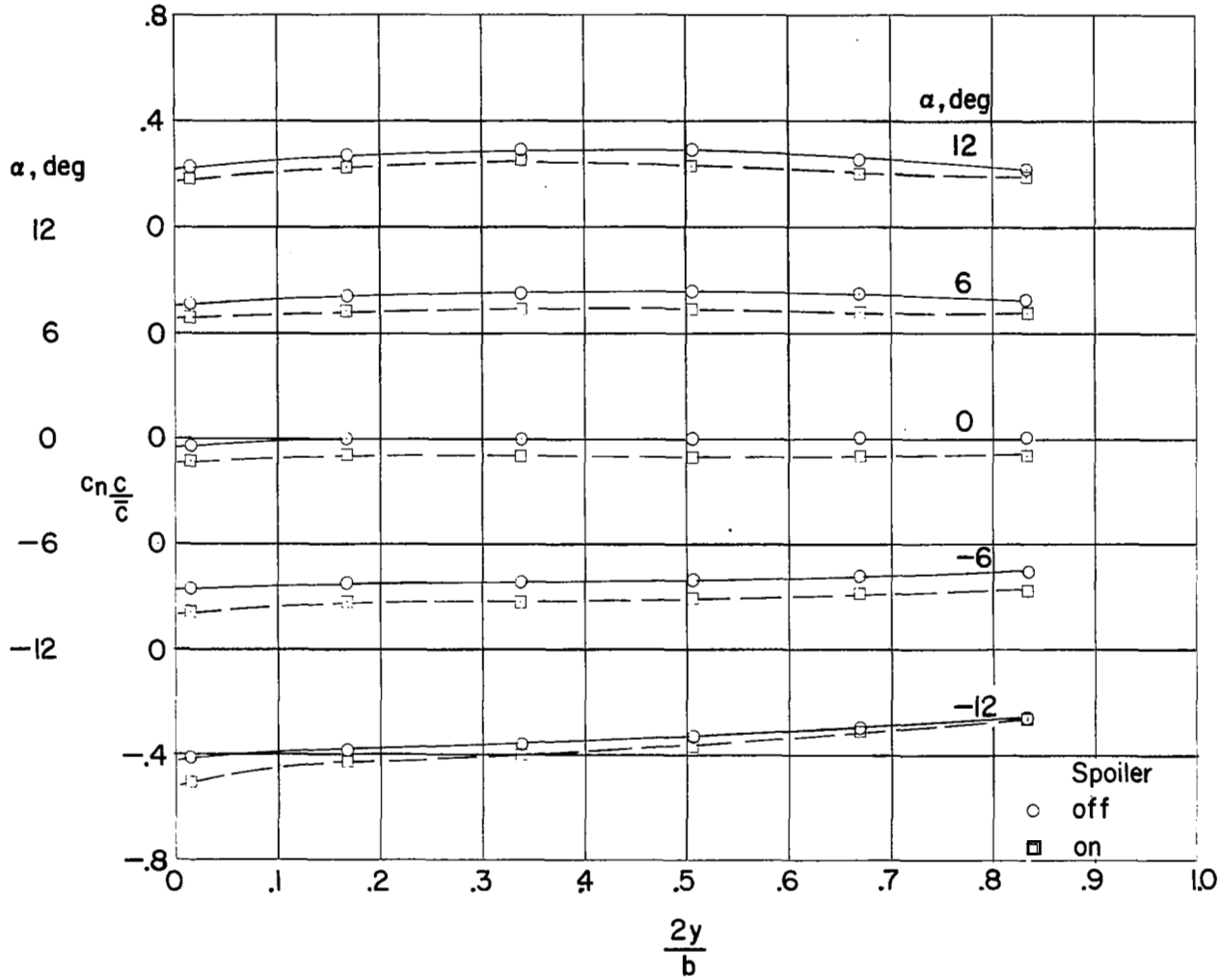

(b) Configuration 22, half-span swept spoiler.

Figure 9.- Continued.

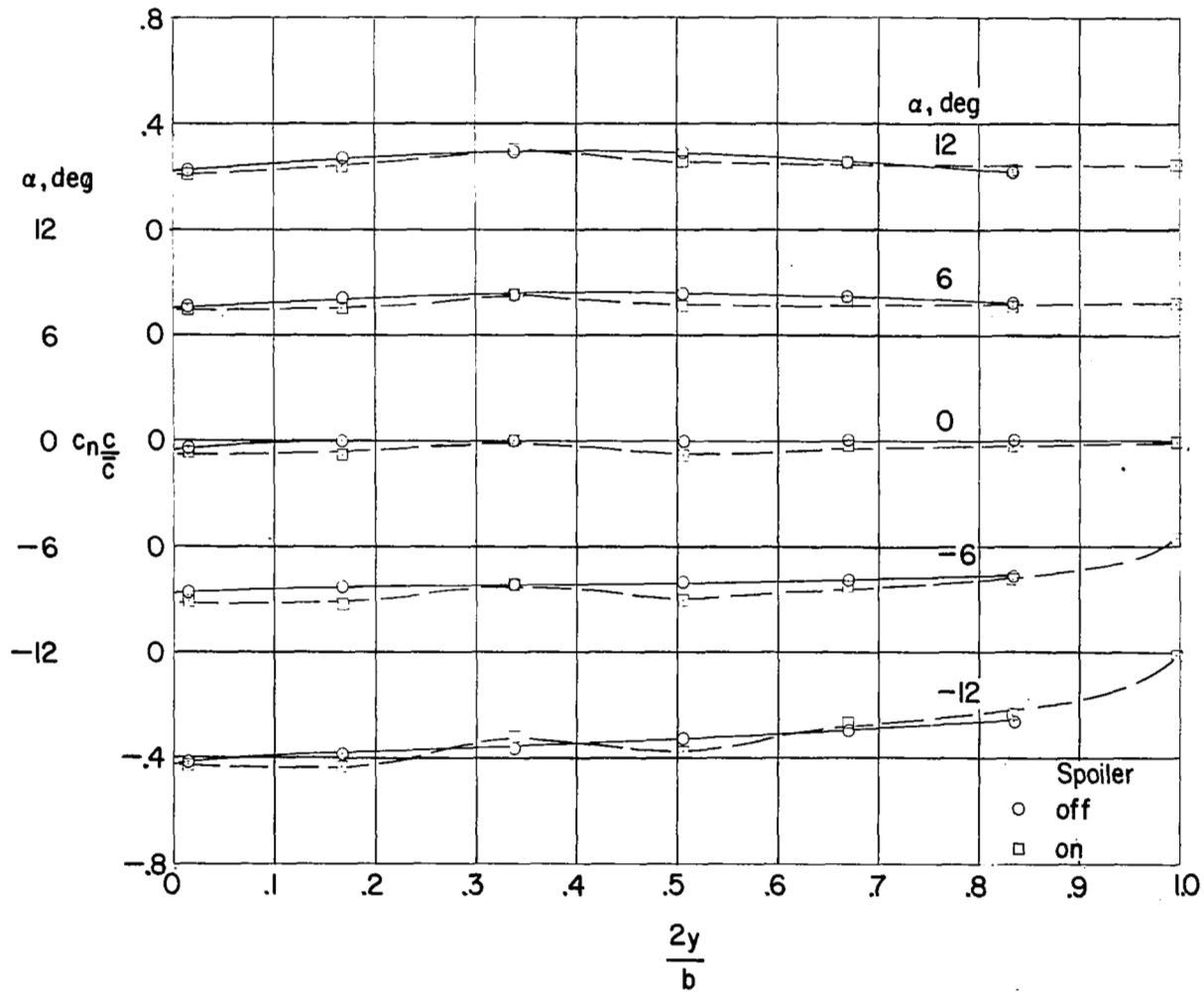

(c) Configuration 23, half-span unswept spoiler.

Figure 9.- Continued.

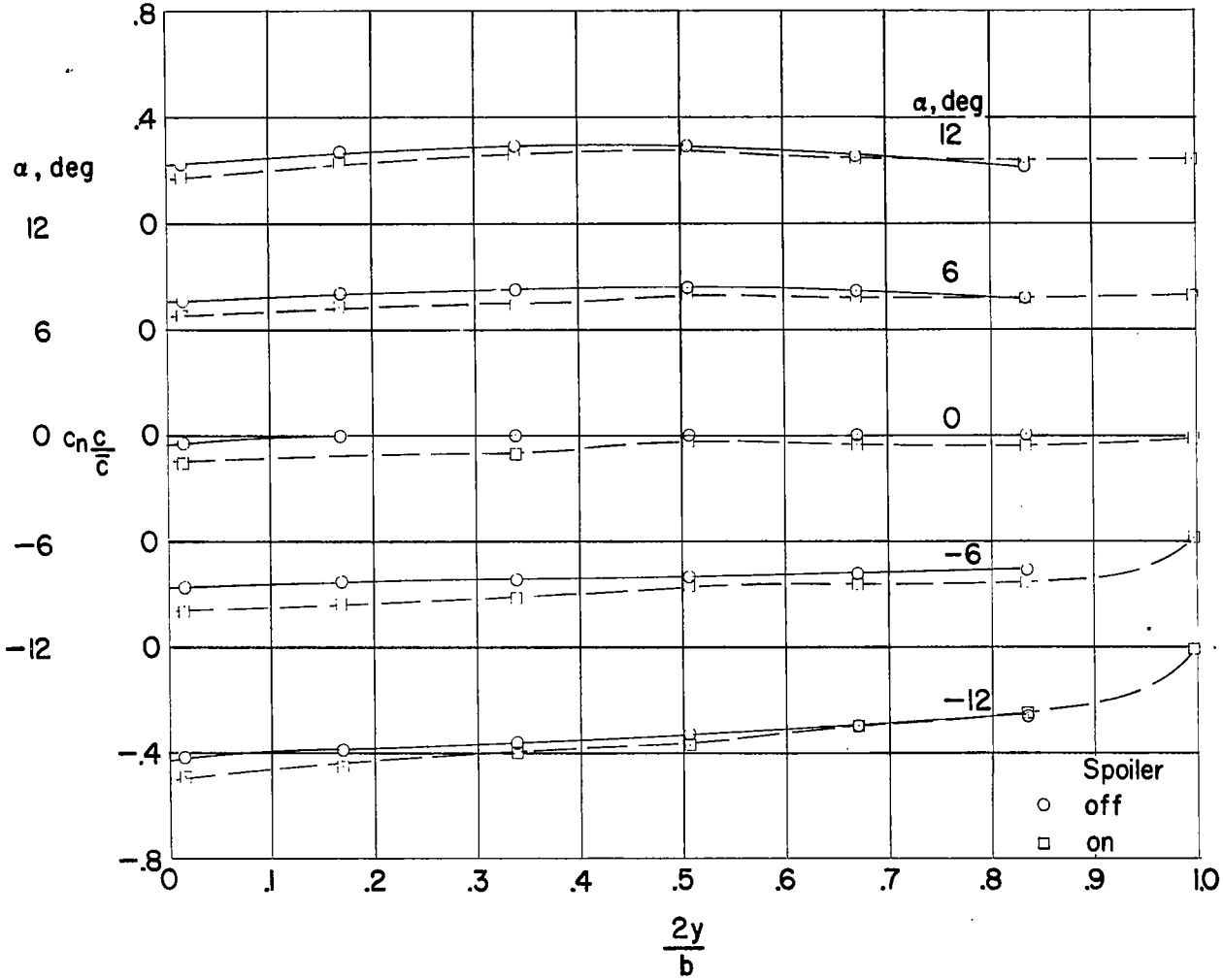

(d) Configuration 24, half-span stepped spoiler.

Figure 9.- Continued.

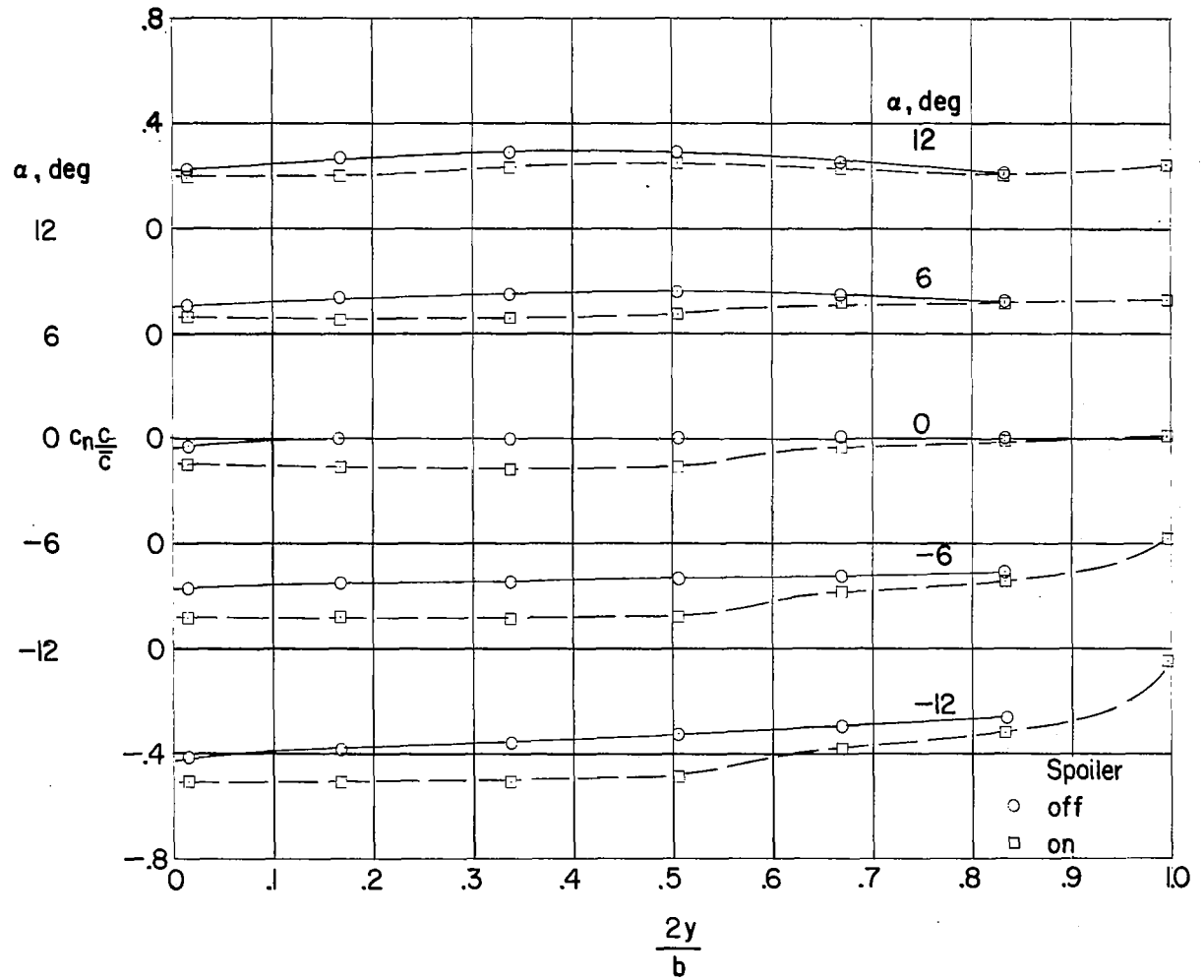

(e) Configuration 25, half-span trailing-edge spoiler.

Figure 9.- Concluded.

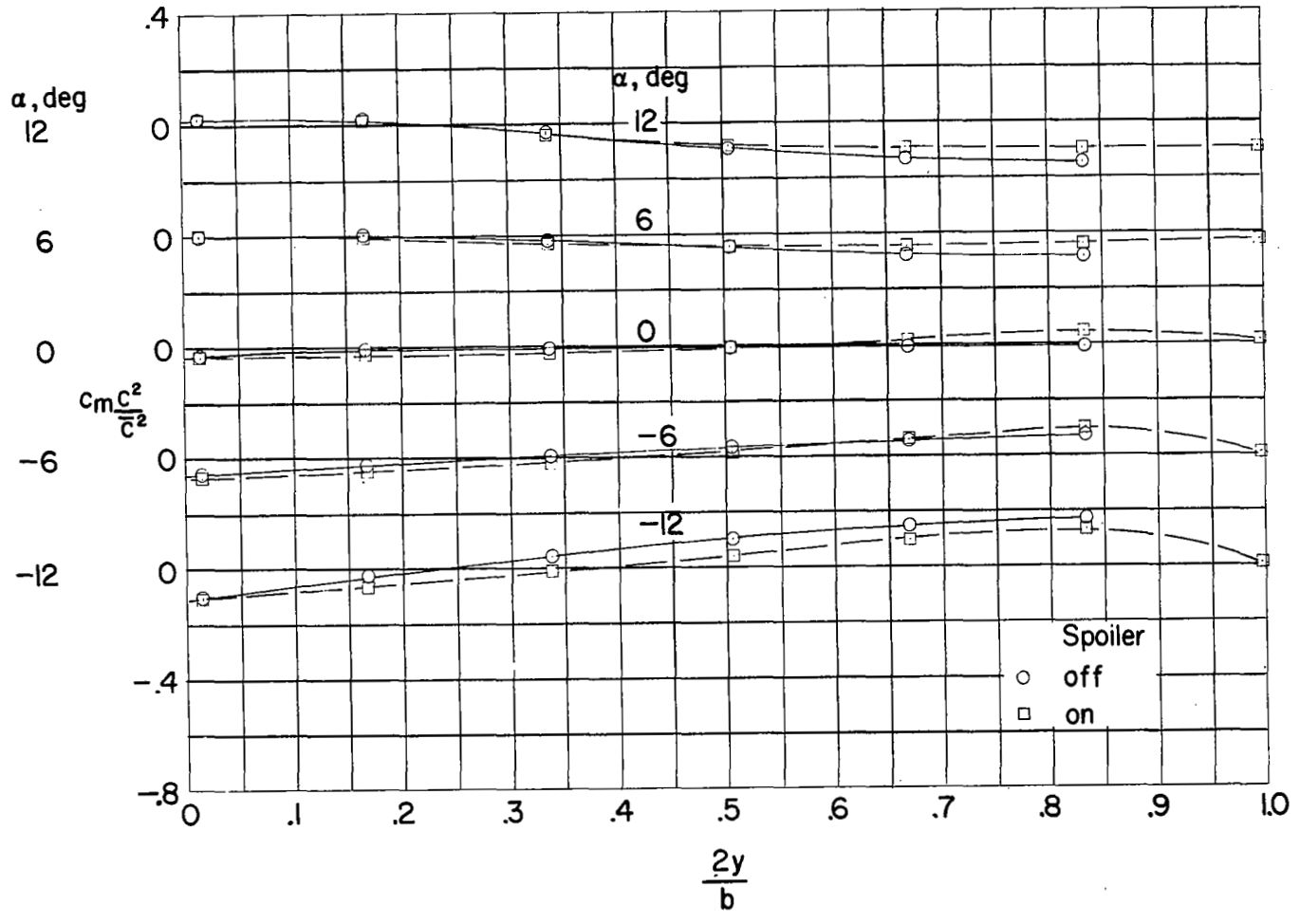

(a) Configuration 21, full-span swept spoiler.

Figure 10.- Spanwise variations of section pitching-moment coefficients for spoiler configurations tested.

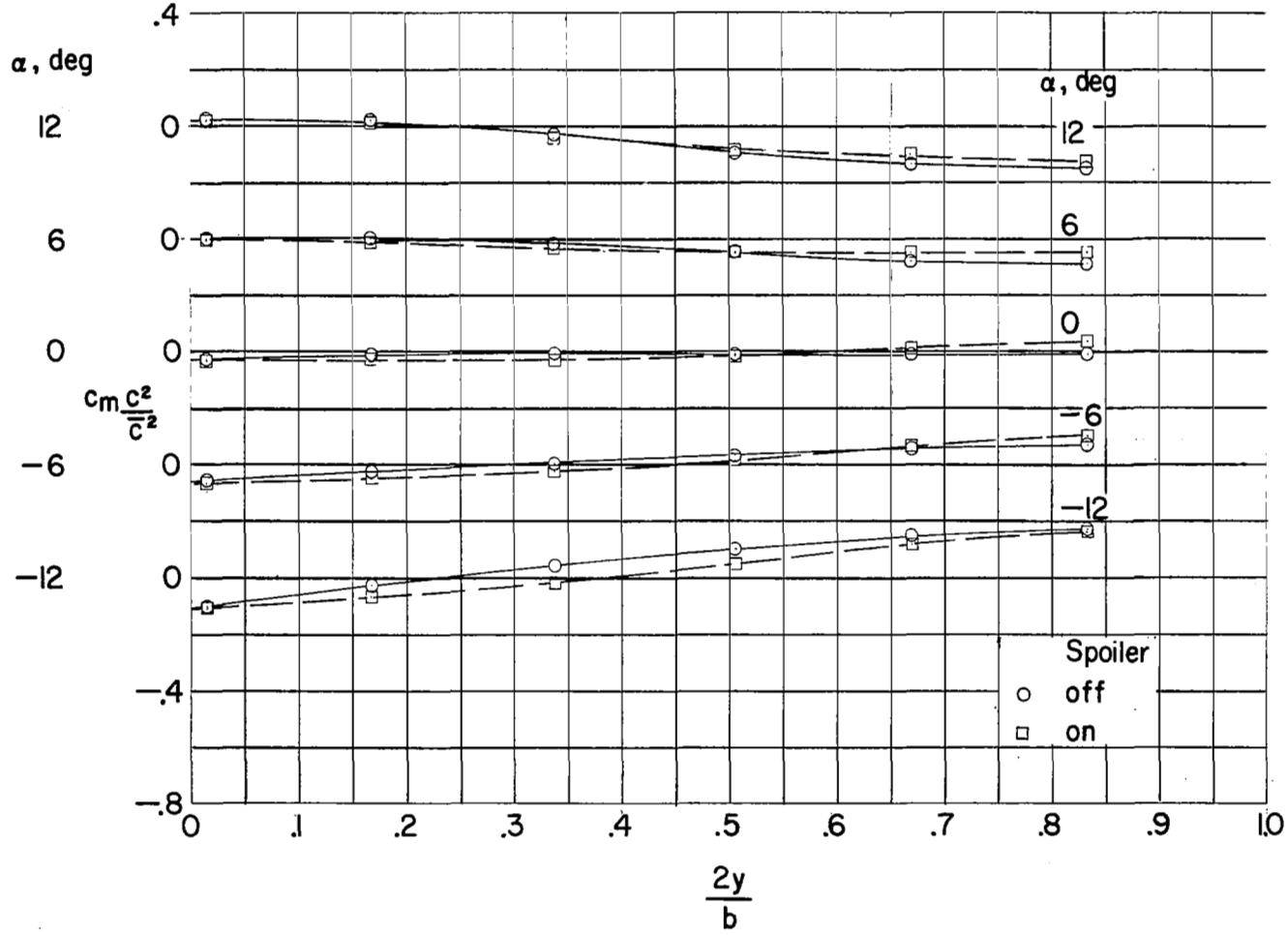

(b) Configuration 22, half-span swept spoiler.

Figure 10.- Continued.

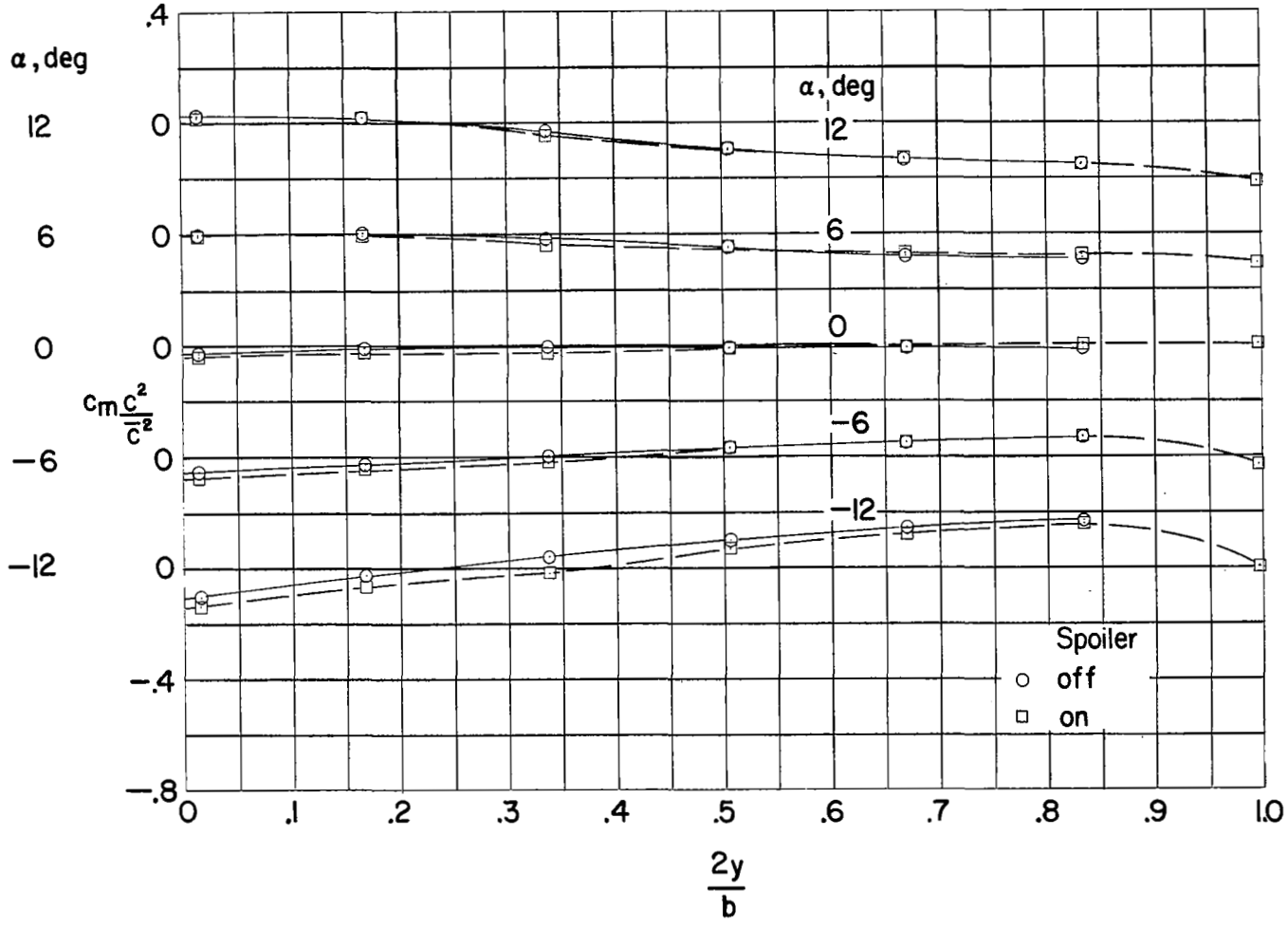

(c) Configuration 23, half-span unswept spoiler.

Figure 10.- Continued.

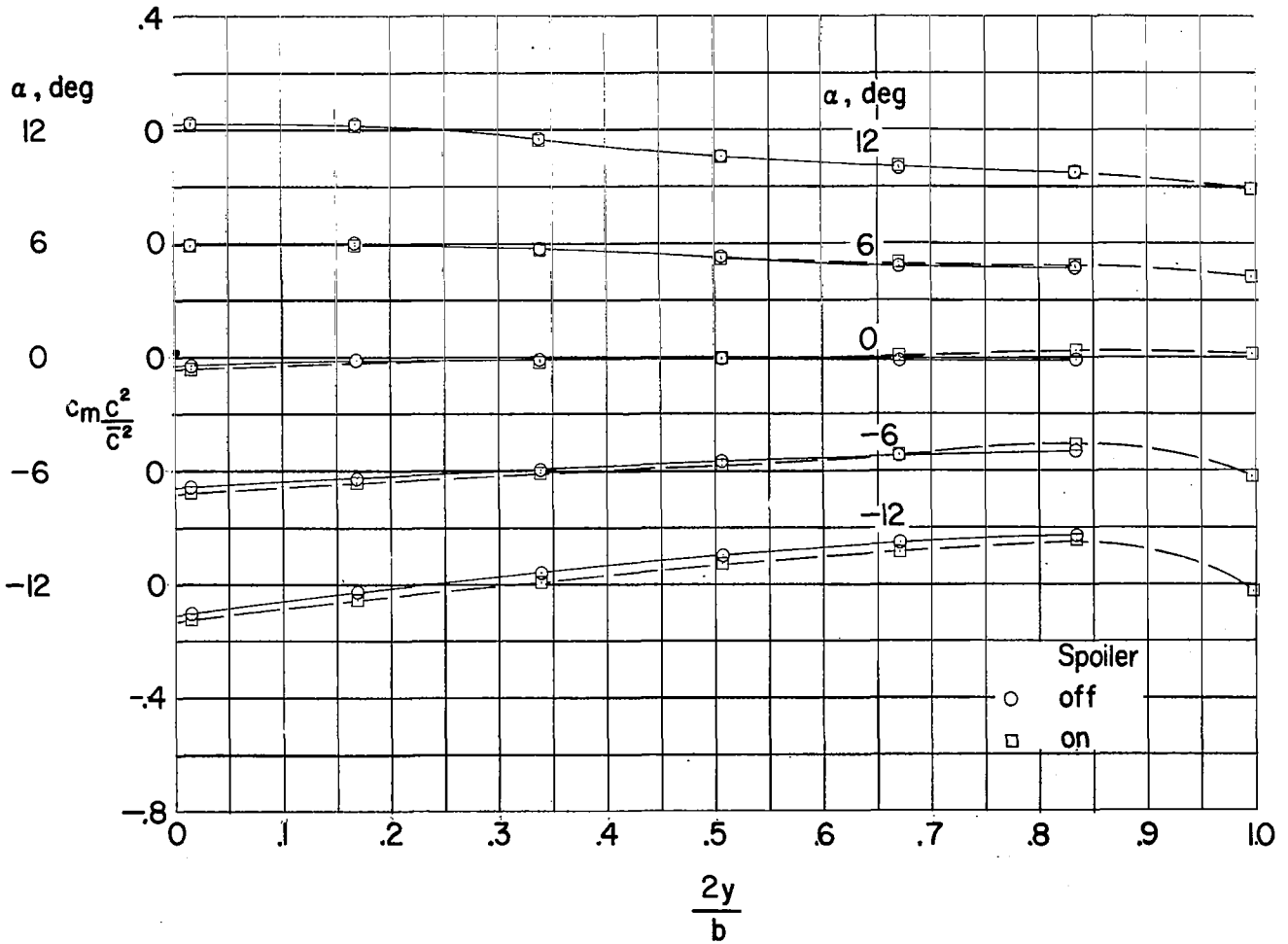

(d) Configuration 24, half-span stepped spoiler.

Figure 10.- Continued.

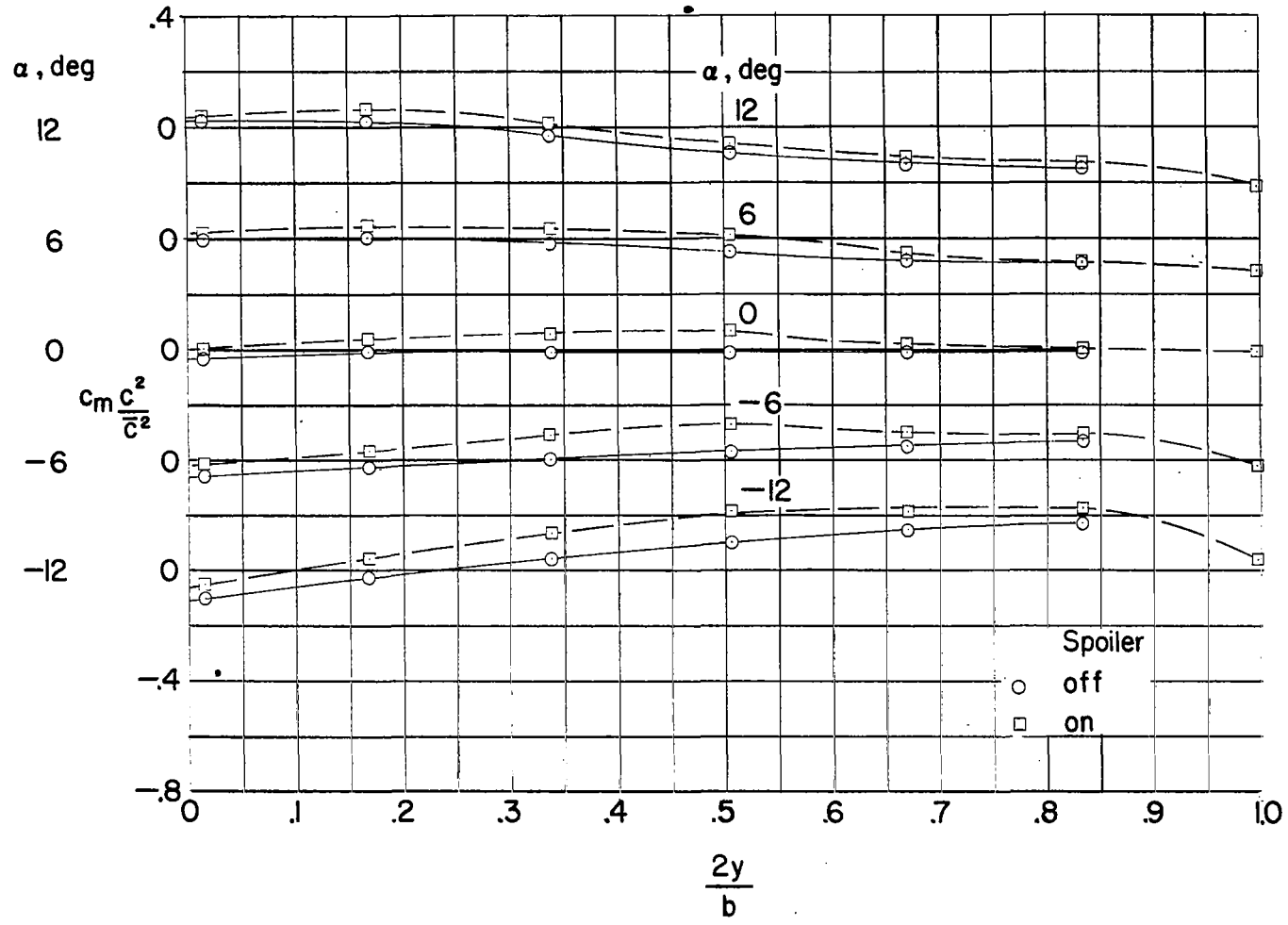

(e) Configuration 25, half-span trailing-edge spoiler.

Figure 10.- Concluded.

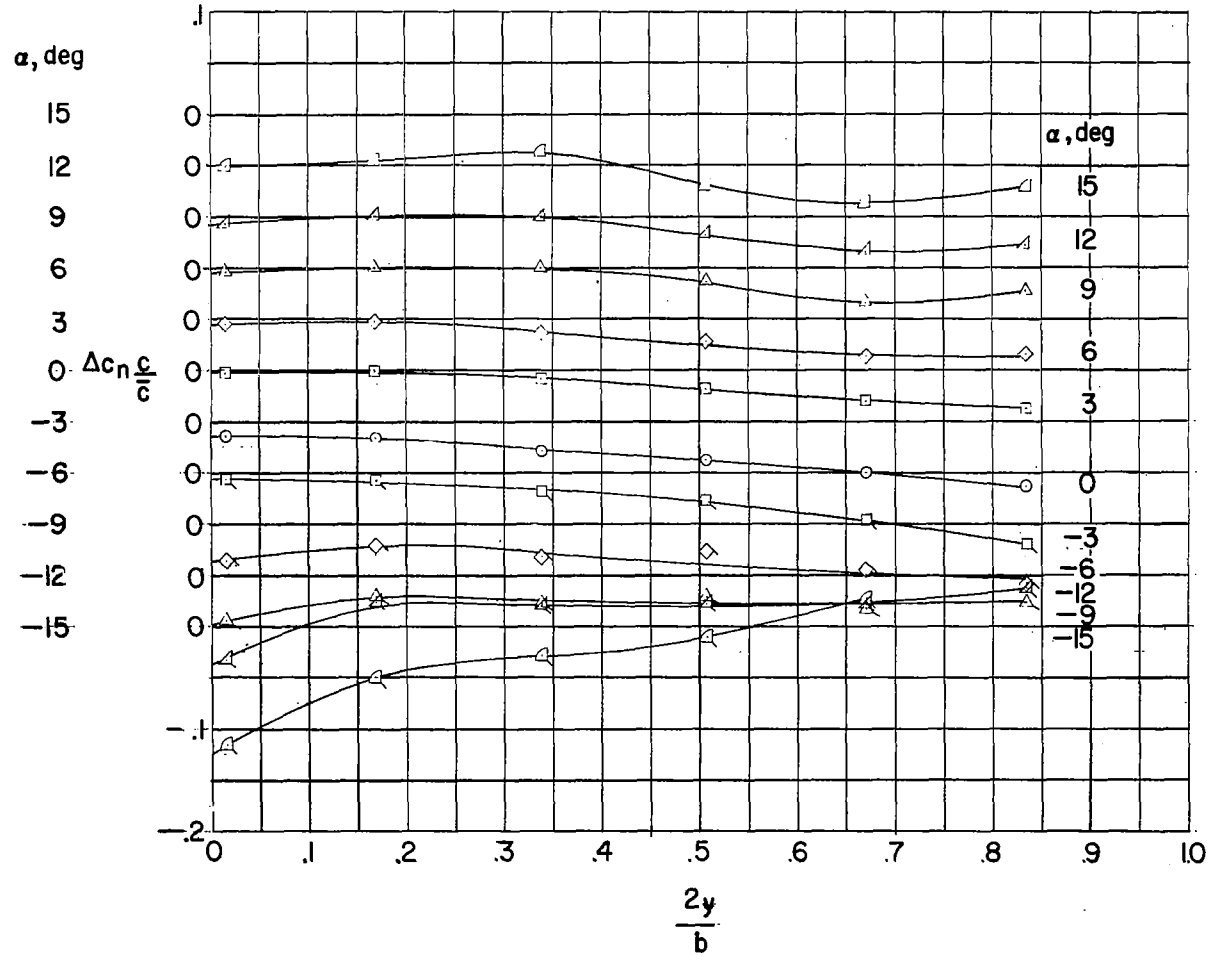

(a) Configuration 21, full-span swept spoiler.

Figure 11.- Spanwise variations of incremental section normal-force coefficients for spoiler configurations tested.

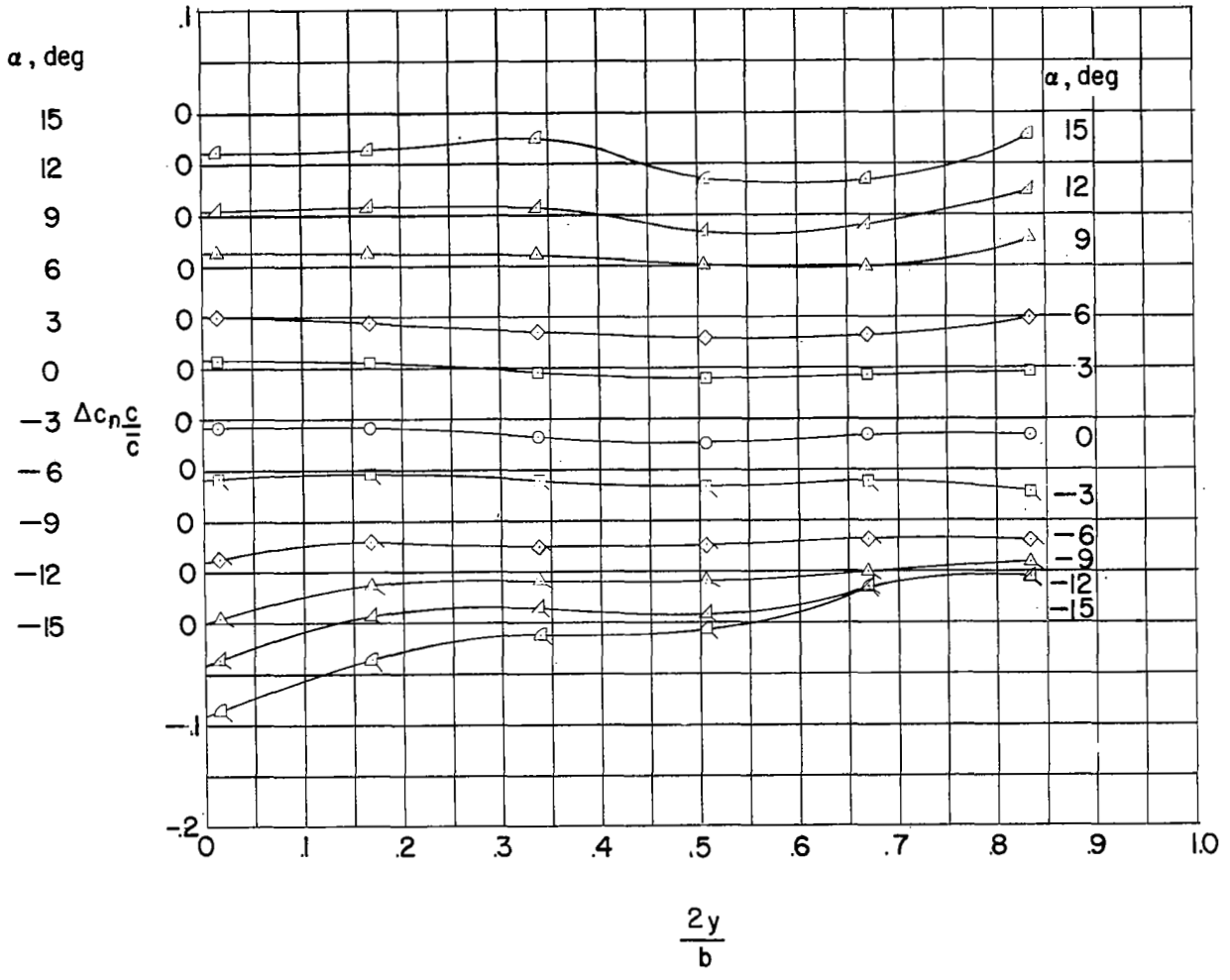

(b) Configuration 22, half-span swept spoiler.

Figure 11.- Continued.

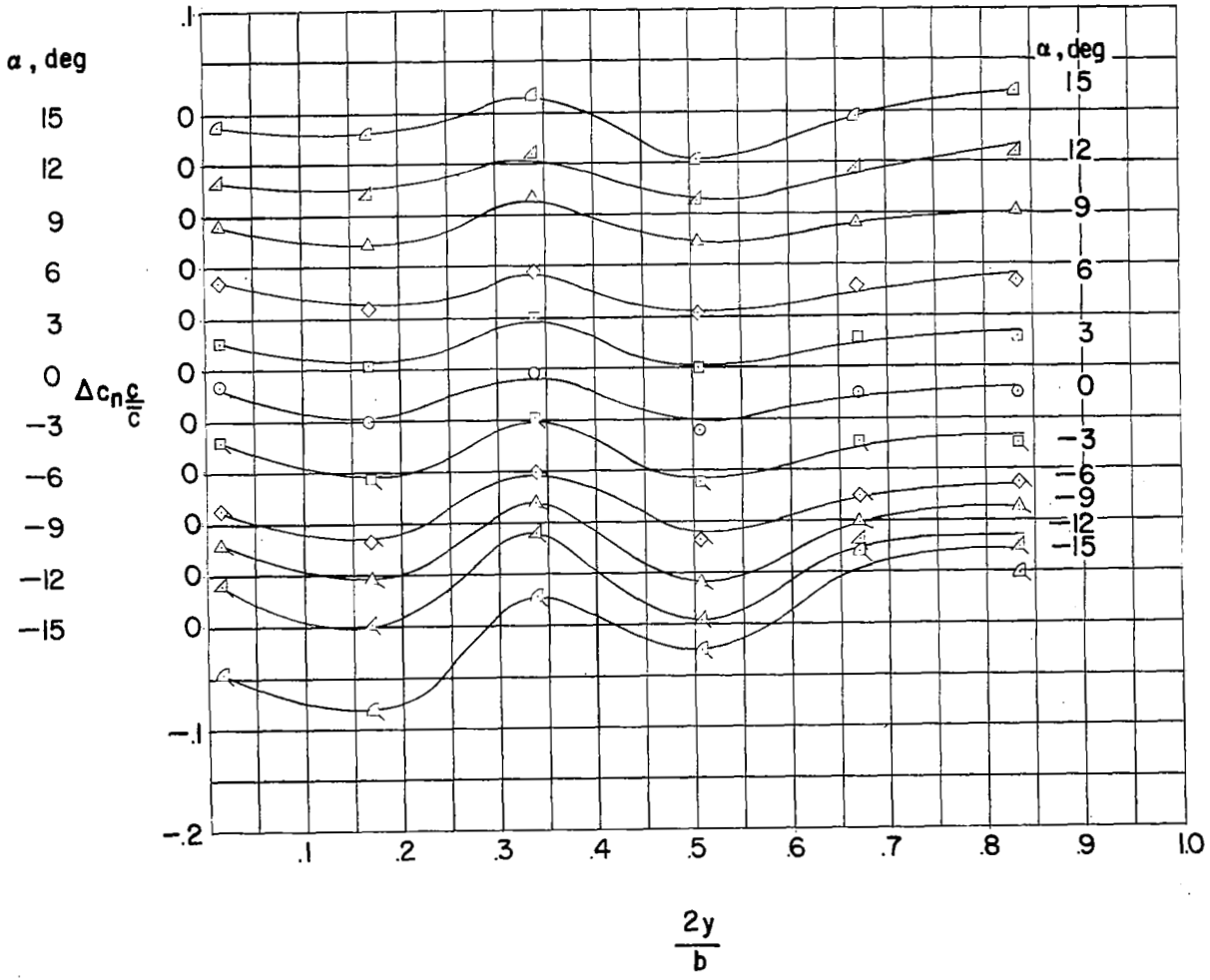

(c) Configuration 23, half-span unswept spoiler.

Figure 11.- Continued.

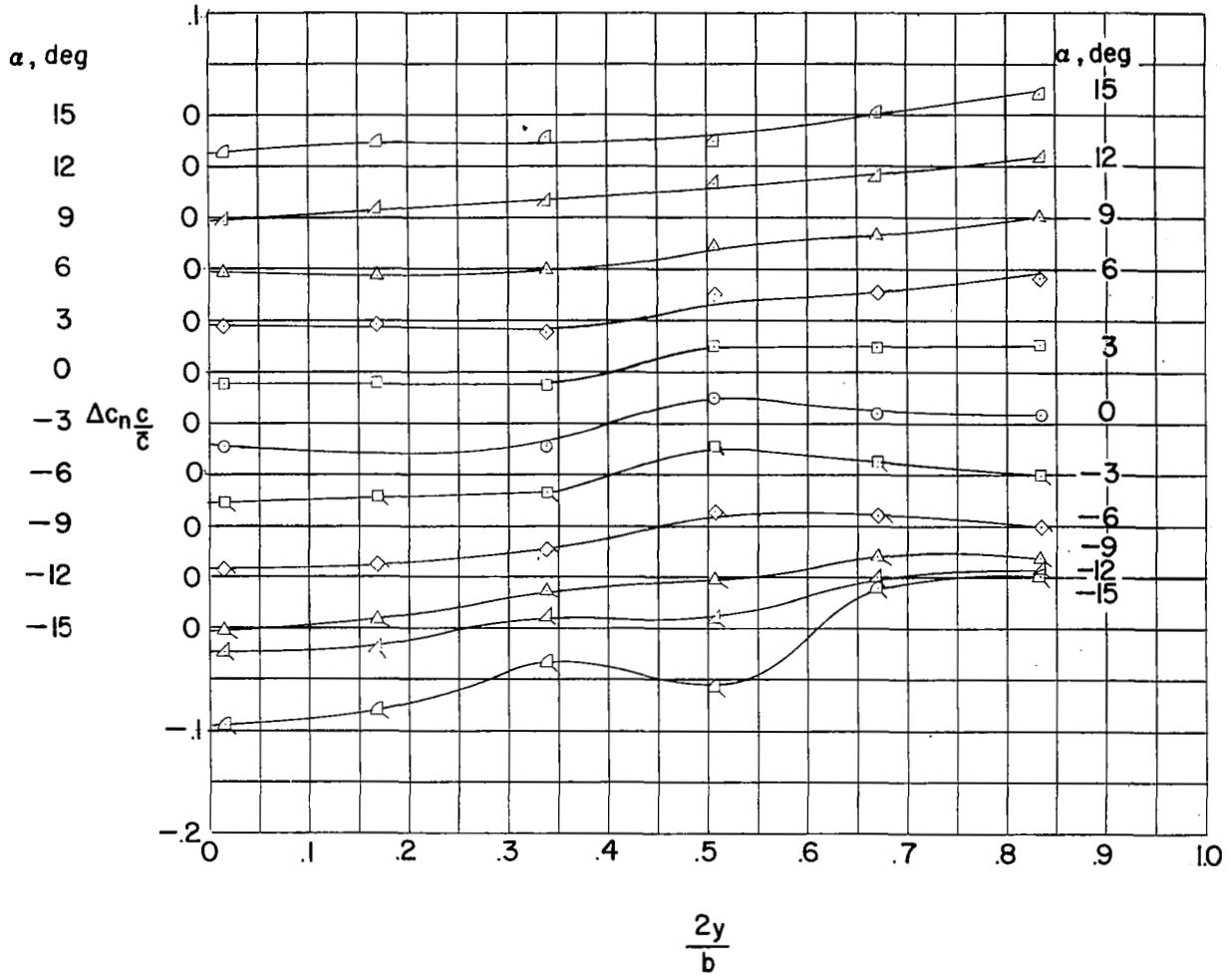

(d) Configuration 24, half-span stepped spoiler.

Figure 11.- Continued.

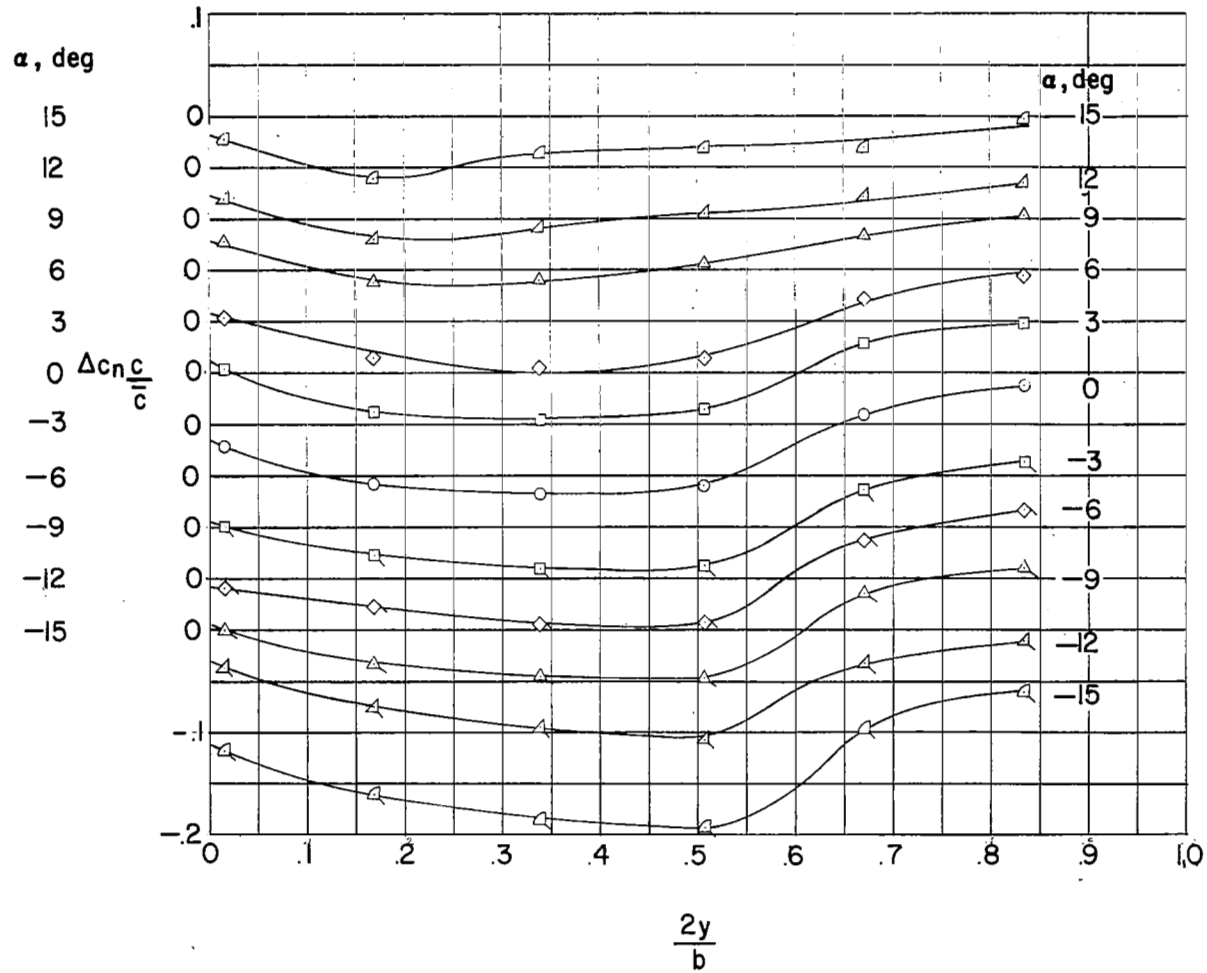

(e) Configuration 25, half-span trailing-edge spoiler.

Figure 11.- Concluded.

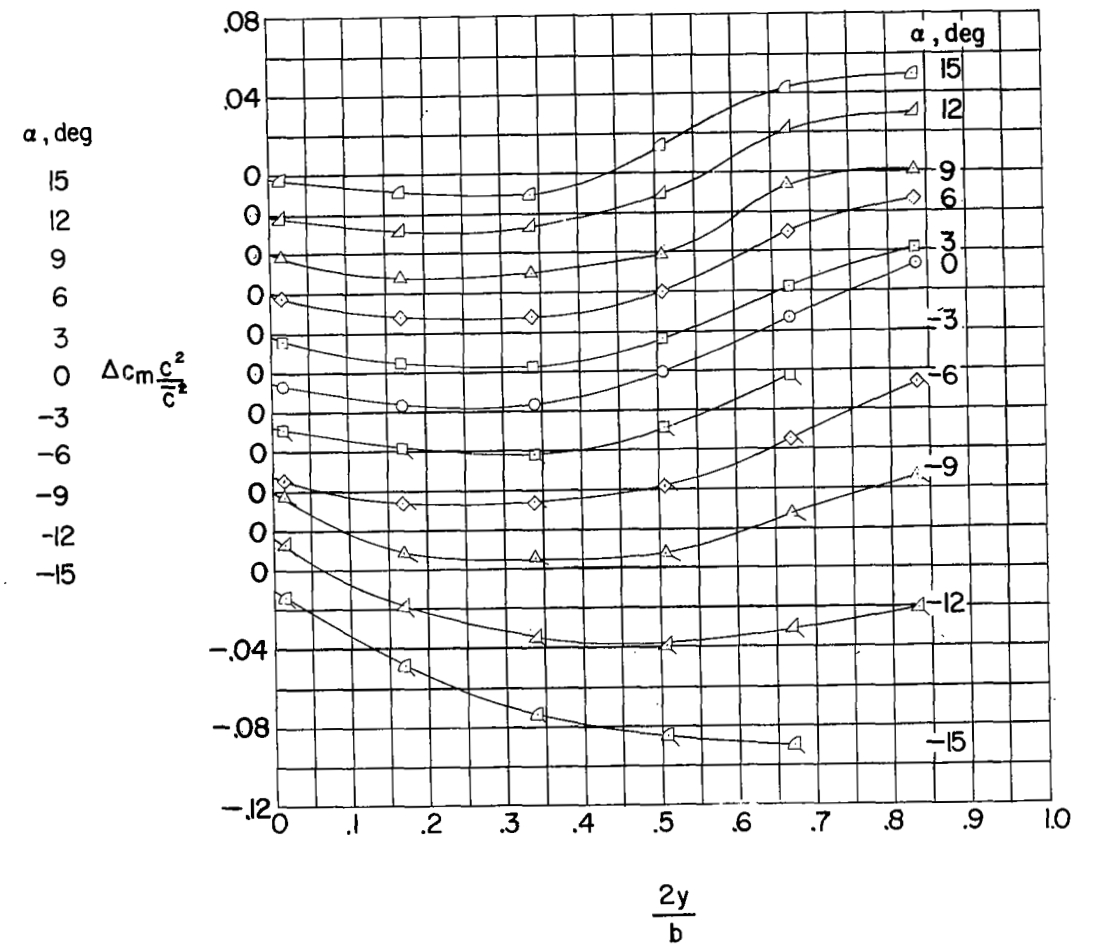

(a) Configuration 21, full-span swept spoiler.

Figure 12.- Spanwise variations of the incremental section pitching-moment coefficients for the spoiler configurations tested.

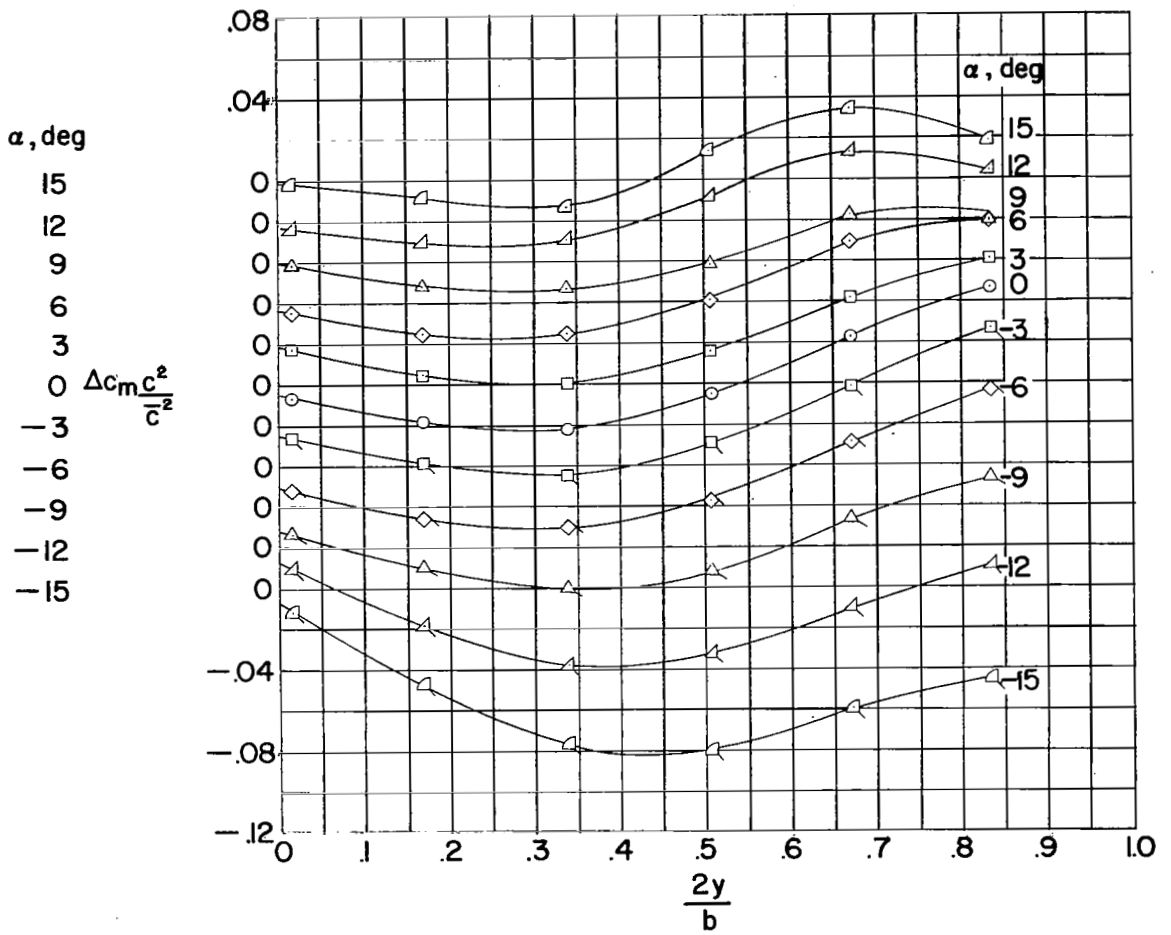

(b) Configuration 22, half-span swept spoiler.

Figure 12.- Continued.

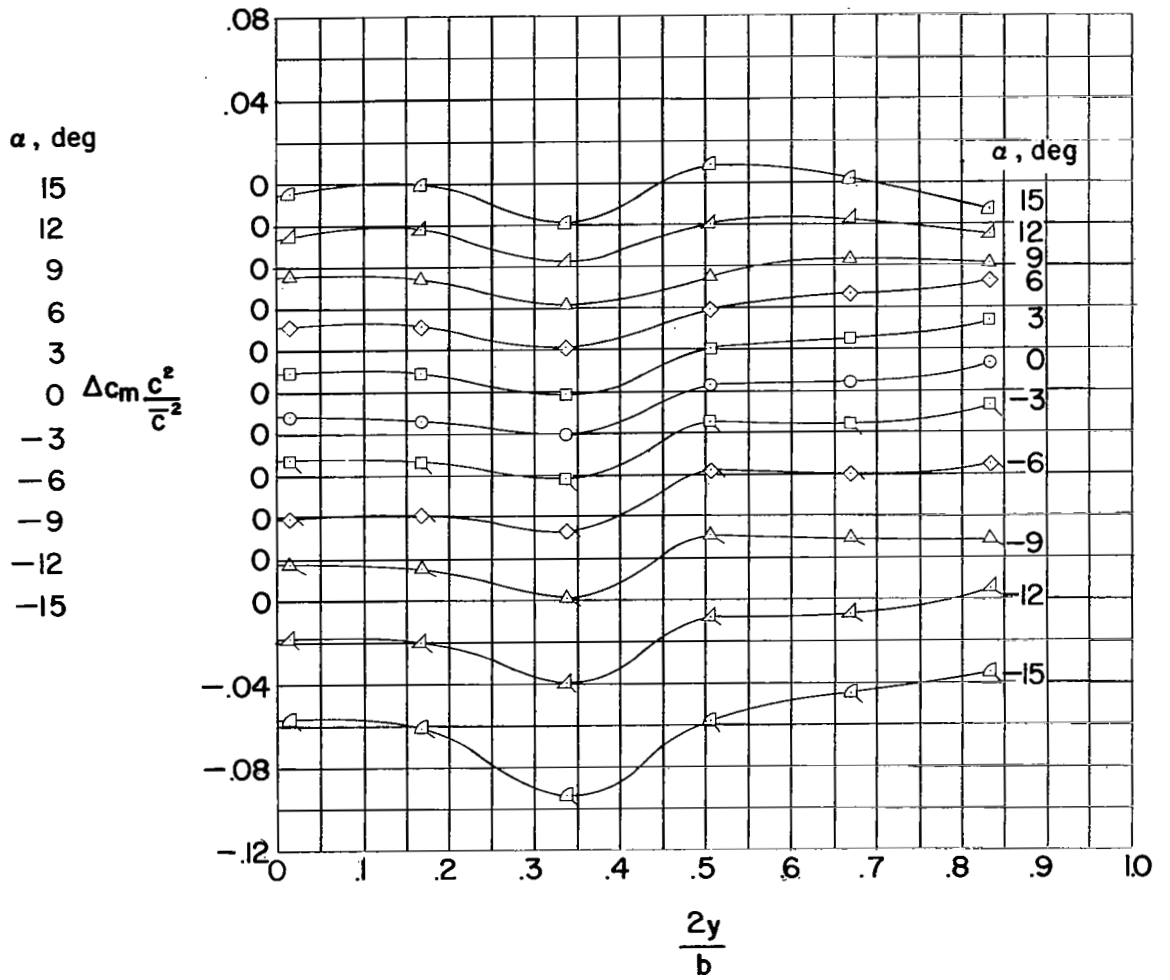

(c) Configuration 23, half-span unswept spoiler.

Figure 12.- Continued.

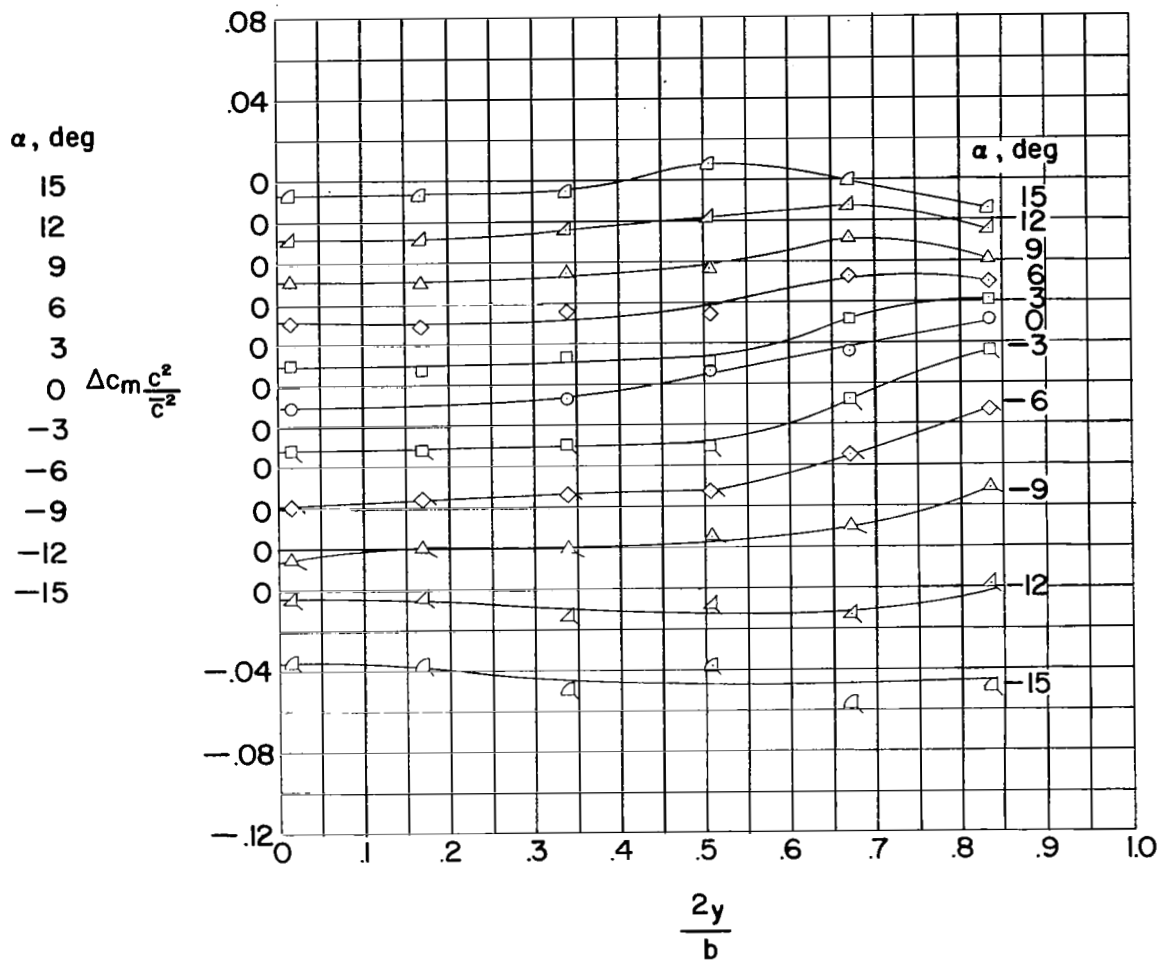

(d) Configuration 24, half-span stepped spoiler.

Figure 12.- Continued.

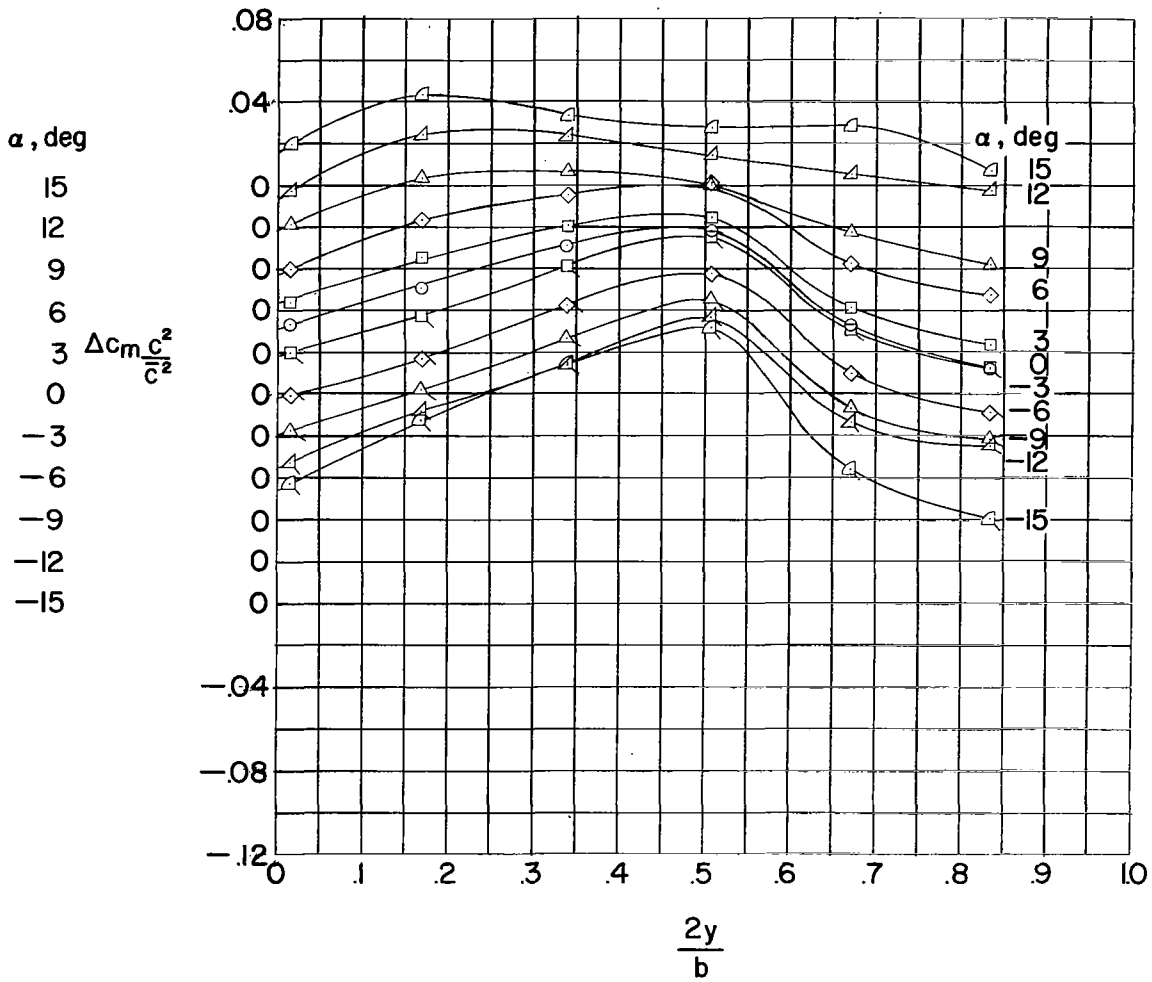

(e) Configuration 25, half-span trailing-edge spoiler.

Figure 12.- Concluded.

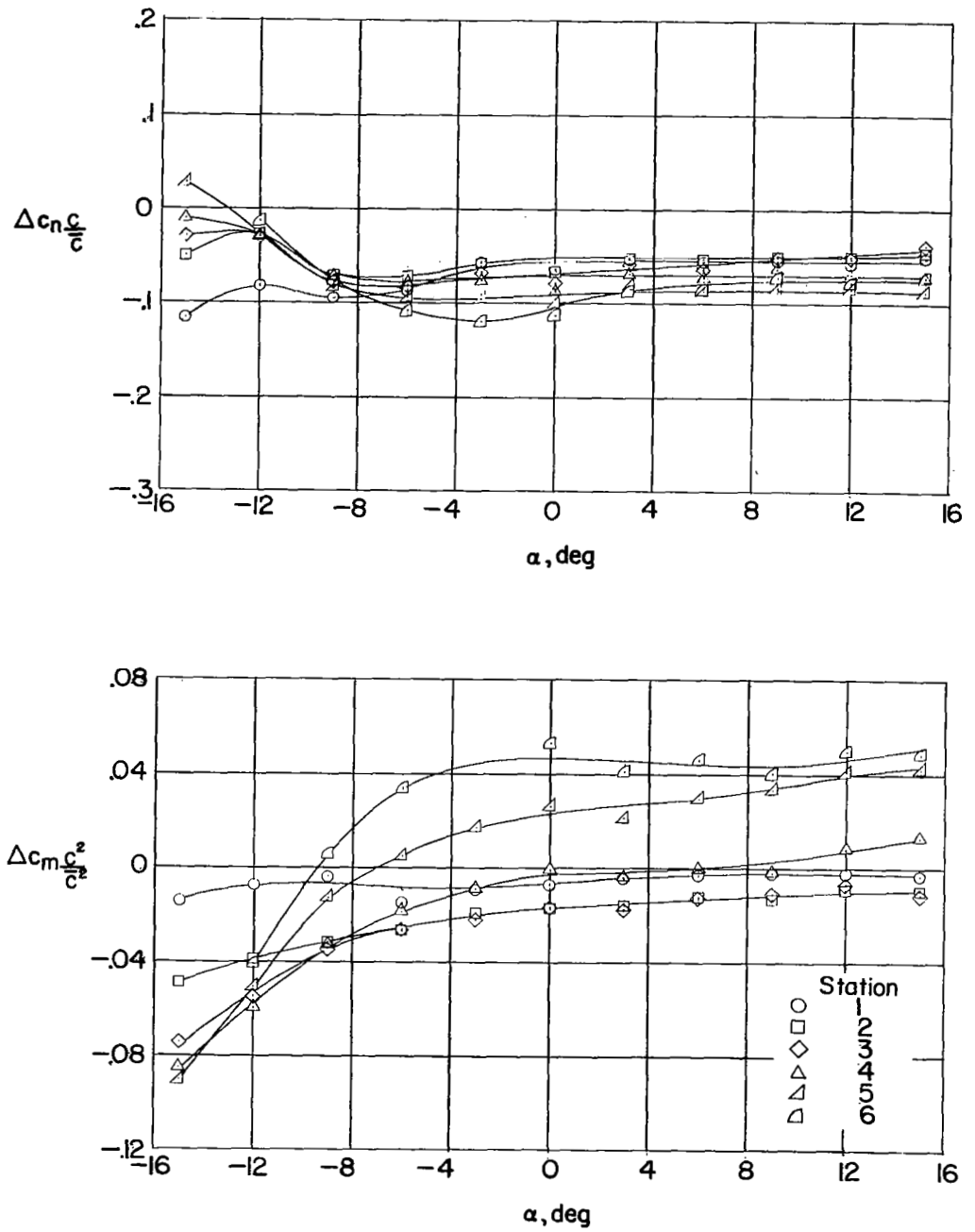

(a) Configuration 21, full-span swept spoiler.

Figure 13.- Variations of incremental section normal-force and pitching-moment coefficients with angle of attack.

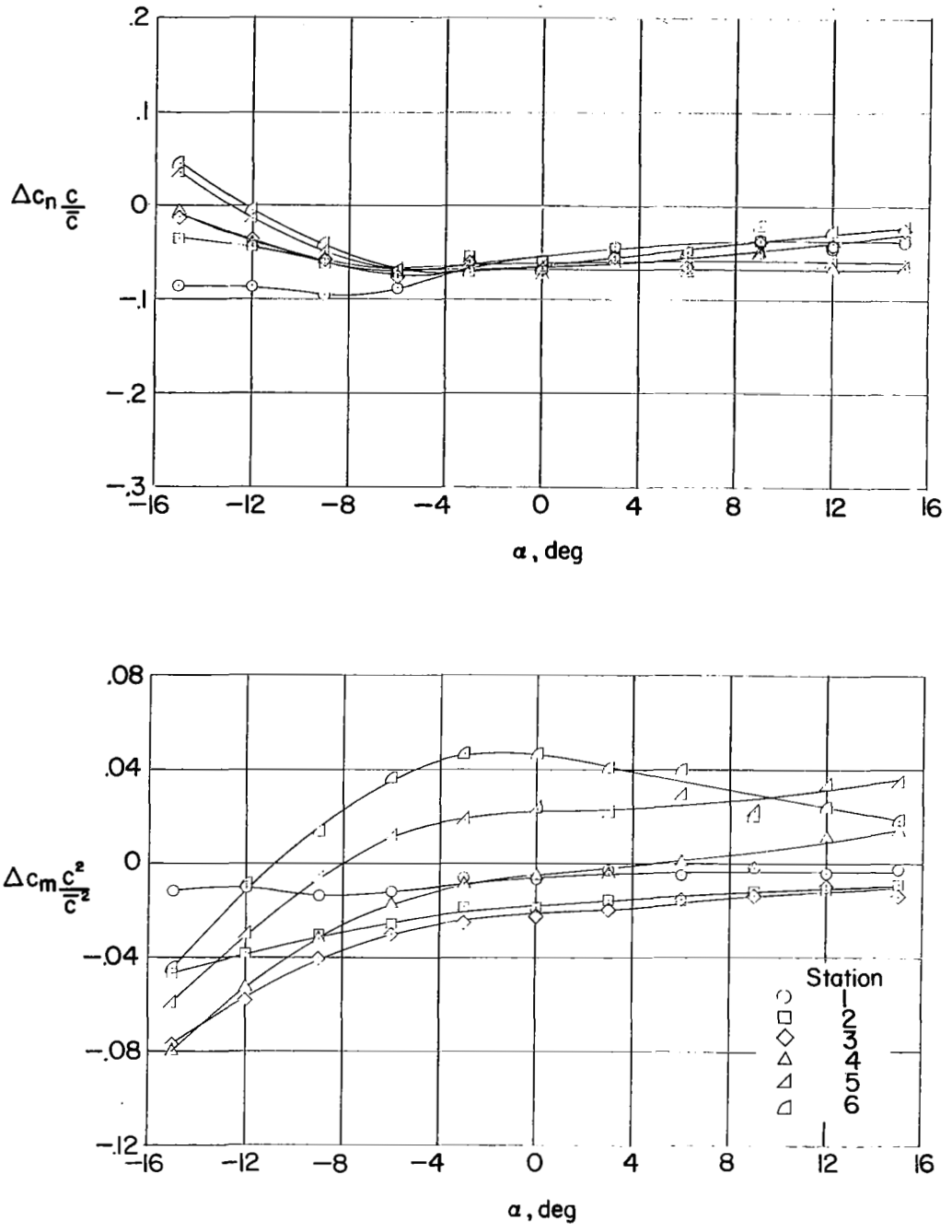

(b) Configuration 22, half-span swept spoiler.

Figure 13.- Continued.

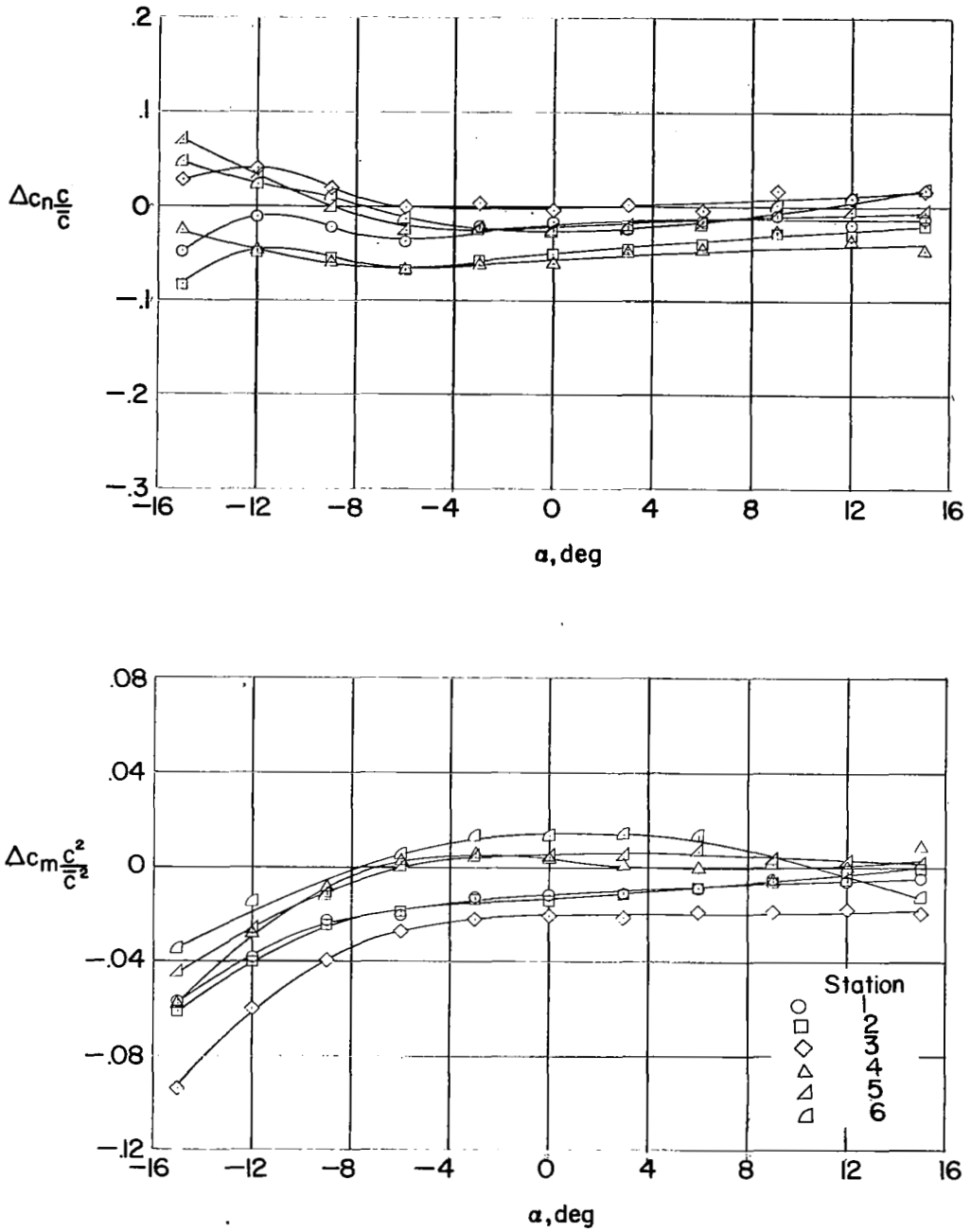

(c) Configuration 23, half-span unswept spoiler.

Figure 13.- Continued.

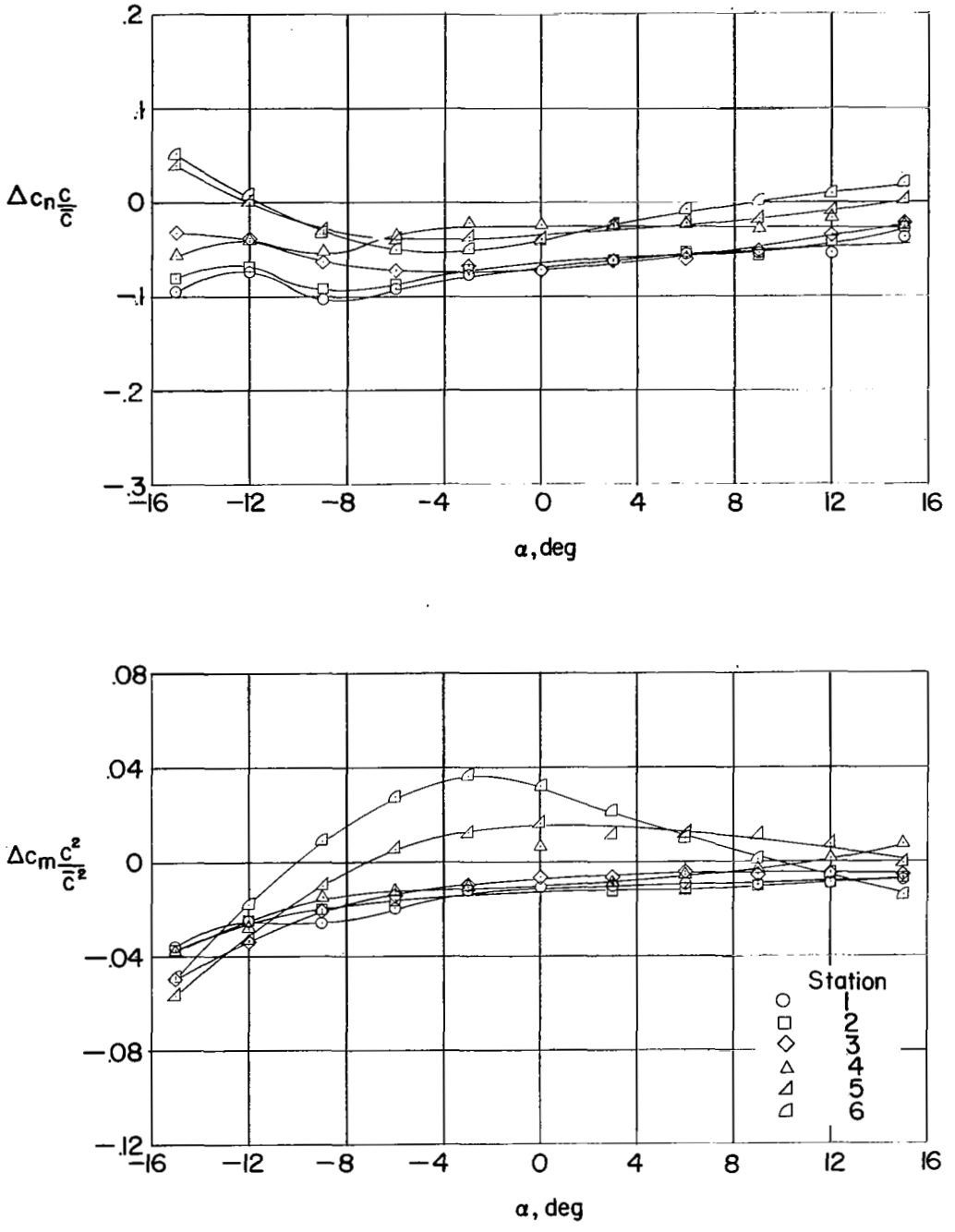

(d) Configuration 24, half-span stepped spoiler.

Figure 13.- Continued.

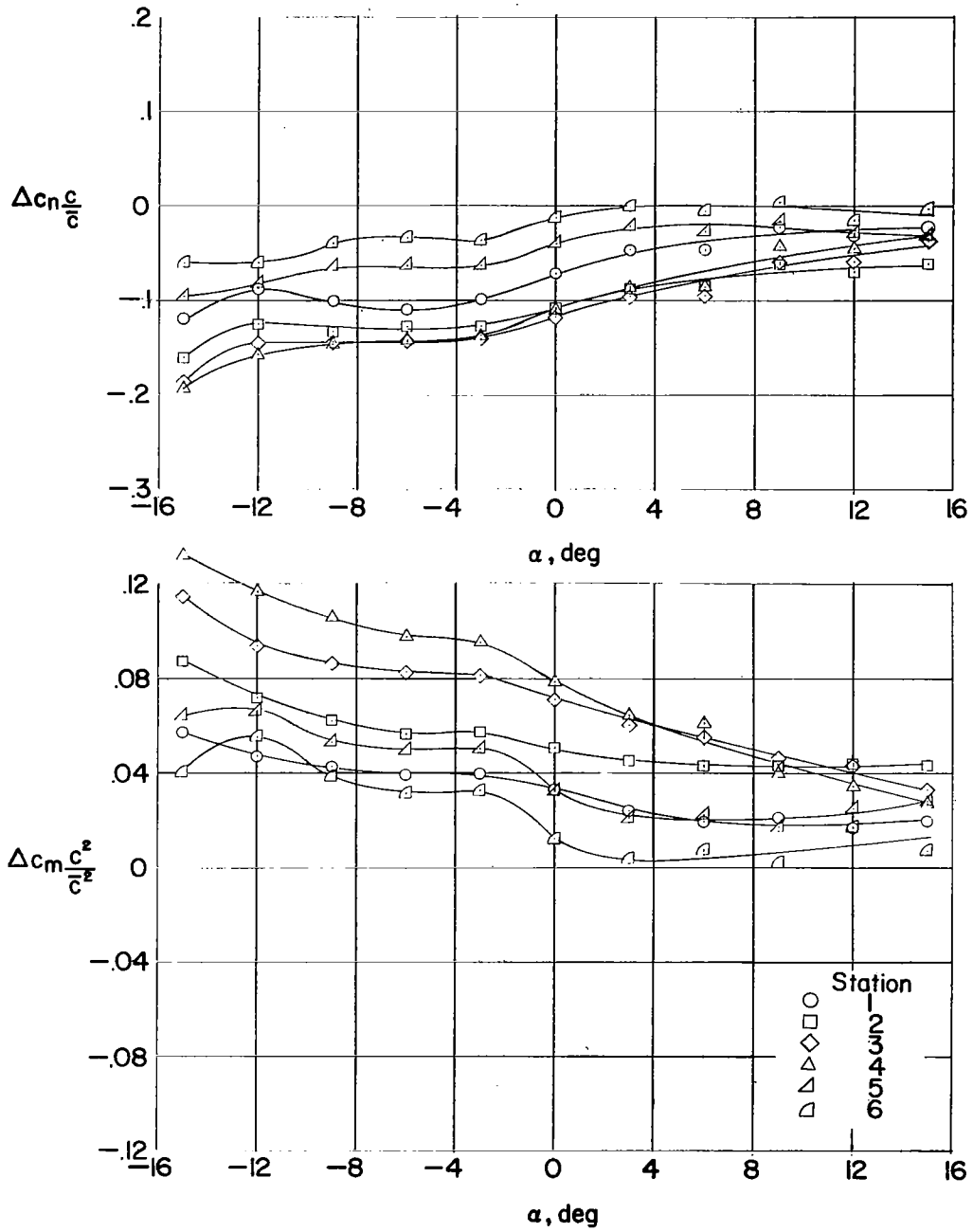

(e) Configuration 25, half-span trailing-edge spoiler.

Figure 13.- Concluded.

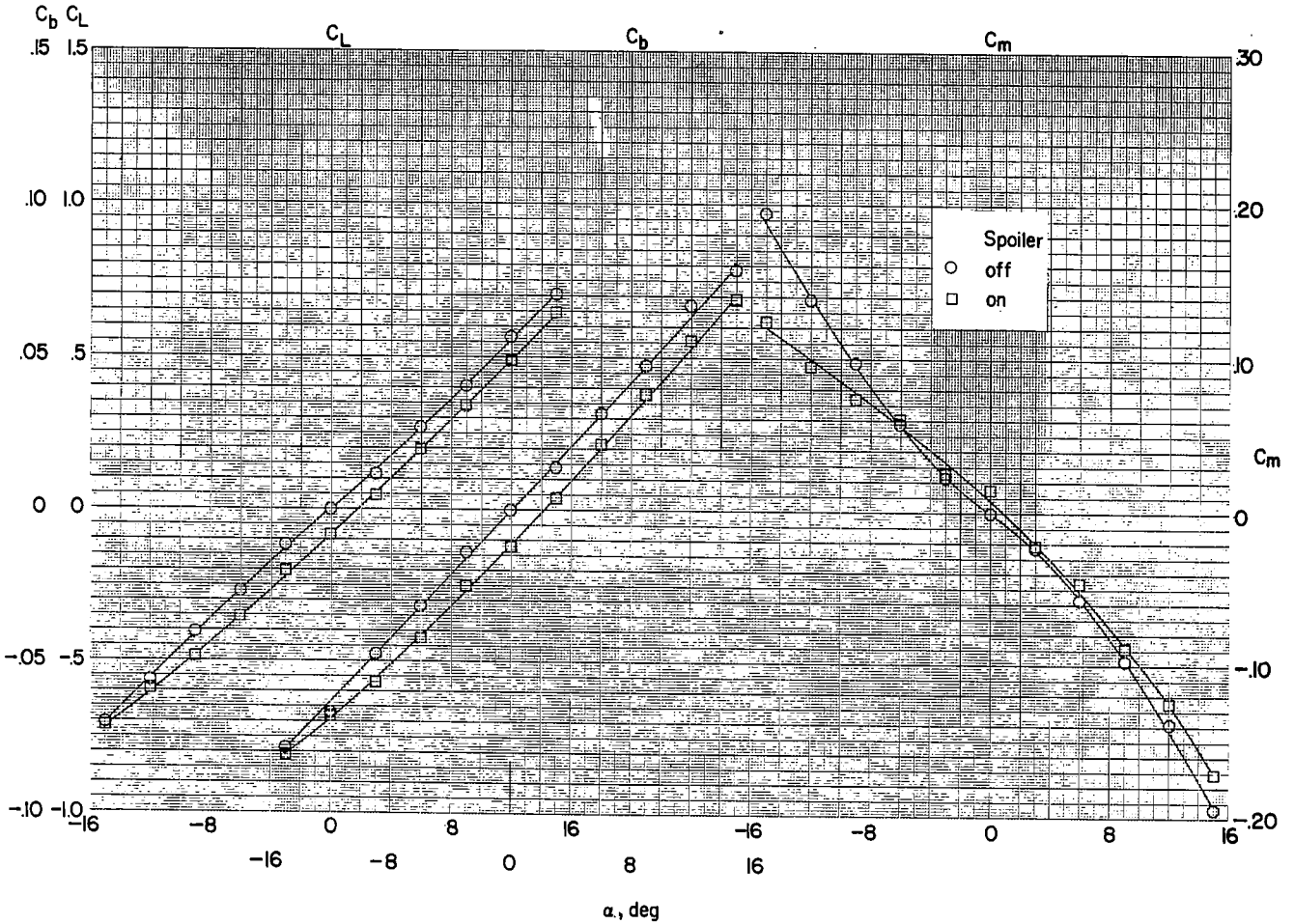

(a) Configuration 21, full-span swept spoiler.

Figure 14.- Variation of wing lift, bending-moment, and pitching-moment coefficients with angle of attack for spoiler configurations tested.

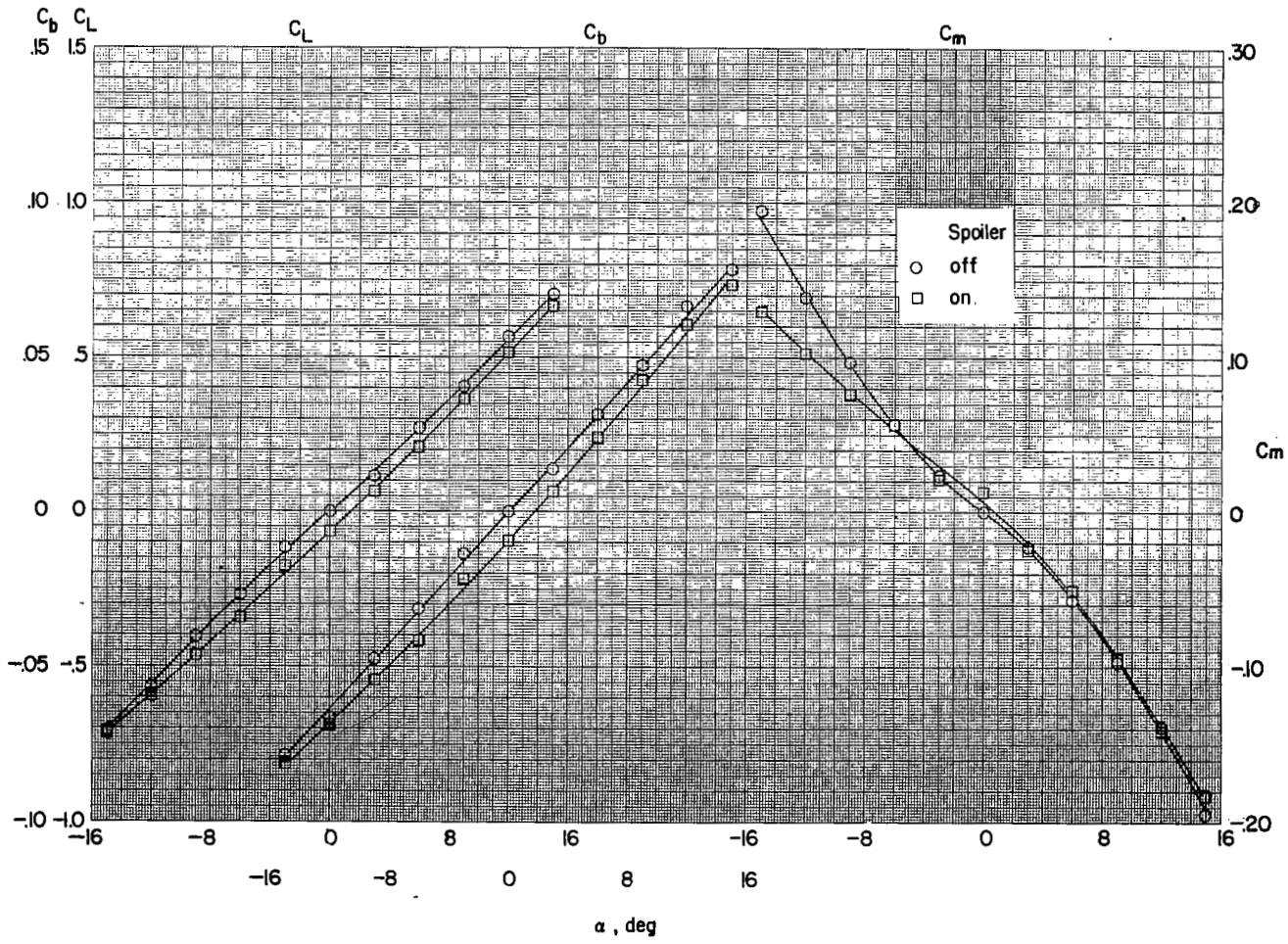

(b) Configuration 22, half-span swept spoiler.

Figure 14.- Continued.

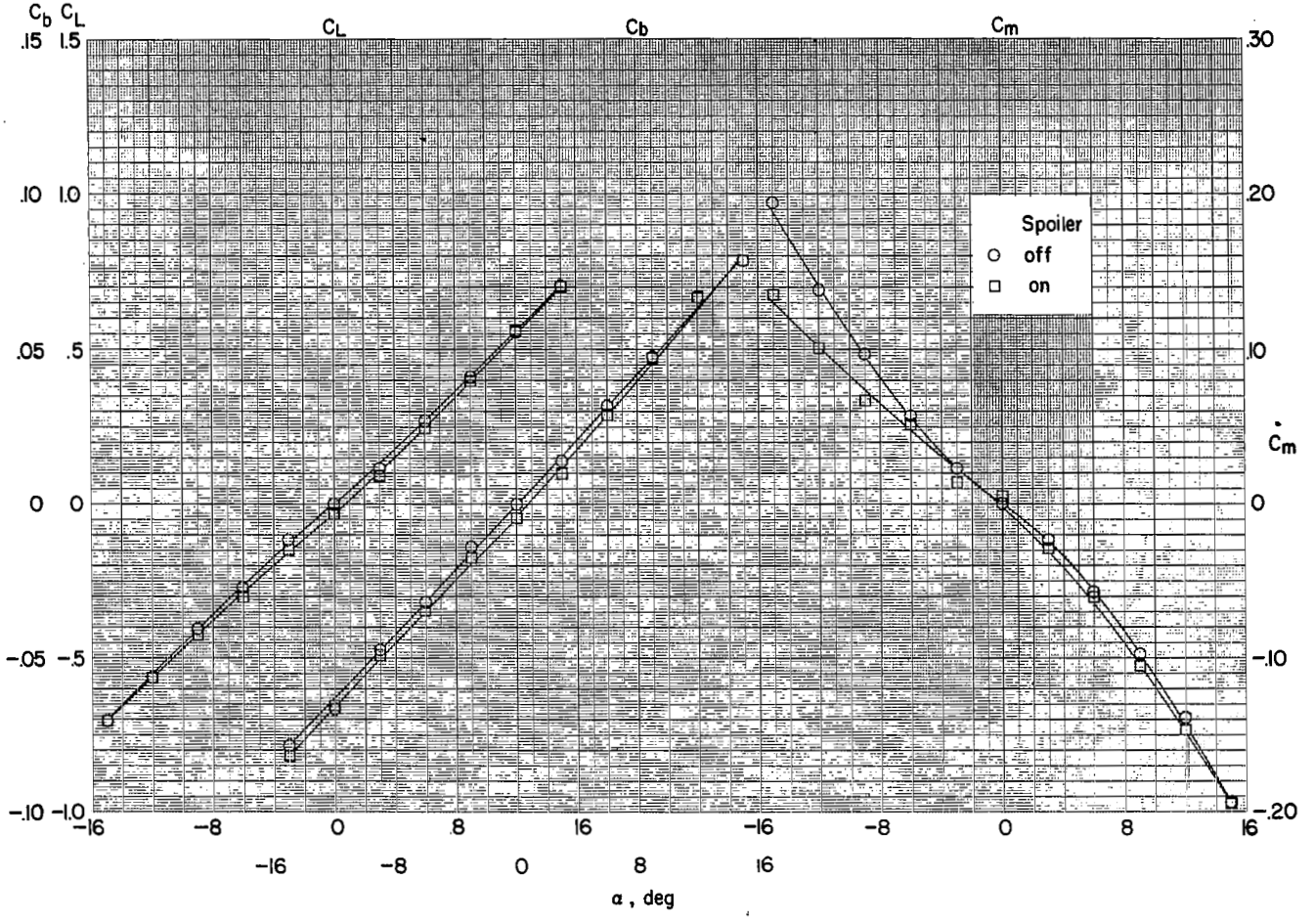

(c) Configuration 23, half-span unswept spoiler.

Figure 14.- Continued.

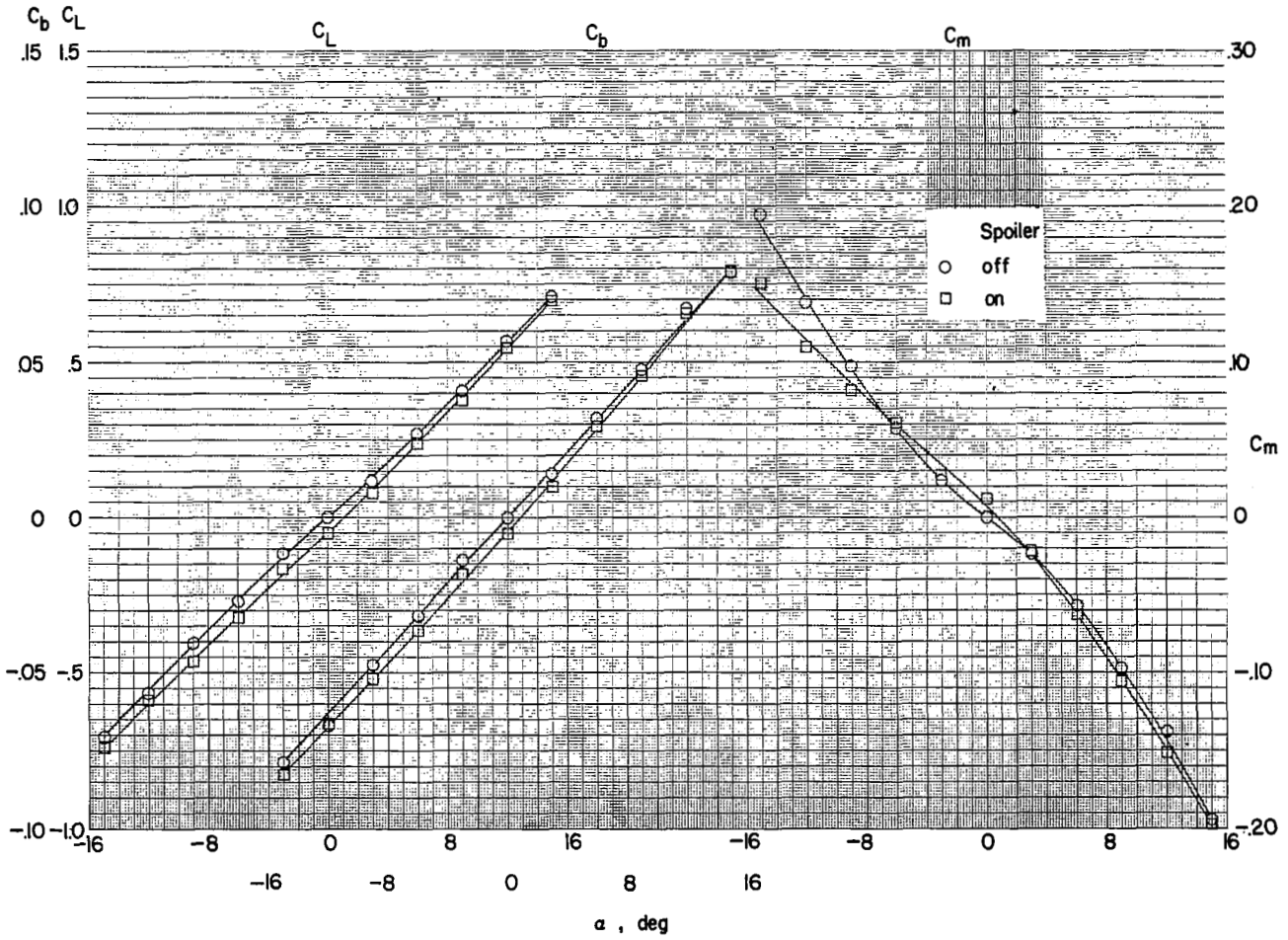

(d) Configuration 24, half-span stepped spoiler.

Figure 14.- Continued.

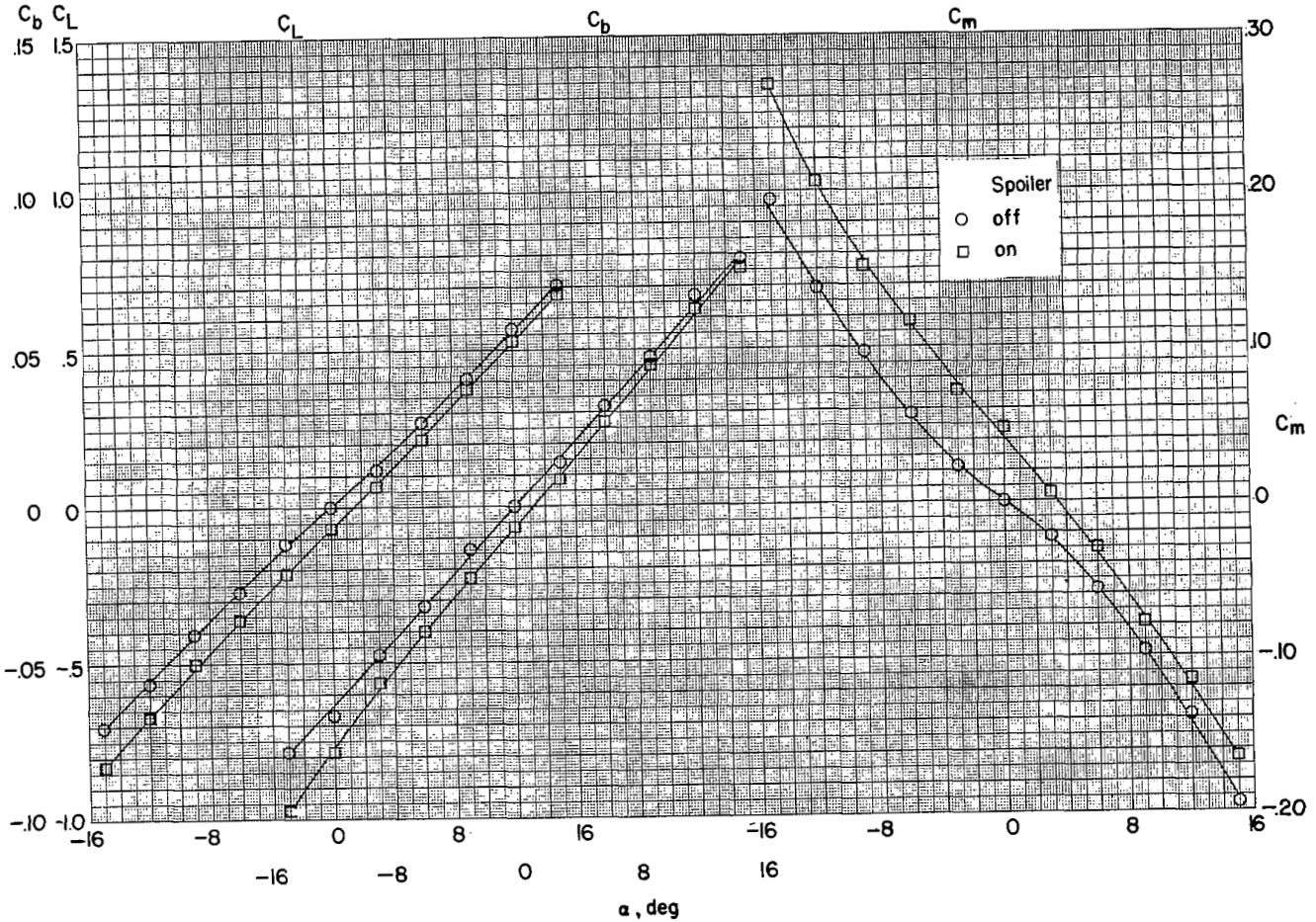

(e) Configuration 25, half-span trailing-edge spoiler.

Figure 14.- Concluded.

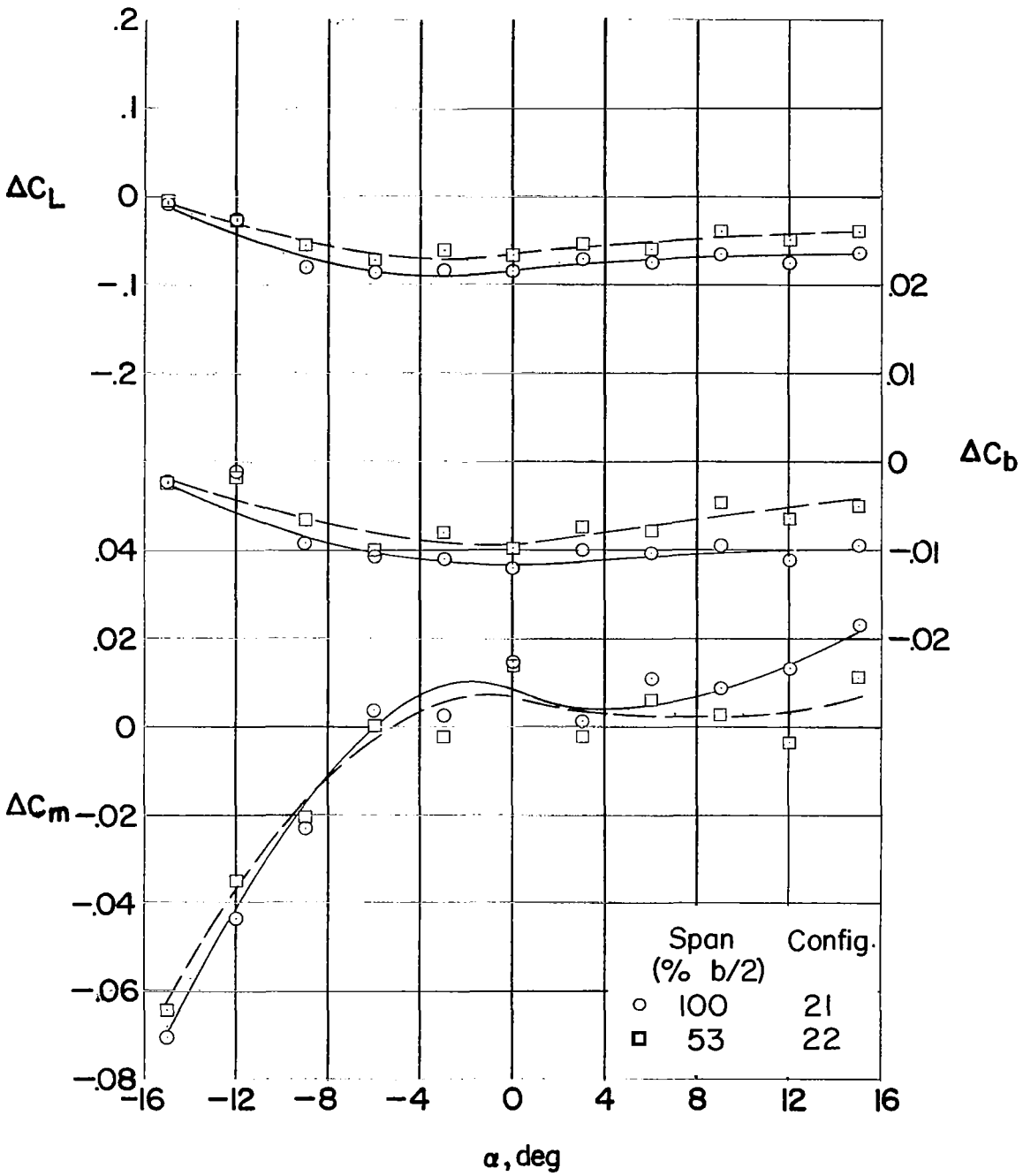

Figure 15.- Variation of incremental lift, bending-moment, and pitching-moment coefficients with angle of attack to show effect of decreasing spoiler span.

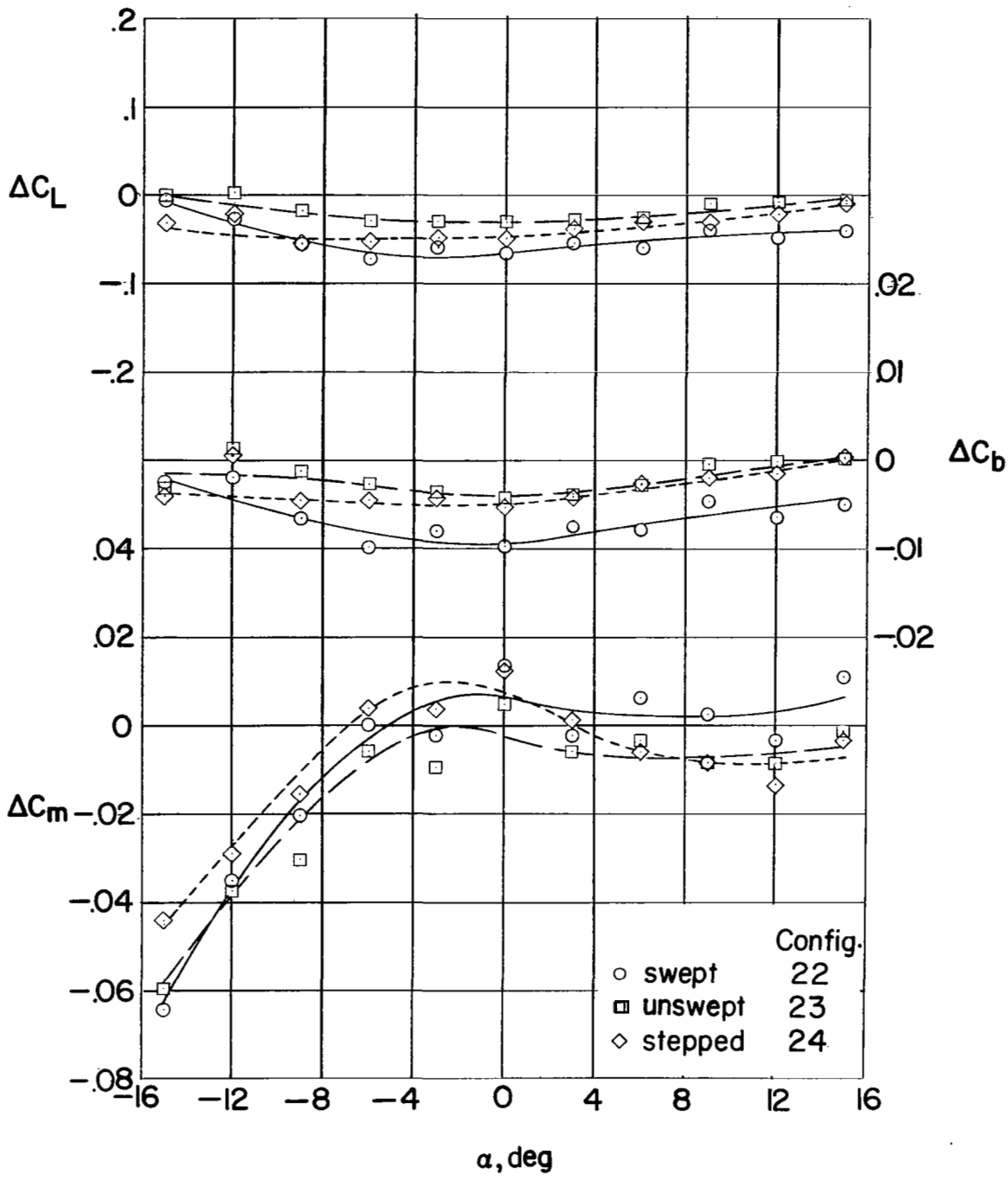

Figure 16.- Variation of incremental lift, bending-moment, and pitching-moment coefficients with angle of attack to show effect of spoiler sweep and spoiler type.

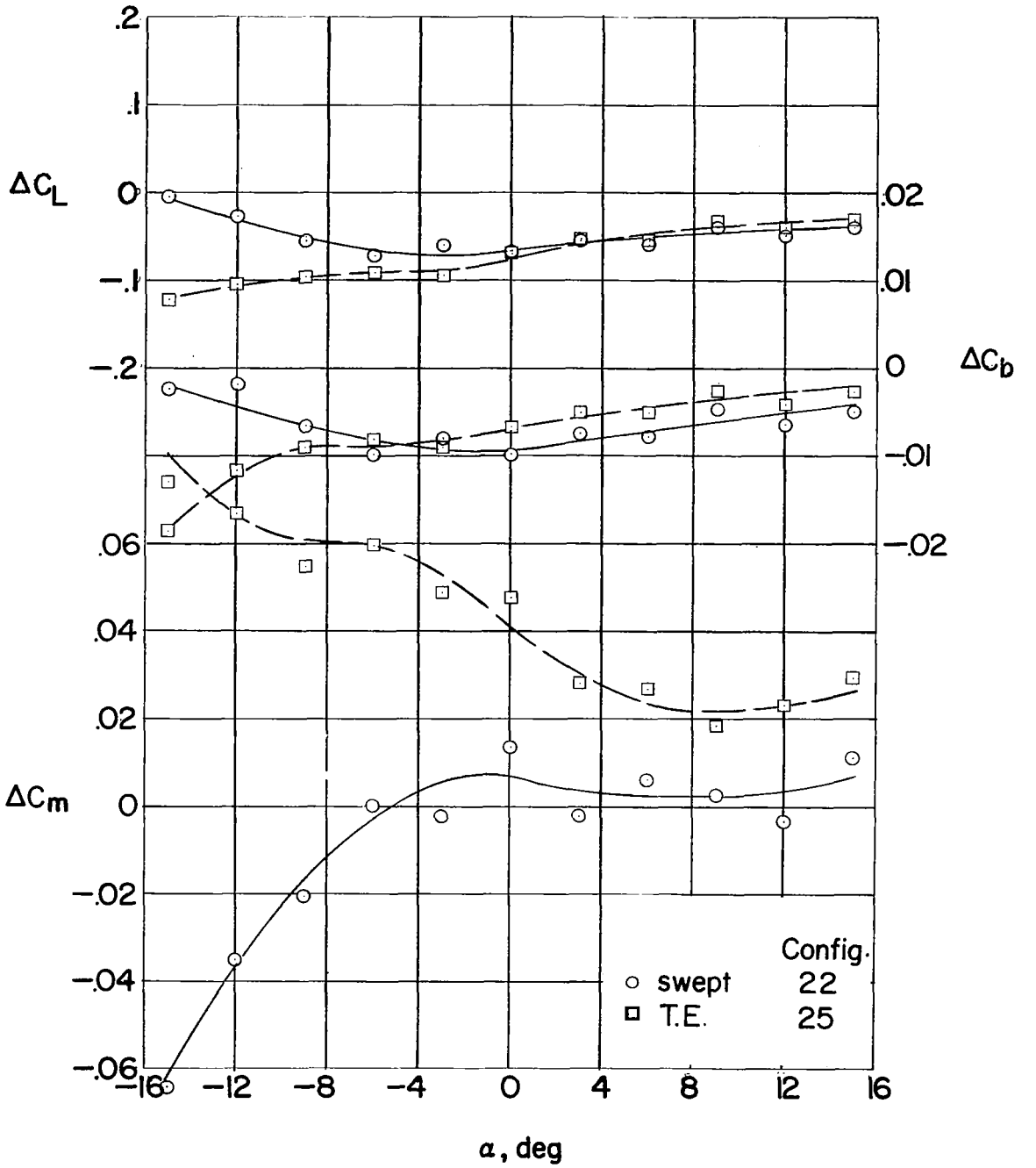

Figure 17.- Comparison of variation of incremental lift, bending-moment, and pitching-moment coefficients with angle of attack for half-span swept spoiler and half-span trailing-edge spoiler configurations.

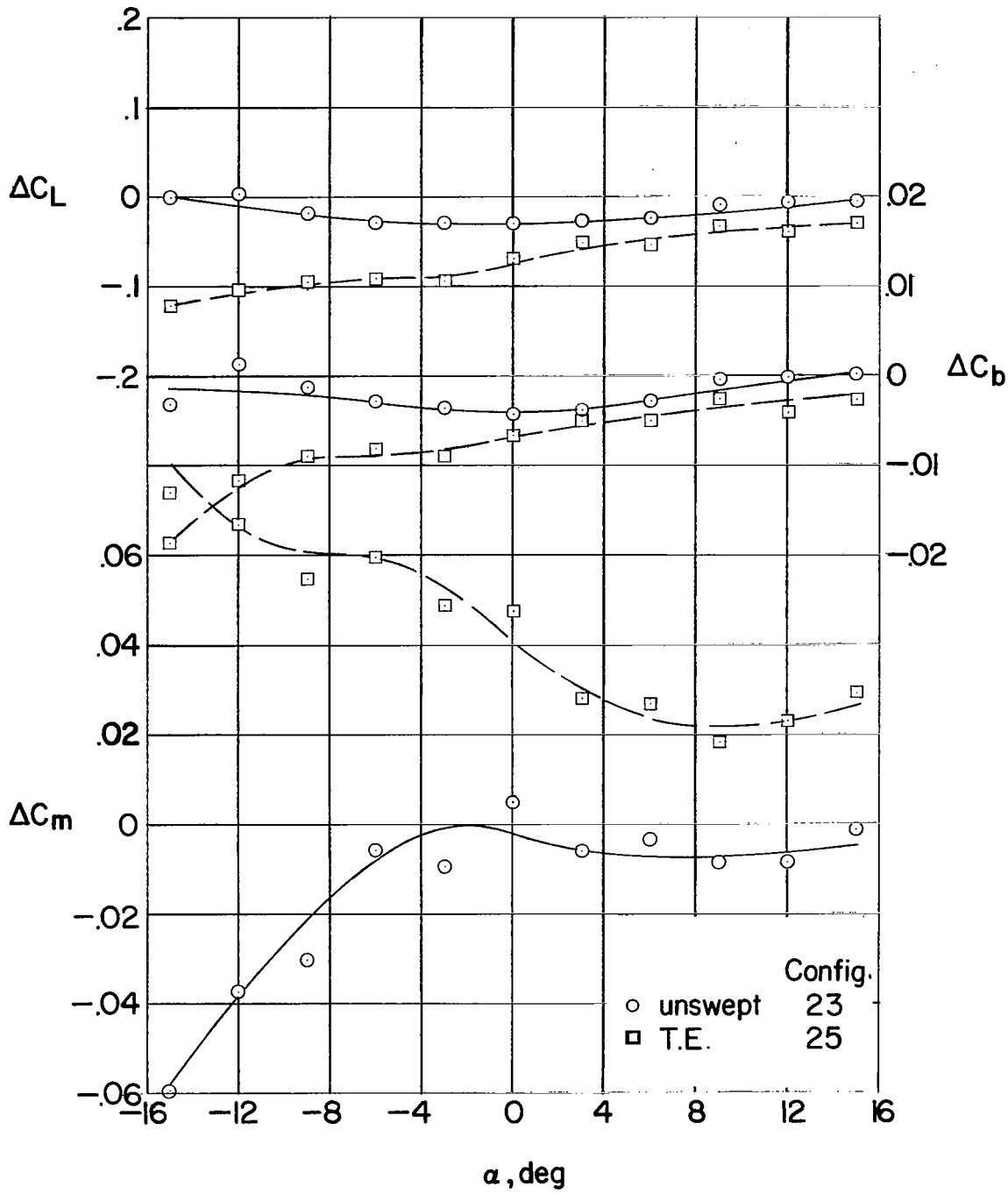

Figure 18.- Comparison of variation of incremental lift, bending-moment, and pitching-moment coefficients with angle of attack for half-span unswept spoiler and half-span trailing-edge spoiler configurations.